# FORMATION AND ENZYME PROCESSING OF 5-CARBOXAMIDO-5-FORMAMIDO-2-IMINOHYDANTOIN, A MAJOR OXIDATION PRODUCT OF GUANINE IN DNA

by

Omar R. Alshykhly

A dissertation submitted to the faculty of
The University of Utah
in partial fulfillment of the requirements for the degree of

Doctor of Philosophy

Department of Chemistry

The University of Utah

December 2015

**The University of Utah Graduate School**

# STATEMENT OF DISSERTATION APPROVAL

The dissertation of **Omar R. Alshykhly**

has been approved by the following supervisory committee members:

| | | |
|---|---|---|
| **Cynthia Burrows** | , Chair | **08/11/15** Date Approved |
| **Amy Barrios** | , Member | **08/11/15** Date Approved |
| **Charles Dale Poulter** | , Member | **08/11/15** Date Approved |
| **Haitao Ji** | , Member | **08/11/15** Date Approved |
| **Bethany Anne Koehntop** | , Member | **08/11/15** Date Approved |

and by **Cynthia Burrows** , Chair/Dean of

the Department/College/School of **Chemistry**

And by David B. Kieda, Dean of The Graduate School.

## ABSTRACT

Oxidative damage to DNA, a factor in cancer, mutation, and aging, is attributed to reactive oxygen species (ROS). ROS are formed exogenously and endogenously and attack DNA showing a preference for reaction with 2-deoxyguanosine (dG) sites. In present work, dG was oxidized by $HO^{\bullet}$ that was generated via iron-Fenton reaction or by X-ray radiolysis of water. Under aerobic conditions and in presence of reductant, the product 5-carboxamido-5-formamido-2-iminohydantoin (d2Ih) was the major lesion formed. The above prescribed conditions are mimic to cellular conditions.

DNA polymerase and base excision repair processing of 2Ih lesion has been evaluated in this study. 2Ih bears a stereocenter in the base and was found as two diasteromers, (*R*)-2Ih and (*S*)-2Ih. Single nucleotide insertion opposite (*R*)-2Ih and (*S*)-2Ih in the template strand catalyzed by the DNA polymerases Klenow fragment $exo^{-}$, DPO4, and Hemo KlenTaq demonstrate these lesions cause point mutations. Specifically, they promote three-fold more G•C → C•G transversion mutations than G•C → T•A, and (*S*)-2Ih was two-fold more blocking for polymerase bypass than (*R*)-2Ih. Both diastereomer lesions were found to be substrates for the DNA glycosylases NEIL1 and Fpg, and poorly excised by endonuclease III (Nth). This part of the study was the first investigation of 2Ih mutagenic potential and 2Ih repair ability by glycosylases. These results suggest that formation of the 2Ih lesions in a cell would be mutagenic in the event that they were not properly repaired.

The last part of this study determined the *N*-glycosidic bond stability of (*R*)-d2Ih and (*S*)-d2Ih lesions at varying pH and the effect of rate enhancement when a nucleophile such as spermine (Spm) was present. The hydrolysis rate constant and $t_{1/2}$ values have been estimated by monitoring the nucleoside *N*-glycosidic bond cleavage reaction. The rate of cleavage was slow at pH 6.4, 7.4, and 8.4, while the rate was twice as fast at pH 5.4 and 4.4. The addition of Spm to the reaction at pH 7.4 increased the hydrolysis seven-fold. This type of hydrolysis in DNA will lead to formation of an abasic site, and eventually this abasic site may be converted to a DNA strand break.

**TABLE OF CONTENTS**

## LIST OF FIGURES

## LIST OF TABLES

## LIST OF ABBREVIATIONS

| | |
|---|---|
| $^1O_2$ | singlet molecular oxygen |
| 2Ih | free base of 5-carboxamido-5-formamido-2-iminohydantoin |
| AP | apurinic/apyrimidinic site |
| ASC | ascorbate |
| BER | base excision repair |
| calcd | calculated |
| CD | circular dichroism |
| cyclo-dG | 5',8-cyclo-2'-deoxyguanosine |
| dATP | adenosine-2'-deoxynucleoside-5'-triphosphate |
| dCTP | cytidine-2'-deoxynucleoside-5'-triphosphate |
| dGTP | guanosine-2'-deoxynucleoside-5'-triphosphate |
| dG | 2'-deoxyguanosine |
| dGh | 5-guanidinohydantoin-2'-deoxyribonucleoside |
| dIz | 2,5-diaminoimidazolone-2'-deoxyribonucleoside |
| dNTP(s) | nucleotide deoxyribotriphosphate(s) |
| dOG | 8-oxo-7,8-dihydro-2'-deoxyguanosine |
| dSp | spiroiminodihydantoin-2'-deoxyribonucleoside |
| dTTp | thimidine-2'-deoxynucleoside-5'-triphosphate |

| | |
|---|---|
| dZ | 2,2,4-triamino-*2H*-oxazol-5-one-2'-deoxyribonucleoside |
| DFT | density functional theory |
| dsDNA | double-stranded DNA |
| *E*.coli | Escherichia coli |
| ECD | electrochemical detector |
| EDTA | ethylene diamine tetraacetic acid |
| ESI | electrospray ionization |
| Fapy-G | formamidopyridine |
| Fapy-dG | formamidopyridine-2'-deoxyguanosine |
| Fpg | formamidopyrimidine DNA glycosylase |
| G | Guanine |
| Gua | free base guanine |
| Gh | guanidinohydantoin |
| HPLC | high-performance liquid chromatography |
| HR | homologous recombination |
| HRMS | High-resolution mass spectrometry |
| Iz | imidazolone |
| MALDI | matrix-assisted laser desorption ionization |
| MMR | mismatch repair |
| MS | mass spectrometry |
| NAC | *N*-acetylcysteine |
| $NaP_i$ | sodium phosphate |
| NEIL1 | human endonuclease VIII like 1 |

| | |
|---|---|
| NER | nucleotide excision repair |
| NHEJ | nonhomologous end joining |
| NMR | nuclear magnatic resonance |
| Nth | endonuclease III |
| $O_2^{\bullet -}$ | superoxide radical anion |
| ODN(s) | Oligonucleotide(s) |
| OG | 8-oxo-7,8-dihydroguanine |
| PAGE | polyacrylamide gel electrophoresis |
| ROS | reactive oxygen species |
| Sp | spiroiminodihydantoin |
| Spm | spermine |
| ssDNA | single-stranded DNA |
| $t_{1/2}$ | half life |
| TCR | transcription coupled repair |
| $T_m$ | melting temperature |
| UV-vis | ultraviolet visible |
| Z | oxazolone |

## ACKNOWLEDGEMENTS

First and foremost, I would like to express my gratitude to Prof. Cynthia Burrows for allowing me to join her laboratory, supporting, guiding, and inspiring me over the past five years. Burrows is an outstanding expert in her research field and is an excellent mentor for me. She always gives me great support and understanding in both professional and personal matters. I am really so proud to be a member in her lab. I would like to thank Dr. Aaron Fleming who was always there to offer help. His patience, generosity and good humor made working in the lab an absolute pleasure from start to finish. Next, I would like to thank my committee members, Prof. Bethany Buck-Koehntop, Prof. Mark Ji, Prof. Dale Poulter, and Prof. Amy Barrios. I want to say thank you for letting my defense be an enjoyable moment, and for your brilliant comments and suggestions. Also, I would like to thank the Burrows lab members for their friendship and support and especially to: Xibo Li, Anton Alenko, Pranjali Ghude, Dr. Na An, Judy Zhu, Dr. Yun Ding, Dr. Jan Reidle, Aaron Rogers, Carla Omaga, and Tony Hanelli.

A special thanks to my family. Words cannot express how grateful I am to my mother, father, brother and my sisters for all of the sacrifices that you have made on my behalf. Your prayers for me were what sustained me thus far. Thanks to my mother-in-law, and father-in-law for their support and encouragement. I would also like to thank all my friends who supported and encouraged me to strive towards my goal. At the end

I would like to express appreciation to my beloved wife who was always with me during the good times and the bad. Finally, thanks to my beloved little daughter, who has been a source of my inspiration and motivation.

# CHAPTER 1

# INTRODUCTION

## Oxidative DNA damage

A significant imbalance between the production of reactive oxygen species (ROS) and antioxidant defense mechanisms leads to oxidative stress.[1] ROS can be formed endogenously[2-5] (Figure 1.1) or exogenously[6] and include smoking and environmental pollution,[1,7] UV light,[8,9] and ionizing radiation.[10-12] ROS such as hydroxyl radical ($HO^{\bullet}$), superoxide radical ($O_2^{\bullet -}$), hydrogen peroxide ($H_2O_2$), singlet oxygen ($^1O_2$), nitric oxide (NO), and peroxynitrite ($ONOO^-$) have been implicated in a number of pathologies including inflammatory diseases,[13,14] Alzheimer's disease,[1,15,16] cancers,[13] stroke,[14] respiratory diseases,[17] acquired immunodeficiency syndrome (AIDS),[18] and the aging process.[13] Many treatments that have been used to combat some of these diseases, ranging from ionization radiation in anticancer therapy to antiretroviral drug therapy in the case of AIDS, have been shown to result in an increase in the production of ROS.[19]

Among all biomolecules subjected to oxidative stress conditions, deoxyribonucleic acid (DNA) as the hereditary unit is the major focus of studies in this field. Oxidative damage to other biomolecules is considered transient, because they are

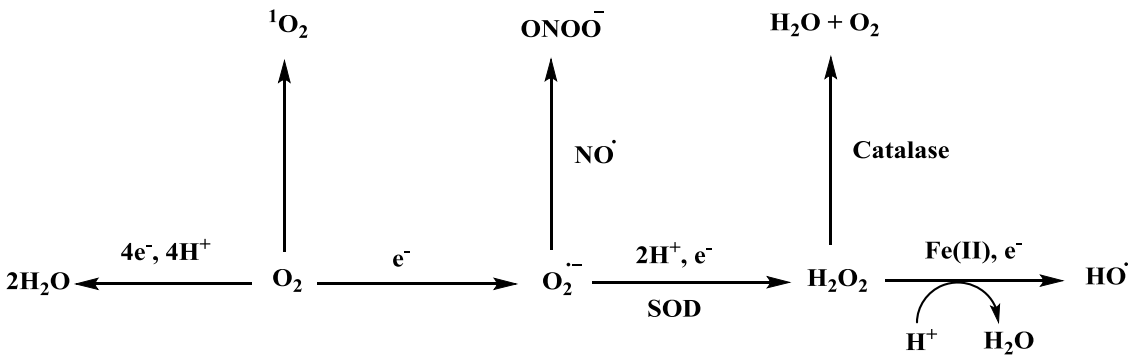


**Figure 1.1.** Formation of ROS endogenously, one-electron reduction of oxygen generates superoxide radical that can be reduced to hydrogen peroxide by superoxide dismutase (SOD). Hydrogen peroxide can go through the Fenton reaction in the presence of a metal such as iron (Fe(II)) to form a hydroxyl radical. Photosensitizers allow the excitation of ground state molecular oxygen to singlet oxygen.

usually degraded and resynthesized. On the other hand, genomic DNA is replicated during cell division, and damage can lead to mutations that alter the sequence permanently. A number of DNA oxidative modifications may be initiated by interaction with ROS, including damage to the deoxyribose moiety of the sugar-phosphate backbone of DNA, nucleobase modifications, single- and double-strand breaks, formation of abasic sites, and DNA-protein crosslinks.[13] Under normal conditions, DNA oxidative damage can be repaired by the cellular machinery, but during oxidative stress the repair mechanisms are unable to cope with the large number of DNA lesions, and some DNA lesions are left unrepaired. The presence of these lesions can cause miscoding and stalling of DNA replication by cellular polymerases, which will alter the gene sequence for the daughter generations. The mutations caused by oxidative stress severely hamper the essential role of preservation and transmission of genetic information between generations. As a result, sensitive DNA repair pathways have evolved to maintain genomic stability and cell viability. Unrepaired DNA lesions may lead to the development of the disease conditions listed above (Figure 1.2). In the specific case of cancers, oxidative damage to DNA is believed to be the precursor to oncogene activation and tumor-suppressor gene inactivation, resulting in unregulated cellular growth (tumorigenesis).[20]

**Guanine oxidation**

DNA bases have lower oxidation potentials compared to the DNA sugar-phosphate backbone and are therefore considered the primary targets of oxidative damage leading to mutagenesis. Guanine (G) is considered a hot spot in DNA for

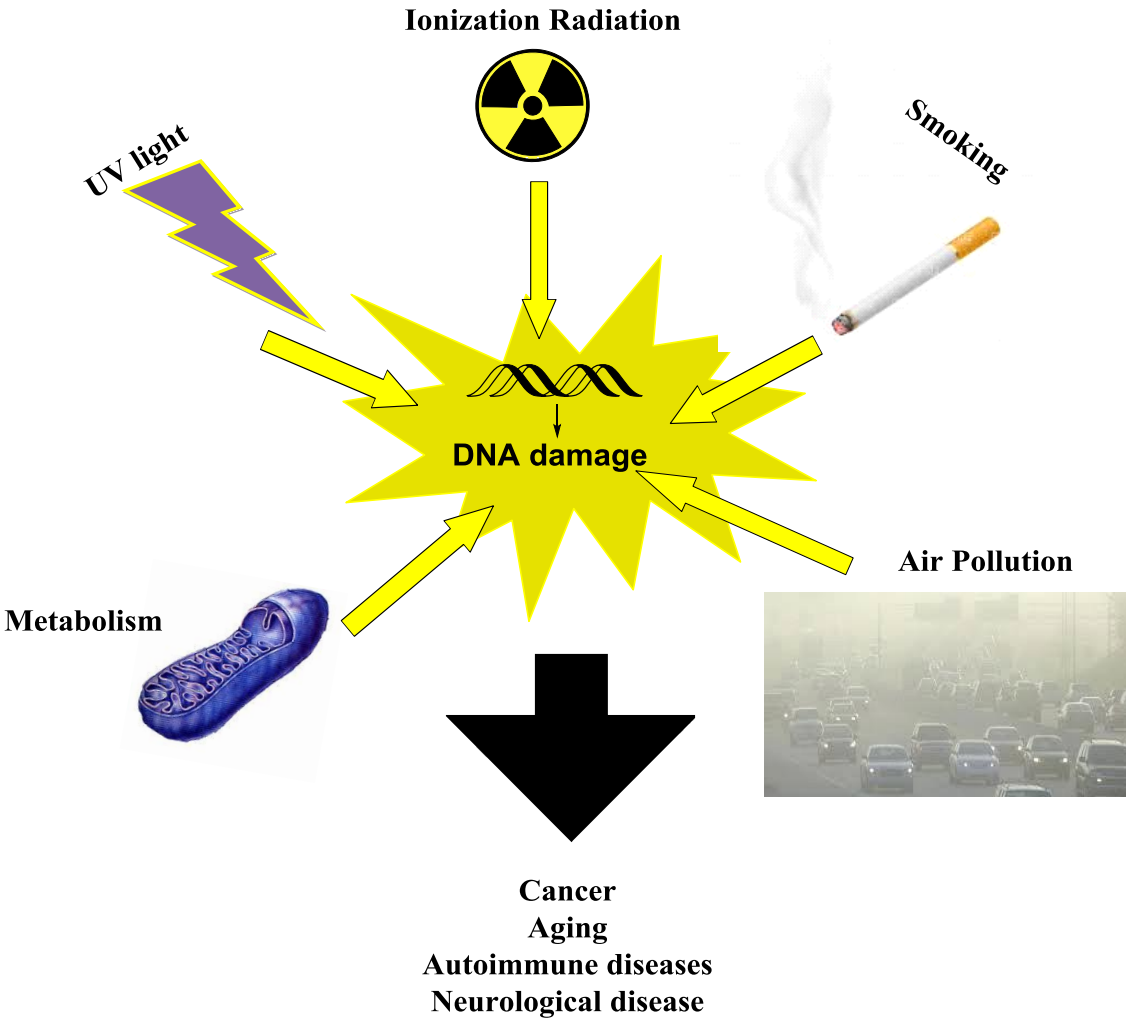


**Figure 1.2.** DNA damage from endogenous and exogenous reactive oxygen species. Unrepaired DNA damage can result in cancer, aging, immune disease, and neurological disorders.

oxidative base damage due to the standard reduction potential of guanine (+1.29 V) being considerably lower than the other native DNA nucleobases (Table 1.1).[21] G is the preferred DNA target for different oxidants such as $HO^{\bullet}$, $^1O_2$, and one-electron oxidation leading to formation of a wide of variety oxidative lesions.[22-26] G can undergo a one-electron oxidation to produce the guanine radical cation ($G^{\bullet+}$). These $G^{\bullet+}$ ($pK_a$ = 3.9)[27] residues are commonly referred to as DNA holes,[28] and they are a much stronger acid than the parent G ($pK_a$ = 9.5).[29] At physiological pH, $G^{\bullet+}$ quickly undergoes deprotonation to form the neutral guanine radical ($G^{\bullet}$, Figure 1.3A).[30] The $G^{\bullet}$ is also one of the major intermediates of the reaction of G with $HO^{\bullet}$. It is also hypothesized that $G^{\bullet}$ undergoes a second one-electron oxidation to form the carbocation ($G^{+}$).[27,31] The resulting carbocation can undergo hydration to produce 8-oxo-7,8-dihydroguanine (OG). As an alternative, $G^{\bullet+}$ can be hydrated to form the $G(OH)^{\bullet}$ radical. This $G(OH)^{\bullet}$ can proceed via one of two pathways: (1) A second one-electron oxidation to form OG,[32] or (2) a one-electron reduction to form 2,6-diamino-4-hydroxy-5-formamidopyrimidine (Fapy-G) (Figure 1.3B).[25,33] On the other hand, $O_2^{\bullet-}$ can also react rapidly with the neutral guanine radical followed by protonation of the adduct and give rise to a hyperoxide adduct at C5 leading to the formation of imidazolone (Iz), which can be further hydrolyzed to give oxazolone (Z) as a major product (Figure 1.3C).[34,35] This mechanism is the same for the oxidation of G by benzophenone and riboflavin (type I photosensitizer).[35-37] OG is a biomarker of oxidative stress *in vivo*.[24,38] Its level was found to increase with several oxidative stressors.[39-41] OG is more easily oxidized than G. Further oxidation of OG can occur due to its low standard reduction potential (+0.74 V vs. NHE),[42] and several groups have reported that OG is susceptible to further

**Table 1.1.** Standard reduction potentials for DNA nucleosides.[21]

| **Deoxynucleosides** | **$E^o$ (V vs. NHE, pH 7)** |
|---|---|
| Deoxyguanosine | 1.29 |
| Deoxyadenosine | 1.42 |
| Deoxythymidine | 1.70 |
| Deoxycytidine | 1.60 |

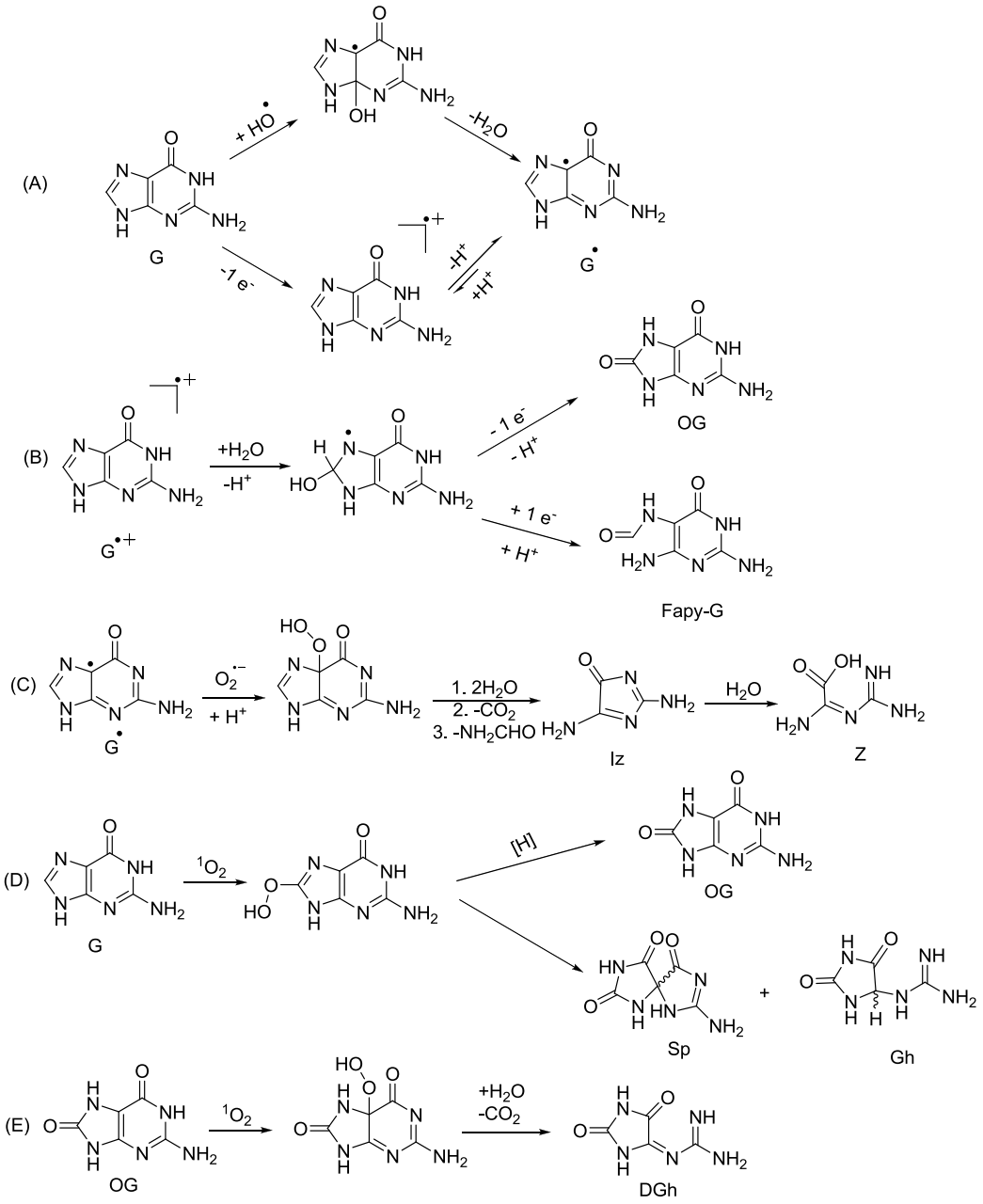


**Figure 1.3.** Pathways for G oxidation. (A) Proposed pathways from G to G$^{\bullet}$, (B) proposed pathways leading to OG and Fapy-G, (C) proposed pathways leading to Iz and Z, (D) proposed pathways leading to Sp and Gh, (E) proposed pathway leading to DGh.

oxidation using other oxidizers including peroxynitrite, iridium hexachloroiridate anion ($[IrCl_6]^{2-}$), $^1O_2$, and the dichromate anion ($[Cr_2O_7]^{2-}$).[43-45] One-electron abstraction leads to the intermediate ($OG^{\bullet+}$), which deprotonates to form the neutral radical form ($OG^{\bullet}$) ($pK_a = 6.6$).[42] Based on the conditions and oxidant type, OG can be oxidized to form a number of hyperoxidized products that can also serve as biomarkers for oxidative stress in cells. The oxidation of OG proceeds through another two-electron oxidation process to form guanidinohydantoin (Gh) and spiroiminodihydantoin (Sp).[43,46,47]

Other reaction channels exist to yield the hydantoins Gh and Sp. G can undergo a [4+2] cycloaddition in the presence of $^1O_2$ to form 4,8-endoperoxide.[48-50] This unstable compound can rearrange to form an 8-hydroperoxy derivative,[51] which is a strong peracid oxidant and in the presence of reducing agent OG is formed as the major lesion. The presence of OG in cellular DNA after treatment with $^1O_2$ supports this pathway.[52] Otherwise, in the absence of reductant, it will form Gh and Sp as the final lesions (Figure 1.3D).[43,46] On the other hand, a [2+2] cycloaddition of OG by $^1O_2$ yields dehydroguanidinohydantoin (DGh) (Figure 1.3E).[53]

**G oxidation by hydroxyl radical**

$HO^{\bullet}$ oxidation or modification of DNA has been, and still is, the subject of research interest. As a physiological and endogenous oxidant, this radical is central to many health problems.[54] The $O_2^{\bullet-}$ is converted to hydrogen peroxide ($H_2O_2$) by antioxidant enzymes such as superoxide dismutases (SOD). $H_2O_2$ produced can be rendered harmless by conversion to water and molecular oxygen by glutathione peroxidase/catalase or can diffuse into the cytoplasm and induce the Fenton reaction or

the Haber-Weiss reaction if it reacts with Fe(II) or Cu(I), respectively, to generate $HO^{\bullet}$ (Figure 1.1), which causes oxidative damage to biomolecules such as DNA.[2,55]

One key target of ionizing radiation in cells is the DNA. The DNA can be damaged by ionizing radiation through indirect or direct ionization. Indirect ionization requires the ionization of other molecules in cells such as water to form $HO^{\bullet}$. Besides $HO^{\bullet}$, the photon itself can also hit the DNA to give a cascade of ionizations to the atoms that make up DNA (Figure 1.4).[12,56] $HO^{\bullet}$ is the ROS with the highest reduction potential (2.31 V vs NHE, pH7).[57,58] $HO^{\bullet}$ is a significant source of DNA damage that can react with almost all DNA bases. It can be added to a double bond to give the $HO^{\bullet}$ adduct or it can abstract a hydrogen atom. The G adduct can be formed at carbon 4, 5, or 8, besides hydrogen abstraction from the sugar moiety (Figure 1.5). These HO-adduct radicals possess different redox properties and are either reducing or oxidizing. [59,60]

The action of $HO^{\bullet}$ on G at the level of the deoxyribonucleoside leads to two intermediate radicals, the hydroxylated radical at C8 $(G8OH)^{\bullet}$ and the neutral guanine radical $G^{\bullet}$ in ≈20 and ≈70 % yield, respectively, relative to $HO^{\bullet}$.[61] The major product of the reaction of $HO^{\bullet}$ with G, $G^{\bullet}$, is proposed to be the result of addition of $HO^{\bullet}$ at C4 or C5, and the latter radical is unstable and loses a molecule of $H_2O$ leading to the neutral guanine radical.[61] $G^{\bullet}$ has oxidative properties as well. In contrast, the attack of $HO^{\bullet}$ at C8 of G yields a reducing neutral radical $(G8OH)^{\bullet}$ that reacts quickly with $O_2$ by electron transfer ($k = 4\times10^9\ M^{-1}\ s^{-1}$) to give rise to OG.[61] The $(G8OH)^{\bullet}$ may be oxidized or reduced depending on the reaction conditions. Thus, the $(G8OH)^{\bullet}$ may be stabilized by reduction. This reaction pathway leads to Fapy-G.[23,26,62] However, in Chapter 2 of this work, we could detect Fapy-G only when we used extreme anoxic conditions

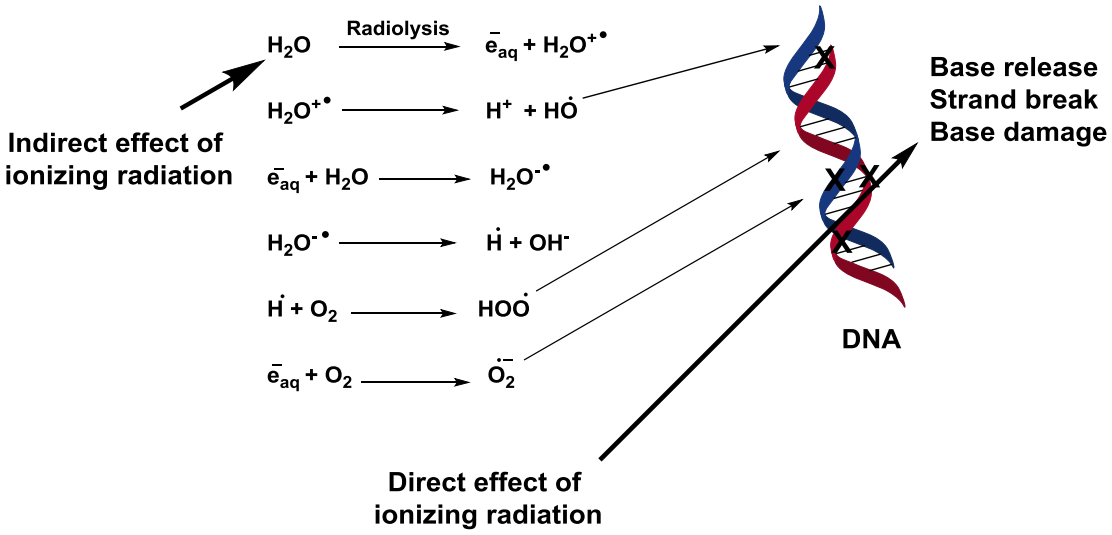


**Figure 1.4.** Direct and indirect effects of ionizing radiation on DNA.

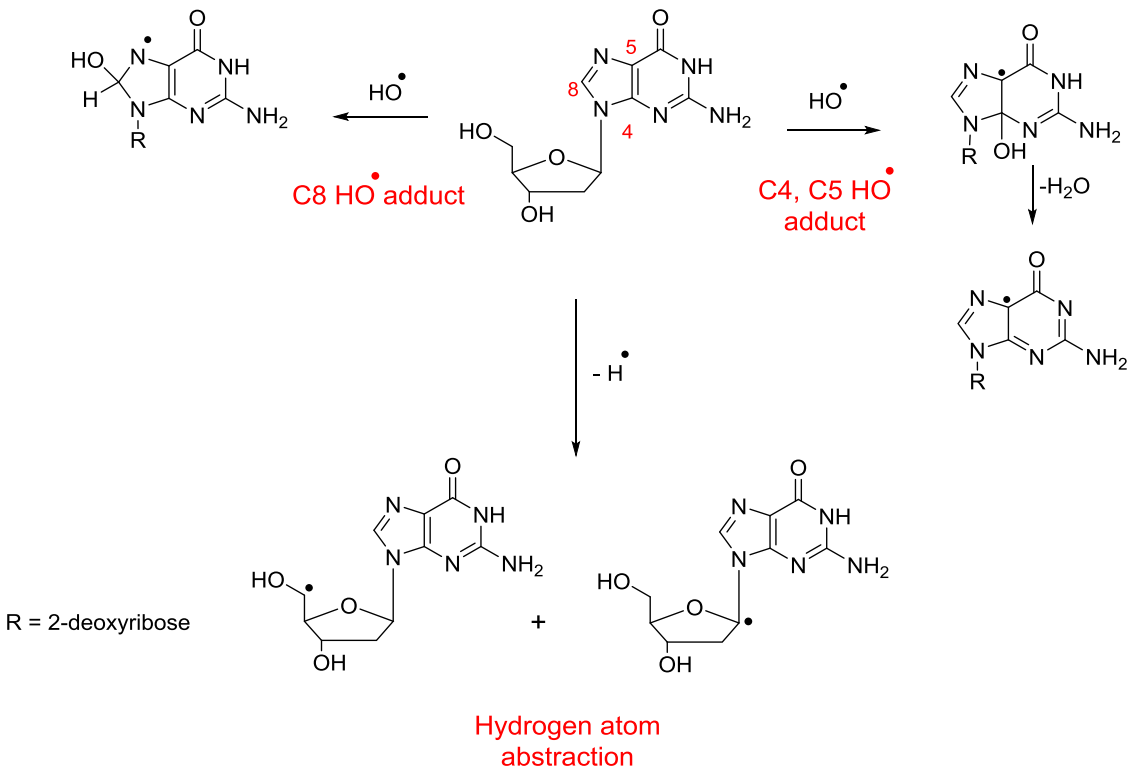


**Figure 1.5.** Proposed pathways of $HO^{\bullet}$ attacking at G. G adducts can form at carbon 4, 5, or 8 besides hydrogen abstraction from the sugar moiety. The G adduct at carbon 4 or 5 leads to the formation the neutral radical $G^{\bullet}$.

(~0% $O_2$). The $G^{\bullet}$ is the same intermediate of guanine oxidation by one-electron transfer.[30] In summary, guanine oxidation by $HO^{\bullet}$ radicals will converge to the same products as for the oxidation by electron transfer or by singlet oxygen.

**History of the 2Ih (G+34) product**

Great progress has been made in the discovery of the oxidative degradation pathway of DNA during the last two decades.[63] Several products have been observed and detected as oxidative damage products in all DNA bases. The G oxidation products starting from OG and ending with Sp and Gh have been detected and well studied. Recent investigations concerning G oxidation have identified another oxidation product that has a mass G+34 and is called 5-carboxamido-5-formamido-2-iminohydantoin (2Ih) from the following oxidation systems: Fenton chemistry with copper ($Cu(II)/H_2O_2$) or lead ($Pb(II)/H_2O_2$), activation of $KHSO_5$ with nickel ($NiCR/KHSO_5$) or manganese complexes ($Mn\text{-}TMPyP/KHSO_5$), dicopper(II)-complex, $CO_3^{\cdot}$, and the epoxidizing agent dimethyldioxirane (DMDO).[64-70] All these previous studies have suggested different pathways to form 2Ih. The story of 2Ih began in our laboratory when Muller and Luo found that the final product formed by G oxidation in oligonucleotides with $NiCR/KHSO_5$ had a 34 amu gain in mass compared to the starting material.[71] Two proposed structures for that product have been suggested (Figure 1.6A). The new product was proposed to be the result of two oxygen atoms being incorporated from $H_2O$ (Figure 1.7A).[71] The Meunier laboratory proposed the product M+34 as the isomeric 5,8-dihydroxy-7,8-dihydroguanine (5,8-di-HO-G) (Figure 1.6B) that was identified by mass spectrometry and was found as the major oxidation product for

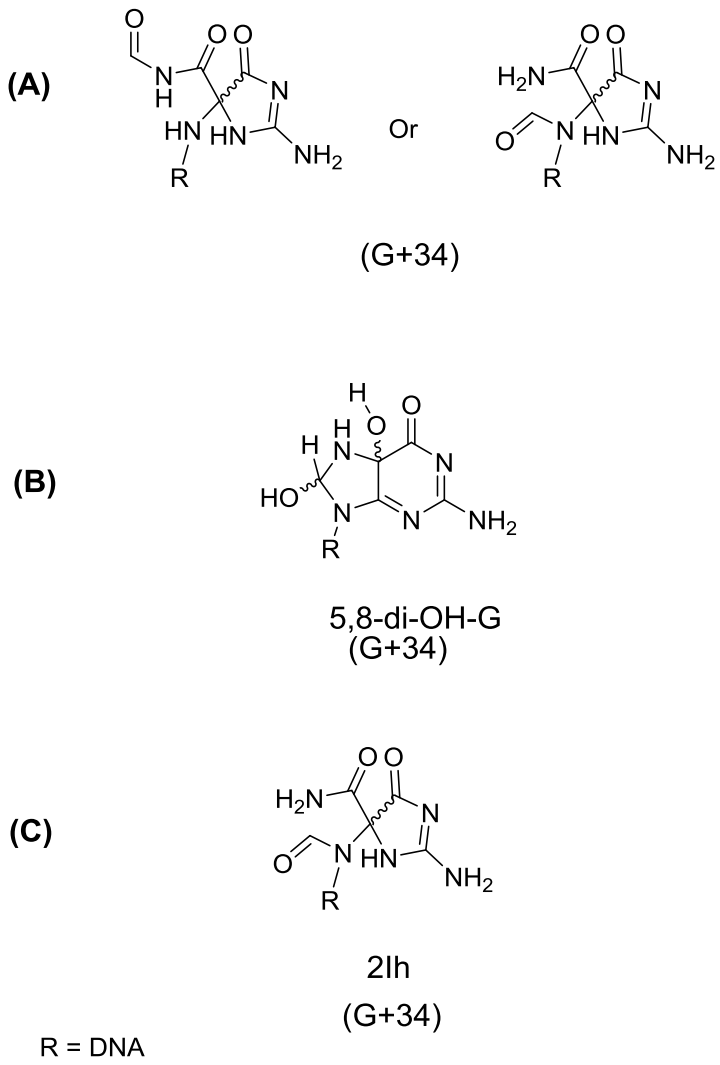


**Figure 1.6.** Proposed structure of the (G+34) product by different groups. (A) Burrows,[71] (B) Meunier[69] and Rokita,[64] (C) Ball.[75]

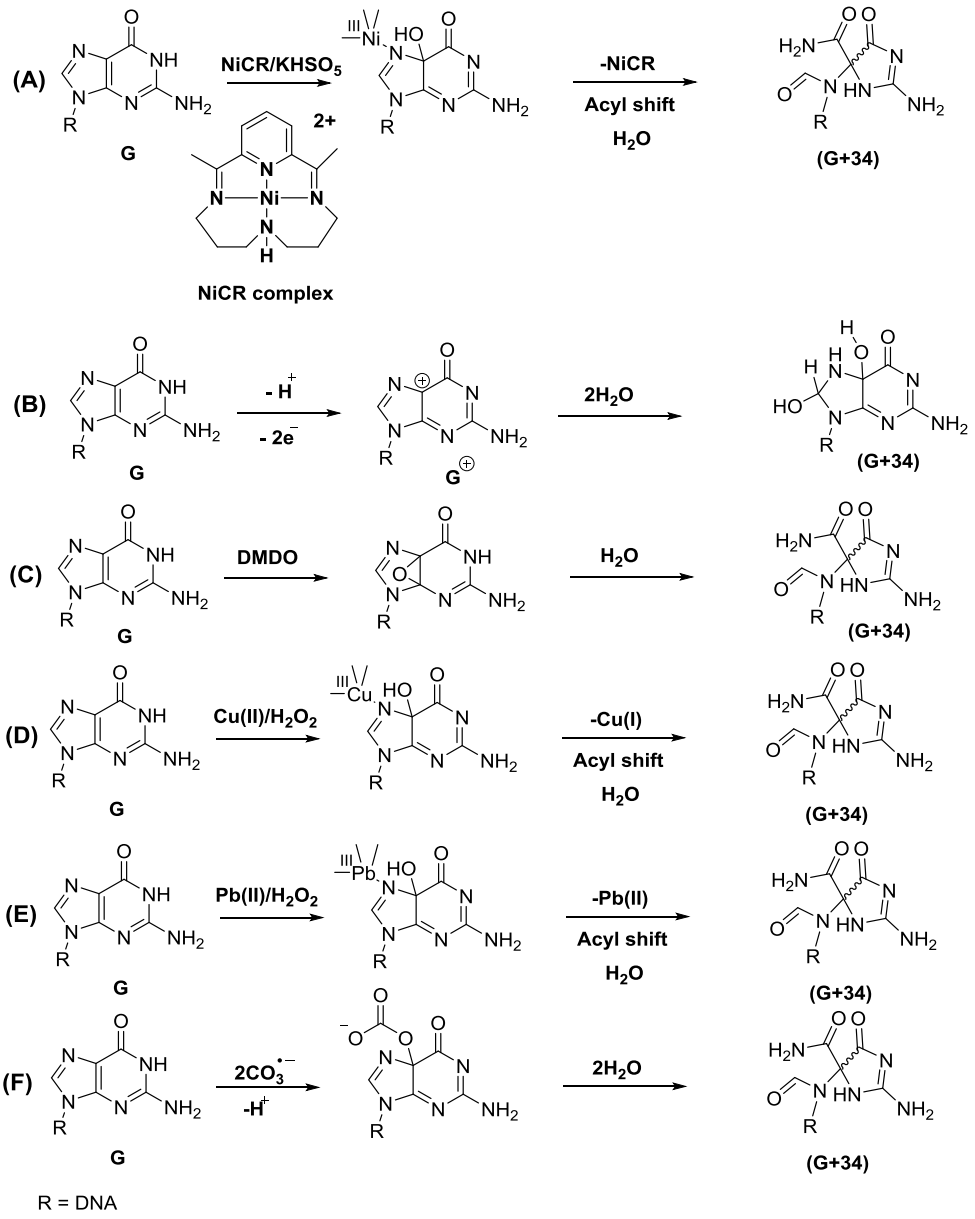


**Figure 1.7.** Proposed pathways to form (G+34) product by different groups. (A and D) Burrows,[66,67,71] (B) Meunier,[69,73] (C) Ball,[70,75] (E) Bohme,[65] (F) Shafirovich.[68]

guanine residues by Mn-TMPyP/$KHSO_5$.[69,72,73] They suggested that the high-valent Mn(V)=O species is responsible for abstraction of two electrons and one proton from guanine to give the guanine cation. The positive charge on the guanine cation has been suggested to be located on C5, and a water molecule could be trapped by the cation, and a second water molecule should be added at C8 of guanine leading to formation of the M+34 oxidation product (Figure 1.7B). Karlin and Rokita reported that M+34 is the result of the oxidation by a dicopper-phenolate complex via a putative hydroperoxo dicopper(II) transient.[64,74] They proposed this M+34 to be 5,8-di-HO-G derivative (Figure 1.6B). The Ball laboratory found that the epoxidation of G with the epoxidizing agent DMDO will form the M+34 product. They suggested that DMDO initially epoxidizes the guanine 4,5 double bond followed by acyl migration and the imidazole ring will be hydrolytically cleaved to give 2Ih (Figure 1.7C). They confirmed the proposed 2Ih structure as an alternative structure to the isomeric 5,8-dihydroxy-7,8-dihydroguanine (Figure 1.6C). They also confirmed the structure of 2Ih as a (5-carboxamido-5-formamido-2-iminohydantoin) via mass spectrometry and complementary (HSQC and HMBC) NMR methods.[70,75]

In 2011, a second study from our laboratory found 2Ih as the only oxidation product by using a NiCR/$KHSO_5$ under specific conditions. It was proposed that the nickle complex coordinates with N7 of G to facilitate formation of 2Ih via addition of the sulfate radical followed by hydrolysis to yield the 5-HO-G intermediate leading to 2Ih (Figure 1.7A).[67] Another study in our laboratory identified 2Ih as a major oxidation product of G by exposure to Cu(II)/$H_2O_2$. It was proposed that a strong oxidizing species, a high-valent Cu(III)-oxo complex, could be coordinated with N7 of

G and effect oxygen atom transfer to the C5 of G leading to 2Ih (Figure 1.7D).[66] The Bohme laboratory found G could be oxidized by Pb(II)/$H_2O_2$ to yield 2Ih as a major product. It was proposed that Pb(II) can bind to N7 of guanine and then interact with $H_2O_2$, analogous to that proposed for oxidation in the presence of NiCR and $KHSO_5$ to make 2Ih (Figure 1.7E).[65] Also, the Shafirovich laboratory found that the oxidation of G by $CO_3^{\cdot -}$ will lead to formation of 2Ih. This study was the first time that 2Ih could be formed without a metal required for oxidation. They proposed the addition of $CO_3^{\cdot -}$ radical to C5 of G followed by hydrolysis with $H_2O$ to yield 2Ih (Figure 1.7F).[68] In the metal-catalyzed studies, the transition metal plays a significant role in 2Ih formation, while $CO_3^{\cdot -}$ demonstrated that the transition metal is not necessary to form 2Ih. According to this, we postulated that other oxidants such as $HO^{\bullet}$ could form 2Ih, as will be discussed in Chapter 2.

**DNA damage repair pathways**

The first step in the repair system is preventing further damage through inactivation of ROS such as $H_2O_2$ by catalase and $O_2^{\bullet -}$ by superoxide dismutase.[76,77] Several antioxidant molecules such as vitamin C, vitamin E, β-carotene, urate, glutathione, and bilirubin are able to quench free radicals.[78] After DNA damage by ROS, various pathways are required for repair. The formation of oxidized lesions in DNA is one of the critical reasons for the induction of carcinogenesis, cellular aging, and neurodegenerative disease.[79] Fortunately, cells are able to efficiently repair DNA damage via several different mechanisms as a means to maintain genomic integrity.[80] Conversely, genomic instability caused by defective DNA damage repair is a hallmark

of cancer, reinforcing the fact that DNA must be repaired properly in order to maintain cellular homeostasis (Figure 1.8).

A cell can respond to DNA damage using a number of mechanisms to repair the DNA, based on the type and extent of damage. Repair of damage involves activation of repair enzymes, numerous phosphorylation events, and recruitment of proteins to the site of damage.[80,81] The damaged lesions are processed by an intricate network of DNA repair pathways. Base excision repair (BER), for example, removes oxidative lesions and other DNA modifications by removing the erroneous base and recruiting polymerase and ligase proteins to repair the damaged strand.[82] DNA adducts that distort the helix are resolved by nucleotide excision repair (NER). During this process, which involves greater than 30 proteins, the damaged nucleotide and the flanking sequence are removed and the complementary strand is used as a template for repair.[83-85] Also, lesions can be bypassed by a system termed translesion synthesis (TLS), which is not an ideal method of repair as it induces error, and thus can be mutagenic.[86] Nucleotide misincorporation generates base-base mismatches during DNA synthesis at variable rates. To prevent such deleterious effects and safeguard the integrity of the genome, cells possess a DNA mismatch repair (MMR) pathway. MMR corrects DNA mismatches generated during DNA replication, thereby preventing mutations from becoming permanent in dividing cells.[87] The various other forms of DNA damage are processed through different pathways. DNA damage causing double-strand breaks can activate DNA damage repair or apoptotic pathways. If the damage can be reversed, the mechanism of repair is classically either nonhomologous end joining (NHEJ) or homologous recombination (HR).[88] Transcription-coupled repair (TCR) is a

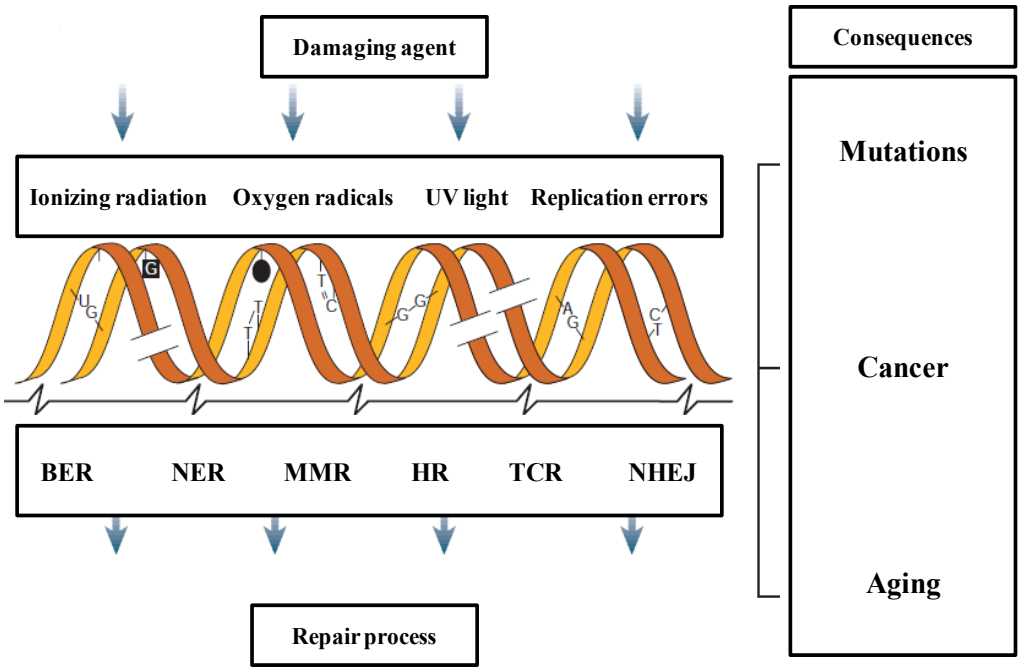


**Figure 1.8.** Various types of DNA-damaging agents, subsequent lesions, repair pathways and potential outcomes in the absence of repair.

subpathway of nucleotide excision repair (NER) that acts specifically on lesions in the transcribed strand of expressed genes.[89] Global genome nucleotide excision repair (GG-NER) is another subpathway of nucleotide excision repair (NER) that detects and eliminates bulky damages in the entire genome, including untranscribed regions and silent chromatin.[90] BER is the most common main pathway involved in excision and repair of oxidative base damage (Figure 1.9).[91,92]

Several repair mechanisms are effective for repair and prevention of DNA damage, but even under normal cellular conditions some levels of damage can persist in DNA. Furthermore, any genetic peculiarities in these repair pathways may lead to predisposition to suffering more severe effects from ROS damage.[93] Indeed, some genetic diseases such as familial colorectal cancers have been linked to increased levels of oxidative damage due to inherited mutations in DNA repair genes.[93] When ROS are excessively produced or insufficiently removed or degraded the protective defense mechanism of a cell can become overwhelmed, a condition known as extreme oxidative stress, and can result in mutagenesis and carcinogenesis or functional disruption and ultimately cell death.[94]

**Mutagenic potential of G oxidation products**

While the OG lesion is only slightly mutagenic with < 10% of OG lesions resulting in G•C → T•A transversion, the hyperoxidized products are more mutagenic than OG. The polymerase studies of Iz, Z, Gh, and Sp demonstrate that these lesions produce the same G•C → T•A transversion mutation observed for OG, but at significantly greater levels. They have also been shown to produce significant levels of

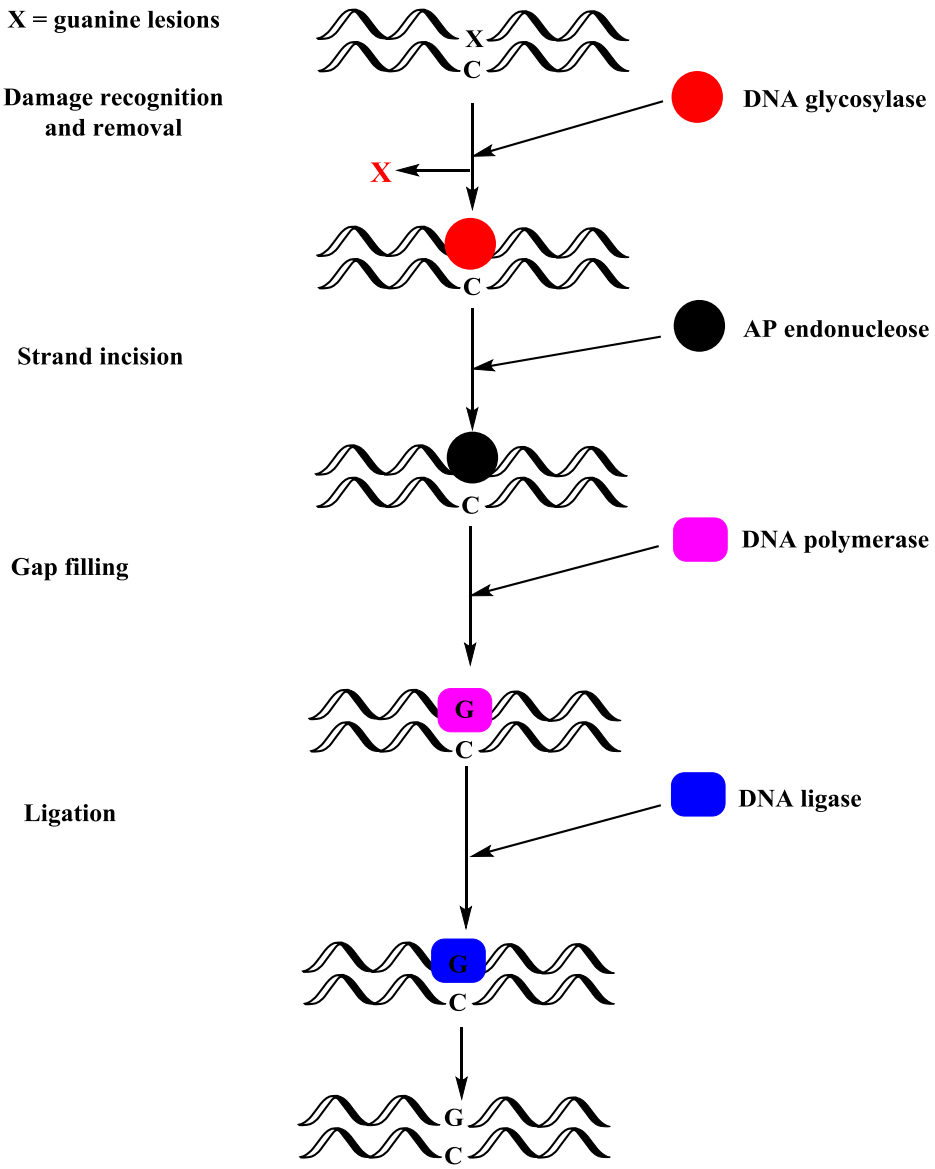


**Figure 1.9.** Base excision repair pathway.

G•C → C•G transversion mutations.[47,95-97]

In *E. coli*, MutM (Fpg) can remove OG from an OG•C base pair, while MutY removes A from an OG•A base pair.[98,99] In mammalian cells, OGG1 acts on the OG•C lesion and MUTYH acts on the A in an OG•A base pair.[100] *In vitro* studies on DNA BER pathway have shown that certain enzymes are able to recognize and remove the hyperoxidized lesions Z, Sp, and Gh. [101-105]

The mutagenic potential of 2Ih, and the ability of glycosylases to recognize and remove it were unknown when we began this study. The study in Chapter 3 is the first to highlight the mutagenic potential and the ability of BER glycosylases to repair 2Ih.

**References**


1. Valko, M., Morris, H., and Cronin, M. T. D. (2005) Metals, toxicity and oxidative stress, *Curr. Med. Chem. 12*, 1161-1208.

2. Wiseman, H., and Halliwell, B. (1996) Damage to DNA by reactive oxygen and nitrogen species: role in inflammatory disease and progression to cancer, *Biochem. J. 313*, 17-29.

3. Cooke, J. P., and Losordo, D. W. (2002) Nitric oxide and angiogenesis, *Circulation 105*, 2133-2135.

4. Liu, Y., Fiskum, G., and Schubert, D. (2002) Generation of reactive oxygen species by the mitochondrial electron transport chain, *J. Neurochem. 80*, 780-787.

5. Petrosillo, G., Ruggiero, F., Pistolese, M., and Paradies, G. (2001) Reactive oxygen species generated from the mitochondrial electron transport chain induce cytochrome c dissociation from beef-heart submitochondrial particles via cardiolipin peroxidation. Possible role in the apoptosis, *FEBS Lett. 509*, 435-438.

6. Cooke, M. S., Evans, M. D., Dizdaroglu, M., and Lunec, J. (2003) Oxidative DNA damage: mechanisms, mutation, and disease, *FASEB 17*, 1195-1214.

7. Klein, C., Frenkel, K., and Costa, M. (1991) The role of oxidative processes in metal carcinogenesis, *Chem. Res. Toxicol. 4*, 592-604.

8. Cadet, J., Douki, T., Pouget, J., Ravanat, J., and Sauvaigo, S. (2001) Effects of UV and visible radiations on cellular DNA, *Curr. Probl. Dermatol. 29*, 62-73.

9. Shigenaga, M., Gimeno, C., and Ames, B. (1989) Urinary 8-hydroxy-2'-deoxyguanosine as a biological marker of in vivo oxidative DNA damage, *Proc. Natl. Acad. Sci. U. S. A. 86*, 9697-9701.

10. Cook, J., Gius, D., Wink, D., Krishna, M., Russo, A., and Mitchell, J. (2004) Oxidative stress, redox, and the tumor microenvironment, *Semin. Radiat. Oncol. 14*, 259-266.

11. Nackerdien, Z., Olinski, R., and Dizdaroglu, M. (1992) DNA base damage in chromatin of gamma-irradiated cultured human cells, *Free Radic. Res. Commun. 16*, 259-273.

12. Cadet, J., Delatour, T., Douki, T., Gasparutto, D., Pouget, J., Ravanat, J., and Sauvaigo, S. (1999) Hydroxyl radicals and DNA base damage, *Mutat. Res. 424*, 9-21.

13. Toyokuni, S., Okamoto, K., Yodoi, J., and Hiai, H. (1995) Persistent oxidative stress in cancer, *FEBS Lett. 358*, 1-3.

14. Shirley, R., Ord, E., and Work, L. (2014) Oxidative stress and the use of antioxidants in stroke, *Antioxidants 3*, 472.

15. Xing, S., Shen, D., Chen, C., Wang, J., and Yu, Z. (2014) Early induction of oxidative stress in a mouse model of Alzheimer's disease with heme oxygenase activity, *Mol. Med. Rep. 10*, 599-604.

16. Christen, Y. (2000) Oxidative stress and Alzheimer's disease, *Am. J. Clin. Nutr. 71*, 621s-629s.

17. Aoshiba, K., Zhou, F., Tsuji, T., and Nagai, A. (2012) DNA damage as a molecular link in the pathogenesis of COPD in smokers, *Eur. Respir. J. 39*, 1368-1376.

18. Aukrust, P., Luna, L., Ueland, T., Johansen, R., Muller, F., Froland, S., Seeberg, E., and Bjoras, M. (2005) Impaired base excision repair and accumulation of oxidative base lesions in CD4+ T cells of HIV-infected patients, *Blood 105*, 4730-4735.

19. Day, B., and Lewis, W. (2004) Oxidative stress in NRTI-induced toxicity: evidence from clinical experience and experiments in vitro and in vivo, *Cardiovasc. Toxicol. 4*, 207-216.

20. Ishii, T., Yasuda, K., Akatsuka, A., Hino, O., Hartman, P., and Ishii, N. (2005) A mutation in the SDHC gene of complex II increases oxidative stress, resulting in apoptosis and tumorigenesis, *Cancer Res. 65*, 203-209.

21. Steenken, S., and Jovanovic, S. V. (1997) How easily oxidizable is DNA? One-electron reduction potentials of adenosine and guanosine radicals in aqueous solution, *J. Am. Chem. Soc. 119*, 617-618.

22. Neeley, W. L., and Essigmann, J. M. (2006) Mechanisms of formation, genotoxicity, and mutation of guanine oxidation products, *Chem. Res. Toxicol. 19*, 491-505.

23. Cadet, J., Berger, M., Douki, T., and Ravanat, J. (1997) Oxidative damage to DNA: formation, measurement, and biological significance, *Rev. Physiol. Biochem. Pharmacol. 131*, 1-87.

24. Burrows, C. J., and Muller, J. G. (1998) Oxidative nucleobase modifications leading to strand scission, *Chem. Rev. 98*, 1109-1152.

25. Cadet, J., Douki, T., Gasparutto, D., and Ravanat, J.-L. (2003) Oxidative

damage to DNA: formation, measurement and biochemical features, *Mutat. Res. 531*, 5-23.

26. Gimisis, T., and Cismas, C. (2006) Isolation, characterization and independent synthesis of guanine oxidation products, *Eur. J. Org. Chem.*, 1351-1378.

27. Steenken, S. (1992) Electron-transfer-induced acidity/basicity and reactivity changes of purine and pyrimidine bases. Consequences of redox processes for DNA base pairs, *Free. Radic. Res. Commun. 16*, 349-379.

28. Reynisson, J., and Steenken, S. (2002) DNA-base radicals. Their base pairing abilities as calculated by DFT, *Phys. Chem. Phys. Chem. 4*, 5346-5352.

29. Close, D. (2013) Calculated pK(a)'s of the DNA base radical ions, *J. Phys. Chem. A. 117*, 473-480.

30. Shafirovich, V., Dourandin, A., Huang, W., and Geacintov, N. (2001) The carbonate radical is a site-selective oxidizing agent of guanine in double-stranded oligonucleotides, *J. Biol. Chem. 276*, 24621-24626.

31. Close, D., Nelson, W., and Bernhard, W. (2013) DNA damage by the direct effect of ionizing radiation: products produced by two sequential one-electron oxidations, *J. Phys. Chem. A. 117*, 12608-12615.

32. Cai, Z., and Sevilla, M. (2003) Electron and hole transfer from DNA base radicals to oxidized products of guanine in DNA, *Radiat. Res. 159*, 411-419.

33. Douki, T., Martini, R., Ravanat, J.-L., Turesky, R. J., and Cadet, J. (1997) Measurement of 2,6-diamino-4-hydroxy-5-formamidopyrimidine and 8-oxo-7,8-dihydroguanine in isolated DNA exposed to gamma radiation in aqueous solution, *Carcinogenesis 18*, 2385-2391.

34. Kino, K., and Sugiyama, H. (2005) UVR-induced G-C to C-G transversions from oxidative DNA damage, *Mutat. Res. 571*, 33-42.

35. Cadet, J., Berger, M., Buchko, G. W., Joshi, P. C., Raoul, S., and Ravanat, J.-L. (1994) 2,2-Diamino-4-[(3,5-di-acetyl-2-deoxy-β-d-erythro-pentofuranosyl) amino]-5-(2H)-oxazolone: a novel and predominant radical oxidation product of 3′,5′-di-acetyl-2′-deoxyguanosine, *J. Am. Chem. Soc. 116*, 7403-7404.

36. Kupan, A., Saulière, A., Broussy, S., Seguy, C., Pratviel, G., and Meunier, B. (2006) Guanine oxidation by electron transfer: one- versus two-electron oxidation mechanism, *Chem. Bio. Chem. 7*, 125-133.

37. Raoul, S., Berger, M., Buchko, G. W., Joshi, P. C., Morin, B., Weinfeld, M., and Cadet, J. J. (1996) Novel oxidation products of deoxyguanosine:oxazolone and

imidazolone nucleosides, *Chem. Soc., Perkin Trans. 2*, 371-381.

38. Doddridge, Z. A., Cullis, P. M., Jones, G. D. D., and Malone, M. E. (1998) 7,8-Dihydro-8-oxo-2‘-deoxyguanosine residues in DNA are radiation damage “hot” spots in the direct γ radiation damage pathway, *J. Am. Chem. Soc. 120*, 10998-10999.

39. Asami, S., Hirano, T., Yamaguchi, R., Tomioka, Y., Itoh, H., and Kasai, H. (1996) Increase of a type of oxidative DNA damage, 8-hydroxyguanine, and its repair activity in human leukocytes by cigarette smoking, *Cancer Res. 56*, 2546-2549.

40. Chen, Q., Marsh, J., Ames, B., and Mossman, B. (1996) Detection of 8-oxo-2'-deoxyguanosine, a marker of oxidative DNA damage, in culture medium from human mesothelial cells exposed to crocidolite asbestos, *Carcinogenesis 17*, 2525-2527.

41. Kasprzak, K. S. (2002) Oxidative DNA and protein damage in metal-induced toxicity and carcinogenesis1,3, *Free Rad. Biol. Med. 32*, 958-967.

42. Steenken, S., Jovanovic, S. V., Bietti, M., and Bernhard, K. (2000) The trap depth (in DNA) of 8-oxo-7,8-dihydro-2'deoxyguanosine as derived from electron-transfer equilibria in aqueous solution, *J. Am. Chem. Soc. 122*, 2373-2374.

43. Luo, W., Muller, J. G., Rachlin, E. M., and Burrows, C. J. (2000) Characterization of spiroiminodihydantoin as a product of one-electron oxidation of 8-oxo-7,8-dihydroguanosine, *Org. Lett. 2*, 613-616.

44. Niles, J. C., Wishnok, J. S., and Tannenbaum, S. R. (2004) Spiroiminodihydantoin and guanidinohydantoin are the dominant products of 8-oxoguanosine oxidation at low fluxes of peroxynitrite: mechanistic studies with $^{18}O$, *Chem. Res. Toxicol. 17*, 1510-1519.

45. Slade, P. G., Hailer, M. K., Martin, B. D., and Sugden, K. D. (2005) Guanine-specific oxidation of double-stranded DNA by Cr(VI) and ascorbic acid forms spiroiminodihydantoin and 8-oxo-2'-deoxyguanosine, *Chem. Res. Toxicol. 18*, 1140-1149.

46. Luo, W., Muller, J. G., Rachlin, E. M., and Burrows, C. J. (2001) Characterization of hydantoin products from one-electron oxidation of 8-oxo-7,8-dihydroguanosine in a nucleoside model, *Chem. Res. Toxicol. 14*, 927-938.

47. Duarte, V., Muller, J. G., and Burrows, C. J. (1999) Insertion of dGMP and dAMP during *in vitro* DNA synthesis opposite an oxidized form of 7,8-dihydro-8-oxoguanine, *Nucleic Acids Res. 27*, 496-502.

48. Ravanat, J., and Cadet, J. (1995) Reaction of singlet oxygen with 2'-deoxyguanosine and DNA. Isolation and characterization of the main oxidation products, *Chem. Res. Toxicol. 8*, 379-388.

49. Kang, P., and Foote, C. (2002) Photosensitized oxidation of $^{13}C$,$^{15}N$-labeled imidazole derivatives, *J. Am. Chem. Soc. 124*, 9629-9638.

50. Sheu, C., Kang, P., Khan, S., and Foote, C. (2002) Low-temperature photosensitized oxidation of a guanosine derivative and formation of an imidazole ring-opened product, *J Am Chem Soc 124*, 3905-3913.

51. McCallum, J., Kuniyoshi, C., and Foote, C. (2004) Characterization of 5-hydroxy-8-oxo-7,8-dihydroguanosine in the photosensitized oxidation of 8-oxo-7,8-dihydroguanosine and its rearrangement to spiroiminodihydantoin, *J. Am. Chem. Soc. 126*, 16777-16782.

52. Ravanat, J.-L., Di Mascio, P., Martinez, G. R., Medeiros, M. H. G., and Cadet, J. (2000) Singlet oxygen induces oxidation of cellular DNA, *J. Biol. Chem. 275*, 40601-40604.

53. Duarte, V., Gasparutto, D., Yamaguchi, L. F., Ravanat, J.-L., Martinez, G. R., Medeiros, M. H. G., Di Mascio, P., and Cadet, J. (2000) Oxaluric acid as the major product of singlet oxygen-mediated oxidation of 8-Oxo-7,8-dihydroguanine in DNA, *J. Am. Chem. Soc. 122*, 12622-12628.

54. Bergtold, D. S., Simic, M. G., Alessio, H., and Cutler, R. G. (1988) Urine Biomarkers for Oxidative DNA Damage, In *Oxygen Radicals in Biology and Medicine* (Simic, M., Taylor, K., Ward, J., and von Sonntag, C., Eds.), pp 483-489, Springer US.

55. Liochev, S. (1999) The mechanism of "Fenton-like" reactions and their importance for biological systems. A biologist's view, *Met. Ions Biol. Syst. 36*, 1-39.

56. Douki, T., Onuki, J., Medeiros, M., Bechara, E., Cadet, J., and Di, M. P. (1998) Hydroxyl radicals are involved in the oxidation of isolated and cellular DNA bases by 5-aminolevulinic acid, *FEBS Lett. 428*, 93-96.

57. Neta, P., Huie, R. E., and Ross, A. B. (1988) Rate constants for reactions of inorganic radicals in aqueous solution, *Adv. Inorg. Chem. 33*, 69-138.

58. Breen, A. P., and Murphy, J. A. (1995) Reactions of oxyl radicals with DNA, *Free Radic. Biol. Med. 18*, 1033-1077.

59. O' Neill, P. (1983) Pulse radiolytic study of the interaction of thiols and ascorbate with OH adducts of dGMP and dG: implications for DNA repair

processes, *Radiat. Res. 96*, 198-210.

60. Candeias, L. P., and Steenken, S. (1989) Structure and acid-base properties of one-electron-oxidized deoxyguanosine, guanosine, and 1-methylguanosine, *J. Am. Chem. Soc. 111*, 1094-1099.

61. Candeias, L. P., and Steenken, S. (2000) Reaction of $HO^{\cdot}$ with guanine derivatives in aqueous solution: formation of two different redox-active OH-adduct radicals and their unimolecular transformation reactions. Properties of G(-H), *Chem. Eur. J. 6*, 475-484.

62. Steenken, S. (1989) Purine bases, nucleosides, and nucleotides: aqueous solution redox chemistry and transformation reactions of their radical cations and e- and OH adducts, *Chem. Rev. 89*, 503-520.

63. Cadet, J., Douki, T., and Ravanat, J.-L. (2008) Oxidatively generated damage to the guanine moiety of DNA: mechanistic aspect and formation in cells, *Acc. Chem. Res. 41*, 1075-1083.

64. Li, L., Murthy, N. N., Telser, J., Zakharov, L. N., Yap, G. P., Rheingold, A. L., Karlin, K. D., and Rokita, S. E. (2006) Targeted guanine oxidation by a dinuclear copper(II) complex at single stranded/double stranded DNA junctions, *Inorg. Chem. 45*, 7144-7159.

65. Banu, L., Blagojevic, V., and Bohme, D. K. (2012) Lead(II)-catalyzed oxidation of guanine in solution studied with electrospray ionization mass spectrometry, *J. Phys. Chem. B. 116*, 11791–11797.

66. Fleming, A. M., Muller, J. G., Ji, I., and Burrows, C. J. (2011) Characterization of 2'-deoxyguanosine oxidation products observed in the Fenton-like system Cu(II)/$H_2O_2$/reductant in nucleoside and oligodeoxynucleotide contexts, *Org. Biomol. Chem. 9*, 3338-3348.

67. Ghude, P., Schallenberger, M. A., Fleming, A. M., Muller, J. G., and Burrows, C. J. (2011) Comparison of transition metal-mediated oxidation reactions of guanine in nucleoside and single-stranded oligodeoxynucleotide contexts, *Inorg. Chem. Acta 369*, 240-246.

68. Rokhlenko, Y., Geacintov, N. E., and Shafirovich, V. (2012) Lifetimes and reaction pathways of guanine radical cations and neutral guanine radicals in an oligonucleotide in aqueous solutions, *J. Am. Chem. Soc. 134*, 4955-4962.

69. Vialas, C., Claparols, C., Pratviel, G., and Meunier, B. (2000) Guanine oxidation in double-stranded DNA by Mn-TMPyP/$KHSO_5$: 5,8-dihydroxy-7,8-dihydroguanine residue as a key precursor of imidazolone and parabanic acid derivatives, *J. Am. Chem. Soc. 122*, 2157-2167.

70. Ye, W., Sangaiah, R., Degen, D. E., Gold, A., Jayaraj, K., Koshlap, K. M., Boysen, G., Williams, J., Tomer, K. B., Mocanu, V., Dicheva, N., Parker, C. E., Schaaper, R. M., and Ball, L. M. (2009) Iminohydantoin lesion induced in DNA by peracids and other epoxidizing oxidants, *J. Am. Chem. Soc. 131*, 6114-6123.

71. Luo, W. (2001) Characterization of purine oxidation products from one-electron oxidants, superoxide and singlet oxygen, Ph.D. Dissertation, University of Utah, Salt Lake City, UT.

72. Pratviel, G., and Meunier, B. (2006) Guanine oxidation: one- and two-electron reactions, *Chem. Eur. J. 12*, 6018-6030.

73. Tomaszewska, A., Mourgues, S., Guga, P., Nawrot, B., and Pratviel, G. (2012) A single nuclease-resistant linkage in DNA as a versatile tool for the characterization of DNA lesions: application to the guanine oxidative lesion "G+34" generated by metalloporphyrin/$KHSO_5$ reagent, *Chem. Res. Toxicol. 25*, 2505-2512.

74. Li, L., Karlin, K. D., and Rokita, S. E. (2005) Changing selectivity of DNA oxidation from deoxyribose to guanine by ligand design and a new binuclear copper complex, *J. Am. Chem. Soc. 127*, 520-521.

75. Ye, W., Sangaiah, R., Degen, D. E., Gold, A., Jayaraj, K., Koshlap, K. M., Boysen, G., Williams, J., Tomer, K. B., and Ball, L. M. (2006) A 2-iminohydantoin from the oxidation of guanine, *Chem. Res. Toxicol. 19*, 506-510.

76. Gaetani, G., Ferraris, A., Rolfo, M., Mangerini, R., Arena, S., and Kirkman, H. (1996) Predominant role of catalase in the disposal of hydrogen peroxide within human erythrocytes, *Blood 87*, 1595-1599.

77. Fridovich, I. (1995) Superoxide radical and superoxide dismutases, *Annu. Rev. Biochem. 64*, 97-112.

78. Guaiquil, V., Vera, J., and Golde, D. (2001) Mechanism of vitamin C inhibition of cell death induced by oxidative stress in glutathione-depleted HL-60 cells, *J. Biol. Chem. 276*, 40955-40961.

79. Beckman, K. B., and Ames, B. N. (1997) Oxidative decay of DNA, *J. Biol. Chem. 272*, 19633-19636.

80. Slupphaug, G., Kavli, B., and Krokan, H. (2003) The interacting pathways for prevention and repair of oxidative DNA damage, *Mutat. Res. 531*, 231-251.

81. Su, T. (2006) Cellular responses to DNA damage: one signal, multiple choices, *Annu. Rev. Genet. 40*, 187-208.

82. Jackson, S., and Bartek, J. (2009) The DNA-damage response in human biology and disease, *Nature 461*, 1071-1078.

83. Rechkunova, N., and Lavrik, O. (2010) Nucleotide excision repair in higher eukaryotes: mechanism of primary damage recognition in global genome repair, *Subcell Biochem. 50*, 251-277.

84. Wang, W. (2007) Emergence of a DNA-damage response network consisting of Fanconi anaemia and BRCA proteins, *Nat Rev Genet 8*, 735-748.

85. Zhang, Y., Rohde, L., and Wu, H. (2009) Involvement of nucleotide excision and mismatch repair mechanisms in double strand break repair, *Curr. Genomics 10*, 250-258.

86. Hoeijmakers, J. (2009) DNA damage, aging, and cancer, *N. Engl. J. Med. 361*, 1475-1485.

87. Li, G.-M. (2008) Mechanisms and functions of DNA mismatch repair, *Cell Res. 18*, 85-98.

88. McCabe, K., Olson, S., and Moses, R. (2009) DNA interstrand crosslink repair in mammalian cells, *J. Cell. Physiol. 220*, 569-573.

89. Ganesan, A., Spivak, G., and Hanawalt, P. (2012) Transcription-coupled DNA repair in prokaryotes, *Prog. Mol. Biol. Transl. Sci. 110*, 25-40.

90. Petruseva, I. O., Evdokimov, A. N., and Lavrik, O. I. (2014) Molecular mechanism of global genome nucleotide excision repair, *Acta Naturae 6*, 23-34.

91. David, S., and Williams, S. (1998) Chemistry of glycosylases and endonucleases involved in base-excision repair, *Chem. Rev. 98*, 1221-1262.

92. Seeberg, E., Eide, L., and Bjoras, M. (1995) The base excision repair pathway, *Trends Biochem. Sci. 20*, 391-397.

93. Al-Tassan, N., Chmiel, N., Maynard, J., Fleming, N., Livingston, A., Williams, G., Hodges, A., Davies, D., David, S., Sampson, J., and Cheadle, J. (2002) Inherited variants of MYH associated with somatic G:C-->T:A mutations in colorectal tumors, *Nat. Genet. 30*, 227-232.

94. Ames, B. N., Sheigenaga, M. K., and Hagen, T. M. (1993) Oxidants, antioxidants, and the degenerative diseases of aging, *Proct. Natl. Acad. Sci. USA. 90*, 7915-7922.

95. Henderson, P. T., Delaney, J. C., Muller, J. G., Neeley, W. L., Tannenbaum, S. R., Burrows, C. J., and Essigmann, J. M. (2003) The hydantoin lesions formed

from oxidation of 7,8-dihydro-8-oxoguanine are potent sources of replication errors *in vivo*, *Biochemistry 42*, 9257−9262.

96. Henderson, P. T., Delaney, J. C., Gu, F., Tannenbaum, S. R., and Essigmann, J. M. (2002) Oxidation of 7,8-dihydro-8-oxoguanine affords lesions that are potent sources of replication errors *in vivo*, *Biochemistry 41*, 914-921.

97. Sugden, K. D., Campo, C. K., and Martin, B. D. (2001) Direct oxidation of guanine and 7,8-dihydro-8-oxoguanine in DNA by a high-valent chromium complex: a possible mechanism for chromate genotoxicity, *Chem. Res. Toxicol. 14*, 1315-1322.

98. David, S. S., O'Shea, V. L., and Kundu, S. (2007) Base-excision repair of oxidative DNA damage, *Nature 447*, 941-950.

99. Michaels, M. L., Tchou, J., Grollman, A. P., and Miller, J. H. (1992) A repair system for 8-oxo-7,8-dihydrodeoxyguanine, *Biochemistry 31*, 10964-10968.

100. Barnes, D. E., and Lindahl, T. (2004) Repair and genetic consequences of endogenous DNA base damage in mammalian cells, *Annu. Rev. Genet. 38*, 445-476.

101. Hazra, T. K., Izumi, T., Boldogh, I., Imhoff, B., Kow, Y. W., Jaruga, P., Dizdaroglu, M., and Mitra, S. (2002) Identification and characterization of a human DNA glycosylase for repair of modified bases in oxidatively damaged DNA, *Proc. Natl. Acad. Sci. 99*, 3523-3528.

102. Leipold, M. D., Muller, J. G., Burrows, C. J., and David, S. S. (2000) Removal of hydantoin products of 8-oxoguanine oxidation by the *Escherichia coli* DNA repair enzyme, FPG, *Biochemistry 39*, 14984-14992.

103. Duarte, V., Gasparutto, D., Jaquinod, M., Ravanat, J., and Cadet, J. (2001) Repair and mutagenic potential of oxaluric acid, a major product of singlet oxygen-mediated oxidation of 8-oxo-7,8-dihydroguanine, *Chem. Res. Toxicol. 14*, 46-53.

104. Leipold, M., Workman, H., Muller, J., Burrows, C., and David, S. (2003) Recognition and removal of oxidized guanines in duplex DNA by the base excision repair enzymes hOGG1, yOGG1, and yOGG2, *Biochemistry 42*, 11373-11381.

105. Hailer, M. K., Slade, P. G., Martin, B. D., Rosenquist, T. A., and Sugden, K. D. (2005) Recognition of the oxidized lesions spiroiminodihydantoin and guanidinohydantoin in DNA by the mammalian base excision repair glycosylases NEIL1 and NEIL2, *DNA Repair 4*, 41-50.

# CHAPTER 2

# 5-CARBOXAMIDO-5-FORMAMIDO-2-IMINOHYDANTOIN, IN ADDITION TO 8-OXO-7,8-DIHYDROGUANINE, IS THE MAJOR PRODUCT OF THE IRON-FENTON OR X-RAY RADIATION-INDUCED OXIDATION OF GUANINE UNDER AEROBIC REDUCING CONDITIONS IN NUCLEOSIDE AND DNA CONTEXTS*

## Introduction

Cellular redox status is a dynamic state that balances reducing and oxidizing species, and if the balance is thrown off in the cell, dysfunction arises.[1] Hydroxyl radical ($HO^{\bullet}$) is a powerful oxidizing species found in the cell that causes redox imbalance due to its particularly high redox potential (2.31 V vs. NHE, pH 7; $HO^{\bullet}(+H^{+})/H_2O$).[2] The Fenton reaction can generate $HO^{\bullet}$ when a redox-active metal effects cleavage of $H_2O_2$, a metabolic product that can easily diffuse within and between cells.[3] Hydrogen peroxide is weakly reactive, but Fe(II) species have the capability to

---

*Partially reproduced with permission from "Alshykhly, O. R., Fleming, A. M., and Burrows, C. J. (2015) 5-Carboxamido-5-formamido-2-iminohydantoin, in addition to 8-oxo-7,8-dihydroguanine, is the major product of the iron-Fenton or X-ray radiation-induced oxidation of guanine under aerobic reducing conditions in nucleoside and DNA contexts, *J. Org. Chem. 80*, 6996-7007."

generate $HO^{\bullet}$ plus Fe(III) via the Fenton reaction (Reaction 1). Furthermore, reducing agents in the cell such as ascorbate (Asc) allows this reaction to be catalytic.[4,5] The unfortunate events that occurred at Fukushima, Japan in 2011 remind us of the dangers of radiation. The high-energy photons released upon radioactive decay are capable of yielding $HO^{\bullet}$ via radiolysis of water (Reactions 3 and 4). The iron-Fenton reaction and X-ray radiolysis of water represent two methods for generating hydroxyl radicals that can oxidize biomolecules,[6,7] such as DNA.[4,5,8] DNA damage plays a significant role in aging and the development of diseases such as cancer.[8]

$$H_2O_2 + Fe(II) \rightarrow Fe(III) + HO^{\bullet} + HO^{-} \quad (1)$$

$$2Fe(III) + Asc \rightarrow 2Fe(II) + \text{dehydroascorbate} \quad (2)$$

$$H_2O + \text{X-ray} \rightarrow e^{-}_{aq} + H_2O^{+\bullet} \quad (3)$$

$$H_2O^{+\bullet} \rightarrow H^{+} + HO^{\bullet} \quad (4)$$

DNA is vulnerable to oxidative insults from $HO^{\bullet}$, and the damage is particularly deleterious because it can cause mutations that are heritable to daughter cells. Notable progress has been made in the discovery of DNA oxidation pathways resulting from radical oxygen species, such as $HO^{\bullet}$, during the last three decades.[4,9-12] In DNA, the most susceptible site is 2'-deoxyguanosine (dG) because the guanine heterocycle has the lowest redox potential (1.29 V vs. NHE, pH 7; $dG^{\bullet}(-H^{+})/dG$) among the four DNA bases.[13] The nucleoside dG is a prime target for direct oxidation or electron transfer-mediated oxidation that can result from $HO^{\bullet}$.[12-14] Oxidative damage to dG yields

products that result from the initial product-forming reaction occurring at one of three sites that include the C5 or C8 positions of the heterocyclic ring, or the 2-deoxyribose unit (Figure 2.1). These products are identified by their characteristic mass changes from the parent nucleoside dG (M).

Sugar oxidation is a commonly observed reaction pathway of dG damage resulting from $HO^{\bullet}$.[11] Products observed along this pathway include 5',8-cyclo-2'-deoxyguanosine (cyclo-dG) diastereomers derived from $H^{\bullet}$ atom abstraction at C5`, and release of the free base guanine (Gua) after hydroxylation of C1`. Direct base release in DNA leads to strand breaks due to the lability of the abasic site so formed.[15-17] The yields of these products are highly dependent on the reaction conditions.[11] Base oxidation of dG leads to two lesions resulting from reaction at C8 that include 8-oxo-7,8-dihydro-2'-deoxyguanosine (dOG), observed in high yield under aerobic oxidizing conditions, or the ring-opened product 2,6-diamino-4-hydroxy-5-formamidopyrimidine-2'-deoxyribonucleoside (Fapy-dG) observed under anaerobic reducing conditions.[18-20] Both dOG and Fapy-dG are mutagenic compounds found *in vivo*,[9] while dOG is a biomarker monitored to assay the extent of cellular oxidative stress.[21] Because dOG has a lower redox potential (0.74 V vs. NHE, pH 7; $dOG^{\bullet}(-H^{+})$/dOG) than dG,[13] it is readily oxidized to the hydantoin lesions spiroiminodihydantoin-2'-deoxyribonucleoside (dSp) and 5-guanidinohydantoin-2'-deoxynucleoside (dGh).[8,22-25] These lesions have been observed *in vivo* and are also highly mutagentic.[26-29] Additionally, oxidation of dG leads to products resulting from initial chemistry occurring at the C5 position of the purine. 2,5-Diaminoimidazolone-2'-deoxyribonucleoside (dIz) and its hydrolysis product 2,2,4-triamino-2*H*-oxazol-5-one-2'-deoxyribonucleoside (dZ) are four-electron oxidation

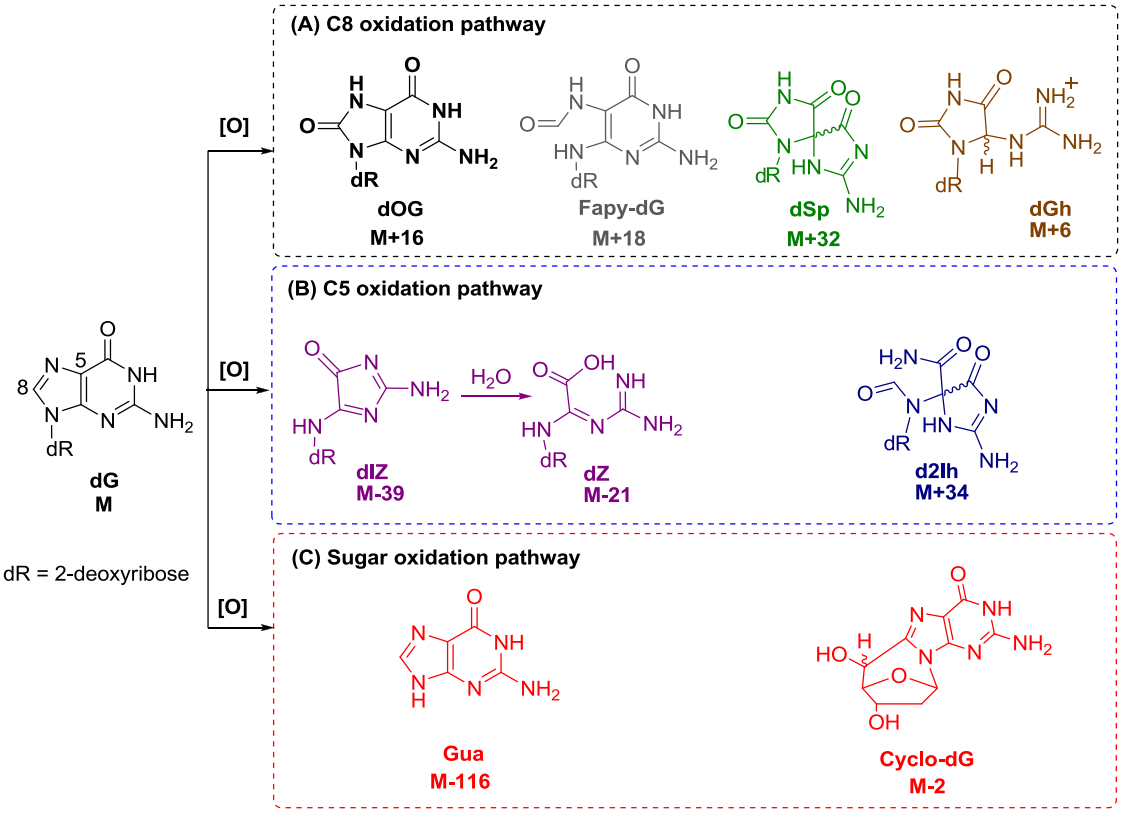


**Figure 2.1.** Structures of dG and its oxidation products. Box A: products observed from initial $HO^{\bullet}$ attack at C8; box B: products observed from initial $HO^{\bullet}$ attack at C5; box C: guanine-derived products observed when oxidation occurs on 2-deoxyribose.

products resulting from exposure to $HO^{\bullet}$ or one-electron oxidants under aerobic conditions.[8,20,30-34] Recent studies concerning dG oxidation have identified 5-carboxamido-5-formamido-2-iminohydantion-2'-deoxyribonucleoside (d2Ih) as a product from Fenton chemistry with copper or lead, activation of $KHSO_5$ with nickel or manganese complexes, $CO_3^{\bullet-}$ oxidations, and the epoxidizing agent dimethyldioxirane.[8,12,35-40] These observations have led us to the question of whether d2Ih is in fact a major product from dG oxidation by hydroxyl radical generated either from the Fe(II)-mediated Fenton reaction or by X-ray radiolysis of water.

Toward this goal, we investigated the formation and yield of dG-oxidation products from the Fe(II)-mediated Fenton reaction or X-ray radiolysis of water while monitoring the effect of reductant concentration (ascorbate or *N*-acetylcysteine) on their yields in the nucleoside, short oligodeoxynucleotide, and λ-DNA contexts. These studies identify d2Ih to be a major guanine oxidation product observed when reactions were conducted with low millimolar amounts of reductant, conditions that mimic the presence of reducing agents such as glutathione, urate, or ascorbate in cells.[41] The results of these studies lead to proposed mechanisms for the formation of d2Ih and to discussions of its possible biological significance.

**Experimental** (representative data are provided in Appendix A)

*Fenton reaction*

A 200-μL solution of dG (3.0 mM, 0.6 μmoles, 0.16 mg) in a buffer (75.0 mM $NaP_i$, pH 7.4) was mixed with Fe(II)/EDTA (0.10 mM, 0.02 μmoles, 0.008 mg), $H_2O_2$ (10.0 mM, 2 μmoles, 0.5 mg), and Asc or NAC (2.0 mM, 0.40 μmoles, 0.03 mg) and

incubated for 1 h at 22 ºC. The Fe(II)/EDTA complex was freshly made by mixing $Fe(NH_4)_2(SO_4)_2$ and $Na_2EDTA$ in a 1:2 ratio 30 min prior to reaction. The Fe(II)/EDTA complex was removed by column chromatography using ion-exchange resin prior to HPLC analysis following the method outlined below.

*X-ray irradiation*

A 200-μL solution containing dG (3.0 mM, 0.6 μmoles, 0.16 mg) in buffer (75.0 mM $NaP_i$, pH 7.4) and Asc or NAC (2.0 mM, 0.40 μmoles, 0.03 mg) was irradiated with an X-ray RS 2000 biological research irradiator source at 22 $^oC$ for variable times (1 - 30 min). The dose rate was 25 Gy/min.[42] This solution was analyzed by the method outlined below.

*Oligodeoxynucleotide and DNA oxidations*

Single-stranded ODN1 or double-stranded ODN2 were oxidized in 20 mM $NaP_i$ (pH 7.4) with 100 mM NaCl at 37 °C. Iron-Fenton oxidations were conducted in a 200-μL reaction volume with ODN (100 μM, 0.01 μmoles, 0.05 mg) to which was added Fe(II)EDTA (0.10 mM, 0.02 μmoles, 0.008 mg), Asc (2.0 mM, 0.40 μmoles, 0.03 mg), and $H_2O_2$ (1.0 mM, 0.2 μmoles, 0.05 mg), the reaction was allowed to proceed for 30 min. The stock solutions of Fe(II)EDTA, Asc, and $H_2O_2$ were all freshly prepared. To irradiate the ODNs, they were placed in the same buffer system as the iron-Fenton reaction followed by X-ray irradiation with a dose rate 25 Gy/min for 30 min (total dose = 750 Gy). For the λ-DNA oxidations, everything was identical to the ODN oxidations with the exception that the λ-DNA (1 μM, 0.1 nmoles, 0.03 mg) was different.

*Hydrolysis of oxidized oligodeoxynucleotides and λ-DNA*

The oxidized ODN or λ-DNA samples were hydrolyzed to the free bases for HPLC analysis. The hydrolysis was performed on the oxidized and lyophilized DNA by adding 50 μL of 70% HF in pyridine for 30 min at 37 ºC. After the reaction, the excess HF was neutralized by adding 1 mL $ddH_2O$ and 80 mg of $CaCO_3$ to the sample. The insoluble salts were removed by centrifugation, and the supernatant was then lyophilized to dryness. Next, the lyophilized samples were dissolved in $ddH_2O$ and submitted to LC-MS and HPLC analysis as a described for the nucleoside studies below.

*Product identification*

Product identification was initially achieved by UPLC-$ESI^+$-MS (100 X 2.1 mm, 1.7 μm) and UPLC-ESI+-MS with a Hypercarb column (100 X 2.1 mm, 5μm). Then, each compound was HPLC purified for further structural analysis. The following masses were observed: Gua *m/z* $[M+H]^+$ calcd 152.1, found 152.1. OG *m/z* $[M+H]^+$ calcd 168.1, found 168.1. dOG *m/z* $[M+H]^+$ calcd 284.2, found 284.1. *R* and *S* diastereomers of cyclo-dG *m/z* $[M+H]^+$ calcd 266.2, found 266.1. Gh *m/z* $[M+H]^+$ calcd 158.1, found 158.1. (*S*)-d2Ih and (*R*)-d2Ih[43] *m/z* $[M+H]^+$ calcd 302.3, found 302.1; $ESI^+$-MS/MS *m/z* $[M+H]^+$ lit.[39] 186, 158, and 141, found 186, 158, and 141. HRMS (ESI-TOF) *m/z* $[M+Na]^+$ calcd for $C_5H_7N_5O_3Na$ 208.0447, found 208.0449. The HRMS value was obtained on the free base 2Ih, due to the nucleoside's instability toward acid. dGh *m/z* $[M+H]^+$ calcd 274.3, found 274.1; HRMS (ESI-TOF) *m/z* $[M+Na]^+$ calcd for $C_9H_{15}N_5O_5Na$ 296.0971, found 296.0980. (*S*)-dSp and (*R*)-dSp[44] *m/z* $[M+H]^+$ calcd

300.2, found 300.1; HRMS (ESI-TOF) *m/z* $[M+Na]^+$ calcd for $C_{10}H_{13}N_5O_6Na$ 322.0764, found 322.0761; $ESI^+$-MS/MS *m/z* $[M+H]^+$ lit.[22] 184, 156, 141, 113, 99, and 86, found 184, 156, 141, 113, 99, and 86. dZ *m/z* $[M+H]^+$ calcd 247.2, found 247.1; HRMS (ESI-TOF) *m/z* $[M+Na]^+$ calcd for $C_8H_{14}N_4O_5Na$ 269.0862, found 269.0870; $ESI^+$-MS/MS *m/z* $[M+H]^+$ lit.[45] 247, 203, and 131, found 247, 203, and 131. The dGh diastereomers were characterized by NMR,[46] dZ was characterized by NMR,[30] cyclo-dG was characterized by X-ray crystallography,[47] the dSp diastereomers have been characterized by X-ray crystallography[48] and NMR,[49] and the diastereomers of d2Ih have been previously characterized by NMR.[39]

*Product quantification*

The oxidation products from the Fe(II)-Fenton reaction or X-ray irradiation reaction were quantified by C18 reversed-phase HPLC and Hypercarb HPLC. First, the reaction mixture was injected on a reversed-phase HPLC (250 X 4.6 mm, 5 μm) to quantify Gua, OG, dOG, and cyclo-dG. The void volume from this run was collected, lyophilized to dryness, and then dissolved with the Hypercarb column starting mobile phase (0.1% acetic acid). Next, the reconstituted void volume was injected on a Hypercarb column (150 X 4.6 mm, 5 μm) to quantify Gh, (*R*)-d2Ih, (*S*)-d2Ih,[43] dGh, (*R*)-dSp, (*S*)-dSp,[44] and dZ. Product peaks were quantified by their absorbance intensity at 240 nm followed by normalization of these intensities by each compound's extinction coefficient at 240 nm. The values for $\varepsilon_{240\ nm}$ ($ddH_2O$) are: dG 14,080, dOG 14,300, cyclo-dG 14,080, Gua 14,080, OG 14,300,[17] dSp 3,280,[22] d2Ih 2,290,[50] dGh and Gh 2410,[51] and dZ 1780.[45] All values are in units of L. $mol^{-1}$. $cm^{-1}$.

## Results and discussion

*Identification of oxidation products*

The nucleoside dG (3 mM) was initially chosen for oxidation by the Fe(II)-mediated Fenton reaction or X-ray irradiation in the absence or presence of ascorbate (Asc) or *N*-acetylcysteine (NAC). All reactions were conducted with 75 mM $NaP_i$ buffer (pH 7.4) at 22 $^{o}$C. The reaction mixtures were initially analyzed by reversed-phase UPLC-$ESI^+$-MS. This allowed for identification of guanine (Gua), 8-oxo-7,8-dihydroguanine (OG), dOG and the diastereomers of cyclo-dG after comparison to known standards. The void volume from this analysis was collected and reanalyzed with a Hypercarb column equipped with an $ESI^+$-MS detector.

This method allowed for detection of Gh, dZ, and the diastereomers of d2Ih, dGh, and dSp. Because dIz hydrolyzes to dZ during preparation of the void volume, only dZ was quantified. The Hypercarb column allowed for the separation of the diastereomer products of d2Ih and dSp for which the absolute configurations for the peaks had been previously determined.[8,43,52] The two diastereomers of dGh are interconvertible and were not quantified individually.[46] Further support for the identification of d2Ih, dSp, and dZ was obtained by $ESI^+$-MS/MS fragmentation of the free bases from in-source fragmentation of the *N*-glycosidic bond of the parent nucleosides. The product dGh failed to be fragmented. The HRMS was conducted to further support the identification of each product.

*Product quantification from the Fe(II)-mediated Fenton reaction*

Product quantification was conducted with reversed-phase HPLC while monitoring peak elution at 240 nm; product peak areas were integrated and normalized based on the product's extinction coefficient at 240 nm ($\varepsilon_{240nm}$).[8] The extinction coefficient for d2Ih has not been experimentally determined, and due to its instability toward *N*-glycosidic bond hydrolysis was not determined in these studies.[52] However, our previous time-dependent density functional theory studies on the UV-vis and ECD properties for dSp and d2Ih allow us to use these previous results to determine the relative difference in extinction coefficient between these two compounds at the wavelength monitored.[43,52] These calculations determined the $\varepsilon_{240nm}$ for d2Ih to be ~30% less than that of dSp; therefore, the $\varepsilon_{240nm}$ value used to quantify d2Ih was calculated to be 2,290 L. $mol^{-1}$. $cm^{-1}$.[50]

The Fenton reaction was initially conducted with the Fe(II)/EDTA catalyst and 10 mM $H_2O_2$ under aerobic conditions to give 5% conversion to product. We elected to conduct reactions to a low overall yield so that primary oxidation products could be identified and compared. In this reaction, the highest absolute product yields observed were dZ (1.5%) and Gua (1.5%) in equal amounts, with the mass balance completed by low yields of cyclo-dG (0.2%), dOG (0.4%), dSp (0.9%) and d2Ih (0.4%), (Table 2.1).

In the next reaction, the same conditions were applied with the addition of 2 mM Asc that led to a 7-fold increase in product formation, as well as a significant change in product distribution. In the presence of Asc, the major dG product detected was d2Ih (13.4%) with lower yields of the 2-deoxyribose oxidation products cyclo-dG (0.9%) and Gua (7.1%), as well as OG (0.6%), and Gh (<0.1%); also, lower yields of dZ (2.7%),

**Table 2.1.** Absolute yields for oxidation of dG by the Fe(II)-mediated Fenton reaction.[a]

| Absolute Yield (%) / Product | Fe(II)/$H_2O_2$/ +Asc/+$O_2$ | Fe(II)/$H_2O_2$/ -Asc/+$O_2$ | Fe(II)/$H_2O_2$/ +Asc/low $O_2$[b] | Fe(II)/$H_2O_2$/ -Asc/low $O_2$[b] |
|---|---|---|---|---|
| **dOG** | 4.9 | 0.4 | 6.6 | 1.9 |
| **dSp** | 5.6 | 0.9 | 6.0 | 3.9 |
| **dGh** | 0.4 | <0.1 | 2.0 | 1.9 |
| **Gh** | <0.1 | <0.1 | N.D. | N.D. |
| **dZ** | 2.7 | 1.5 | N.D. | N.D. |
| **d2Ih** | 13.4 | 0.4 | 3.3 | 1.0 |
| **cyclo-dG** | 0.9 | 0.2 | 1.9 | 1.2 |
| **Gua** | 7.1 | 1.5 | N.D. | N.D. |
| **OG** | 0.6 | <0.1 | N.D. | N.D. |
| **dG** conversion% | 35.8 | 5.0 | 20.0 | 9.9 |

[a] Reported values represent the average of three trials that have errors of ~8% of the value.

N.D. = not detected. [b]Low $O_2$ represents a partial reduction in the $O_2$ concentration by bubbling argon into the sample for 10 min which was later found to be insufficient to completely remove $O_2$.

dOG (4.9%), dSp (5.6%), and dGh (0.4%) were observed (Table 2.1).

These Asc-dependent studies revealed two key observations: (1) the reaction yields dramatically increased (7-fold) with Asc because the Fe(II)/EDTA complex can redox cycle in the presence of reductant (Reaction 2); and (2) d2Ih was the major product observed when Asc was present. Because dSp and dGh are further oxidation products of the precursor dOG,[22] the yield of d2Ih (13.4%) was compared to the combined yields of dOG, dSp, and dGh (10.9%), and it was found that the yield of d2Ih was higher than that of dOG and its products.

In the next set of reactions, the role of $O_2$ was studied. First, a reaction was conducted with dG in the presence of Fe(II)/EDTA and $H_2O_2$ under low $O_2$ conditions achieved by bubbling argon into the sample for 10 min that was insufficient to completely remove $O_2$. In this reaction, the overall conversion of dG to product was 10%, and the major product observed was dSp (3.9%), with low yields of dOG (1.9%), dGh (1.9%), d2Ih (1.0%) and the sugar oxidation product cyclo-dG (1.2%), (Table 2.1). The addition of 2 mM Asc to the low $O_2$ reaction increased the dG conversion by 2-fold (20%), and changed the product distribution, giving dOG (6.6%) and dSp (6.0%) in high yield and low yields of d2Ih (3.3%), dGh (2.0%), and cyclo-dG (1.9%), (Table 2.1). These low $O_2$ studies indicated the yield of d2Ih was at a minimum under these conditions. Additionally, the major products observed under low $O_2$ conditions were dOG and its further oxidation product dSp.

**Where is Fapy-dG?** Many literature sources point to the presence of Fapy-dG as a guanine oxidation product formed under anaerobic, reducing conditions.[53-55] In our present low $O_2$ studies, this elusive compound was not observed, even after exhaustive

searching of the LC-MS data. This led us to probe deeper into the formation of Fapy-dG, using the following conditions to make this compound from dG by the iron-Fenton reaction. First, the reaction had to be rigorously purged with argon for >30 min prior to addition of $H_2O_2$ with 2 mM Asc, and the HPLC mobile phase was changed from running buffered [20 mM $NH_4OAc$ (pH 7)] water and MeCN to unbuffered $ddH_2O$ and MeCN. These changes allowed observation of a broad hump after the void volume in the reversed-phase HPLC chromatogram with a UV-vis signature consistent with Fapy-dG ($\lambda_{max}$ = 270 and 218 nm),[53] and a defined peak that eluted after dG with a similar UV-vis profile.[53] The broad hump was consistent with literature reports because Fapy-dG exists as anomers of two different sugar configurations.[53,54] LC-$ESI^+$-MS of all these new peaks only found masses consistent with the Fapy free base, as well as a peak with mass Fapy + 18.

These observations identify that Fapy-dG is not stable to laboratory manipulation as it is for d2Ih, dOG, dSp, or dGh, and it appears to be sensitive to nucleophilic buffers in the HPLC mobile phase, e.g., $NH_4OAc$. Further test reactions that had argon bubbled through them for a few seconds up to a min before $H_2O_2$ addition did not furnish the Fapy peaks. The Fapy peaks only appeared after purging the system with argon for >30 min. To reiterate, in cases with low $O_2$ and Asc present, dOG was the major product observed, and when $O_2$ was at ambient concentrations with Asc present, the major product was d2Ih. These observations identify Fapy-dG to be very challenging to obtain; it is only observed under extreme anoxic conditions (~100% argon and ~0% $O_2$), conditions under which cells cannot survive. If Fapy-dG was formed in a cell, detection of the nucleoside would be problematic due to the hydrolytic

instability of the *N*-glycosidic bond. This later feature is in contrast to d2Ih, dOG, dSp, and dGh that are all at least stable enough to allow their characterization under very mild conditions (22 °C in water buffered at pH 7).

Finally, Fapy-dG has a low redox potential (1.1 V vs. NHE),[54] rendering it subject to further oxidation; however, this is also the case for dOG (0.7 V vs. NHE),[13] that has an even lower redox potential, and we detect and quantify this intermediate species and its further oxidation products dSp and dGh. Thus, the conditions outlined do not simply over oxidize Fapy-dG causing its loss. We conclude that Fapy-dG is not a major contributor to the product distribution of guanosine oxidation by hydroxyl radical under cellularly relevant conditions.

*Reducing agent-dependent studies for the iron-mediated Fenton reaction*

In cells, two main small-molecule reductants are found in high concentrations, ascorbate and glutathione, found at concentrations of 0.8 – 3 mM and 1 – 10 mM, respectively.[41] Knowing that d2Ih yields increase when Asc was present during the Fe(II)-mediated Fenton oxidation of dG (Table 2.1), we then studied the role of increasing reductant concentrations on the relative yields of the products. In addition, the nature of the reductant was studied, in which we chose *N*-acetylcysteine (NAC) as a model for glutathione. Note that protection of the amine group of cysteine with an acetyl group prevents amine adduct formation with dG oxidation intermediates.[56,57]

Titration of reductant Asc from 0 - 5 mM into the Fe(II)-mediated Fenton reaction oxidation of dG provided the following trends in the relative product distributions (Figure 2.2A): (1) As the Asc concentration increased, the reaction yield

increased, supporting the role of Asc in allowing the iron catalyst to redox cycle between Fe(II) and Fe(III) and thereby increasing the production of $HO^{\bullet}$ (Reactions 1 and 2). (2) The amount of 2-deoxyribose oxidation decreased (~10%) as the concentration of reductant Asc increased. These observations negate the involvement of Asc reductant in sugar oxidation, and it is likely that Asc inhibits this pathway. (3) The relative yields of dOG, dSp, and dGh slightly increased (~6%) with more Asc. (4) The Asc concentration was shown to be critical in the relative yields of the C5 products, dZ and d2Ih. When Asc was not present, the major C5-oxidation product was dZ (also a major product overall); however, as Asc was titrated into the reaction, the relative yield of dZ decreased and d2Ih increased until it was the major product of the reaction at Asc > 2 mM (Figure 2.2A). Within the range of physiological Asc concentrations (1 - 3 mM),[41] d2Ih was always the major oxidation product detected (Figure 2.2A).

Moreover, when the study was conducted with variable NAC concentrations, the same trends as the Asc were observed (Figure 2.2B). Again, the most notable observation is that d2Ih was the major oxidation product observed in reactions conducted with > 2 mM thiol concentrations (Figure 2.2B), even when considering a comparison of d2Ih (~37%) with the combined yields of dOG, dSp, and dGh (~30%), (Figures 2.2A and B) with 2 mM reductant.

*$H_2O_2$ concentration-dependent studies for the iron-mediated Fenton reaction*

In the next set of studies, dG oxidation product distributions versus the $H_2O_2$ concentration in the range of (0 – 10 mM) was studied and monitored in the HPLC with a static amount of either (0.8 mM Asc or 3 mM NAC) as a reductant in the reaction,

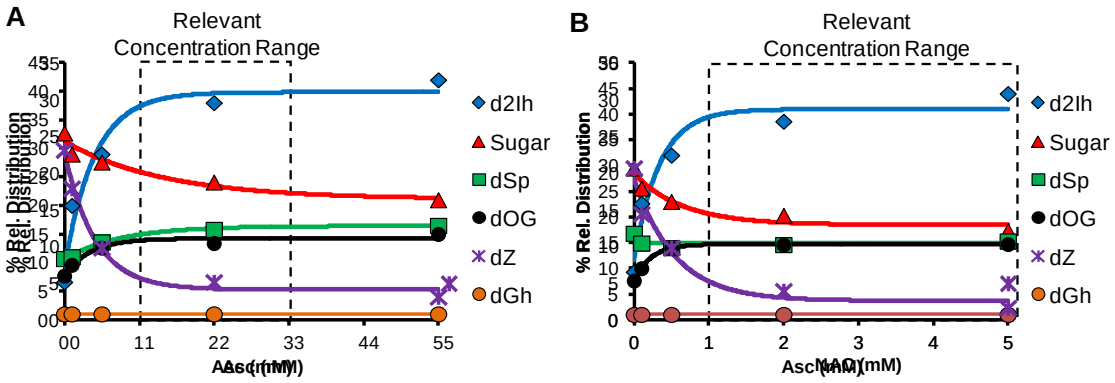


**Figure 2.2.** Effect of reductant concentration on relative product distributions observed from the Fe(II)-mediated Fenton reaction. The reactions were conducted with 3 mM dG, 10 μM Fe(II)/EDTA, 10 mM $H_2O_2$ in 75 mM $NaP_i$ buffer (pH 7.4) at 22 $^oC$ while varying the concentration of Asc (panel A) or NAC (panel B) from 0 – 5 mM. Data points represent the average of three trials with an error in each value of 3 - 10%.

(Figure 2.3A and B, respectively). Key observations from these studies include: (1) As expected, the reaction yield increased as more $H_2O_2$ was added to the reaction. (2) With increased $H_2O_2$ concentrations, the flux of $HO^{\bullet}$ increased, and the relative yield of dSp increased at the expense of dOG. This observation supports dOG as the intermediate leading to dSp.[10,12] (3) Both dZ and d2Ih increased as a function of $H_2O_2$ concentration (0 – 10 mM). Moreover, the amount of d2Ih increased 4-fold when Asc was the reductant while dZ increased 3-fold (Figure 2.3A). In the $H_2O_2$-dependent studies with NAC, d2Ih increased 13-fold while dZ increased 3-fold when $H_2O_2$ increased from 0 – 10 mM (Figure 2.3B). These studies demonstrate that the yield of d2Ih is maximal under conditions that boost formation of $HO^{\bullet}$.

*Product quantification from X-ray-mediated oxidation of dG*

Next, oxidation of dG was conducted with an X-ray source at a dose rate of 25 Gy/min for 30 min (total dose = 750 Gy). Initial studies without reductant gave a 45% conversion of dG to product. The major oxidation products observed were dZ (14.7%), dSp (10.8%) and Gua (12.4%), and in low absolute yields were d2Ih (2.9%), dOG (1.4%) and dGh (1.4%). Next, Asc (2 mM) was added to the reaction to give the following changes in the yields: (1) The absolute conversion of dG to product decreased with Asc (2.5-fold), as expected, because Asc quenches radical reactions.[58] (2) The major products were now d2Ih (6.3%), dSp (3.9%), and Gua (4.1%), with the mass balance completed by low yields of dZ (1.1%), dOG (2.5%), cyclo-dG (0.5%), and dGh (<0.1%). The most striking observation was that d2Ih was the major oxidation product when Asc was present during X-ray mediated oxidations; however, this is in contrast to

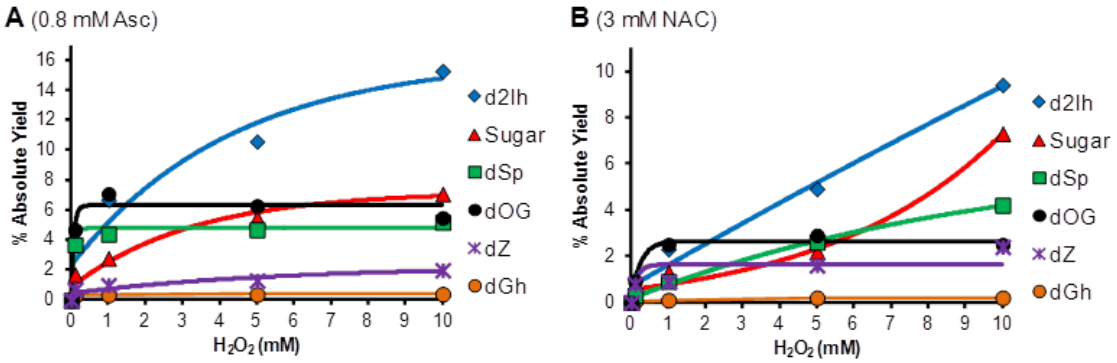


**Figure 2.3.** Effect of $H_2O_2$ concentration on the absolute product distributions from the Fe(II)-Fenton reaction. The reactions were conducted with 3 mM dG, 10 μM Fe(II)/EDTA, and with either 0.8 mM Asc (panel A) or 3 mM NAC (panel B) in 75 mM $NaP_i$ (pH 7.4) at 22 $^oC$, while varying the concentration of $H_2O_2$ from 0 – 10 mM. Data points represent the average of three trials with an error in each value of 5 - 11%.

studies without Asc where dZ was the major oxidation product quantified (Table 2.2). When considering the yield of d2Ih (6.3%) in comparison to the combined yields of dOG, dSp, and dGh (6.4%), the initial split between d2Ih and the C8 products was nearly equal with x-ray irradiation when reductant was present. Because the X-ray reactions required the reaction vessel to be open to the atmosphere, studies were not conducted under anaerobic conditions.

*Reducing agent-dependent studies for the X-ray mediated oxidations*

Reactions with and without Asc suggest a major role for reductant in the product distributions for X-ray mediated oxidations (Table 2.2). Therefore, studies were conducted with the reductants Asc or NAC titrated (0 – 5 mM) into the X-ray-mediated reaction mixture while monitoring the product yields (Figure 2.4A and B). From these studies, the following observations were made in X-ray-mediated oxidations: (1) As the reducing agent concentration increased, the reaction yield significantly decreased. (2) The relative yield of dOG increased (6-fold) as a function of reductant concentration (Figures 2.4A and B), while the yield of dSp decreased about (1.5-fold) and dGh decreased about (3-fold). This result supports the conclusion that the reductant quenched the further oxidation of dOG to the hydantoins. (3) The yields of the sugar oxidation products were not significantly changed by the increase in reductant concentration (Figure 2.4A and B). (4) The reductant had the most dramatic effect on the C5-pathway products, dZ and d2Ih. When reductant was not present, dZ was the major product and d2Ih was observed in very low yield; however, when Asc or NAC was increased to relevant concentrations, d2Ih was the major oxidation product

**Table 2.2.** Absolute yields for oxidation of dG by X-ray radiolysis of water.[a]

| Absolute Yield (%) / Product | X-ray +Asc/+$O_2$ | X-ray -Asc/+$O_2$ |
|---|---|---|
| **dOG** | 2.5 | 1.4 |
| **dSp** | 3.9 | 10.8 |
| **dGh** | 0.2 | 1.4 |
| **Gh** | <0.1 | 0.5 |
| **dZ** | 1.1 | 14.7 |
| **d2Ih** | 6.3 | 2.9 |
| **cyclo-dG** | 0.5 | 0.1 |
| **Gua** | 4.1 | 12.4 |
| **OG** | 0.2 | N.D. |
| **dG** conversion % | 18.8 | 45.3 |

[a] Reported values represent the average of three trials, and the error in each value was 4 - 10%. N.D. = not detected.

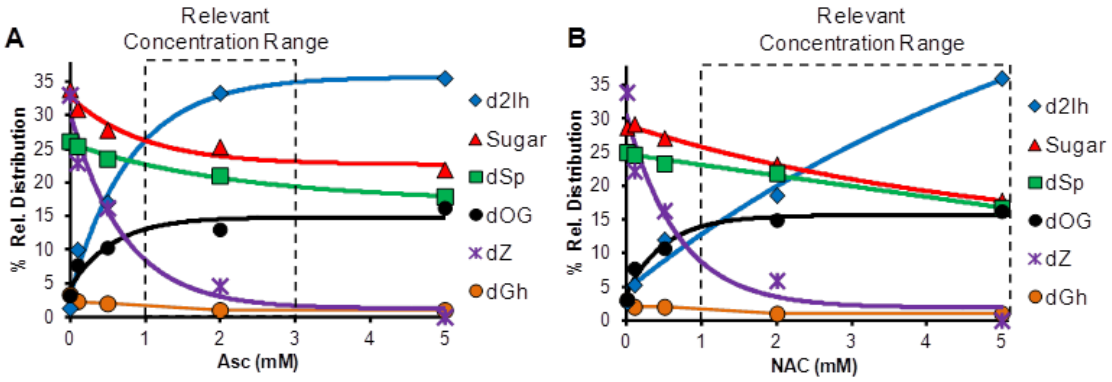


**Figure 2.4.** Effect of reductant concentration on the dG-oxidation product yield from the X-ray reaction. The reactions were conducted with 3 mM dG in 75 mM $NaP_i$ (pH 7.4) at 22 $^oC$ with a 30 min exposure to 25 Gy/min X-ray source (total dose = 750 Gy) while varying the concentration of Asc (panel A) or NAC (panel B) from 0 – 5 mM. Data points represent the average of three trials with an error in each value of 3 - 10%.

observed with very little dZ detected.

*Total X-ray dose effect on dG oxidation product distributions*

In the next set of reactions, dG was irradiated with X-rays at a rate of 25 Gy/min while varying the time (total dose) and keeping the Asc concentration static (2 mM). As the total dose of X-rays increased from 25 - 750 Gy the following trends were observed. (1) As expected, the overall reaction yield increased. (2) The yield of dSp and dGh increased at the expense of dOG with increasing X-ray dose. (3) The yield of sugar chemistry increased with increasing X-ray dose. (4) The yield of dZ and d2Ih both increased as a function of the X-ray dose, and d2Ih was always the major C5-oxidation pathway product, as well as being the major product of the reaction overall (Figure 2.5).

*Proposed pathways leading to dG oxidation products*

Under all of the conditions studied, products derived from sugar oxidation were observed. Oxidation at the 5'-carbon yields the 5'-carbon-centered radical that attacks C8 of the heterocyclic ring of dG to furnish an intermediate radical that loses another electron and proton to furnish cyclo-dG. Oxidation at the 1', 2', 3', 4' or 5' carbons also yields a carbon-centered radical that reacts with $O_2$, and many of these pathways ultimately cause cleavage of the *N*-glycosidic bond releasing Gua.[11,17] Evidence of these sugar oxidation pathways was determined by quantification of Gua release. The yield of cyclo-dG in the Fenton reaction was maximal under anaerobic reducing conditions and was observed to be at a minimum under the aerobic and non-reducing

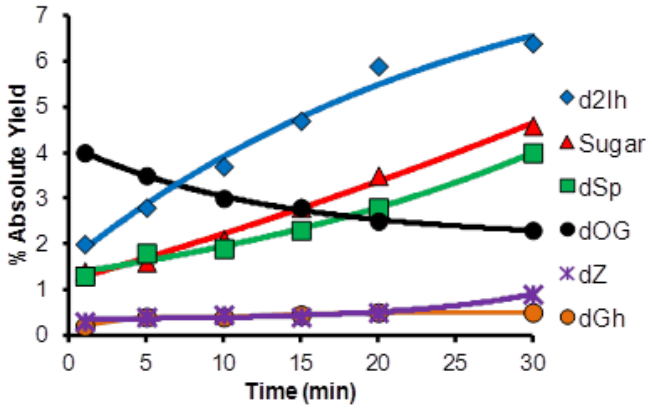


**Figure 2.5.** Effect of X-ray irradiation time on dG-oxidation product distributions. The reactions were conducted with 3 mM dG, 2 mM Asc in 75 mM $NaP_i$ (pH 7.4) at 22 $^oC$ while varying the exposure time (0 – 30 min) to an X-ray source that was delivered at a rate of 25 Gy/min. Data points represent the average of three trials with an error in each value of 3 - 10%.

conditions (Table 2.1). In contrast, base release to give Gua was observed to be maximal under aerobic and reducing conditions and not observable under anaerobic conditions (Table 2.1). These results further support the role of $O_2$ in effecting base release from 2-deoxyribose oxidation (Figure 2.6).[11] Moreover, this reaction was not sensitive to the presence of reductant. However, under anaerobic conditions the 5'-carbon radical was not trapped by $O_2$, but rather added into the heterocyclic ring at C8 leading to cyclo-dG, and again this reaction was not sensitive to the presence of reductant. Also observed in very low yield were OG and Gh, two products that are derived from further oxidation of Gua (Table 2.1). The observation of Gh and not Sp under these conditions (pH 7.4 and 22 $^{o}$C) is consistent with a previous observation that oxidations of the free base OG only give Gh and not Sp.[59] In the X-ray mediated oxidation of dG, $O_2$-dependent studies could not be conducted; therefore, only product dependence on reductant was studied. In this study, the products derived from sugar oxidation were not greatly affected by the presence of reductant (Table 2.2). Other products resulting from oxidation of the 2-deoxyribose sugar in dG were not observed by LC-ESI$^{+}$-MS.

Oxidation of dG at the C8 position yields dOG and Fapy-dG.[4,12] Mechanistically, these products form when HO$^{\bullet}$ adds at the C8 carbon to yield 8-HO-dG$^{\bullet}$ intermediate. This intermediate can be further oxidized to yield dOG, or can be reduced and ring opened to yield the Fapy-dG.[4,12] Under all conditions, dOG was observed; however, we did not detect the Fapy-dG in these studies without exhaustive removal of $O_2$. In both the Fenton reaction and the X-ray irradiation oxidations, the yield of the dOG was at a maximum when the reductant (Asc or NAC) was present,

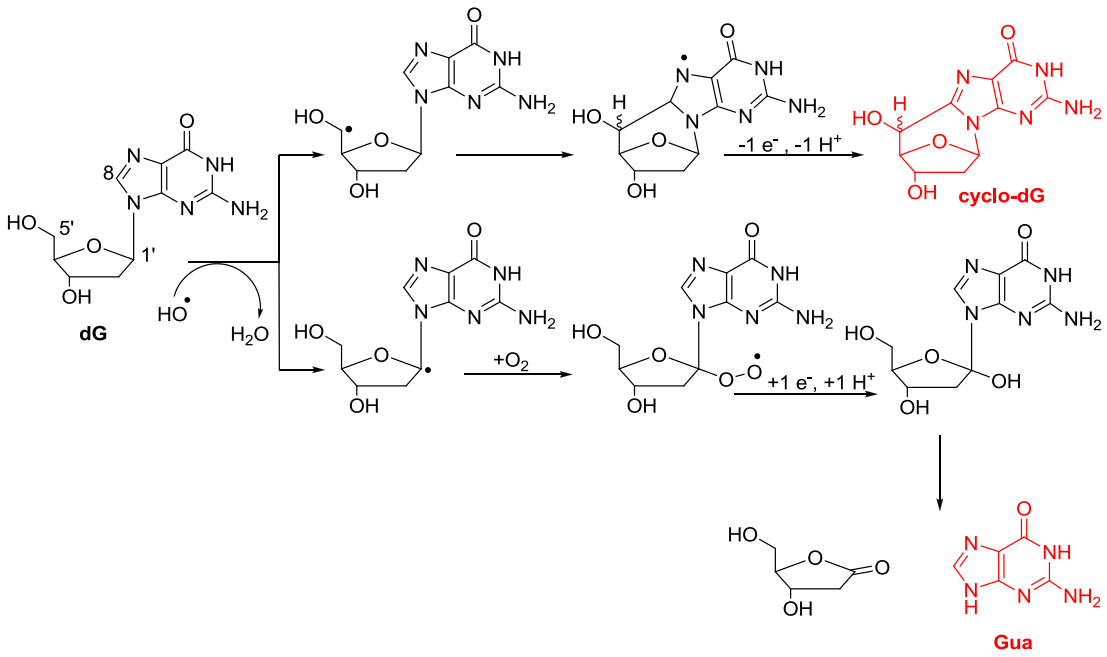


**Figure 2.6**. Proposed pathway for products derived from sugar oxidation. For the sake of brevity, only oxidation of the 1'-carbon leading to Gua is shown.

which appears to be inconsistent with previous (Figure 2.7). results;[19] however, the current studies were conducted under aerobic conditions (Tables 2.1 and 2.2), while the previous studies were conducted under anaerobic conditions.

Because dOG can undergo further oxidation to hydantoin products (Figure 2.8),[22] the presence of reductant suppresses the further oxidation and addresses why dOG concentrations are highest under oxidations conducted with reductant. In conclusion, $HO^{\bullet}$-mediated oxidation of dG via Fe(II)-Fenton chemistry and X-ray irradiation affects oxidation at C8 of dG to yield dOG as the dominant product along this pathway under low oxidant flux with $O_2$ and reductant present (Figures 2.3A, B, and 2.5). Furthermore, as the oxidant flux increases, the yield of dOG decreases due to further oxidation to dSp.

The low redox potential of dOG renders this nucleoside labile toward further oxidation to yield the hydantoins dSp and dGh (Figure 2.8).[13,22] Two-electron oxidation of dOG followed by water attack at C5 yields 5-HO-dOG that bifurcates along two pathways to either dSp or dGh.[22,46,51,52] Acyl migration to dSp dominates under conditions of higher pH (pH > 5.8) and unencumbered contexts such as nucleosides, single-stranded DNA, and G-quadruplexes, while the yield of dGh is highest at low pH (pH < 5.8) or sterically encumbered contexts such as double-stranded DNA.[22,46,51,52,60] These and previous observations explain why dSp was the major hydantoin observed in all unencumbered nucleoside studies. As previously stated, the yield of dOG was highest when reductant was present at relevant concentrations (Figures 2.2 and 2.4). In contrast, the yield of dSp was highest in the absence of reductant.

This observation supports dOG being the stable intermediate that leads to dSp,

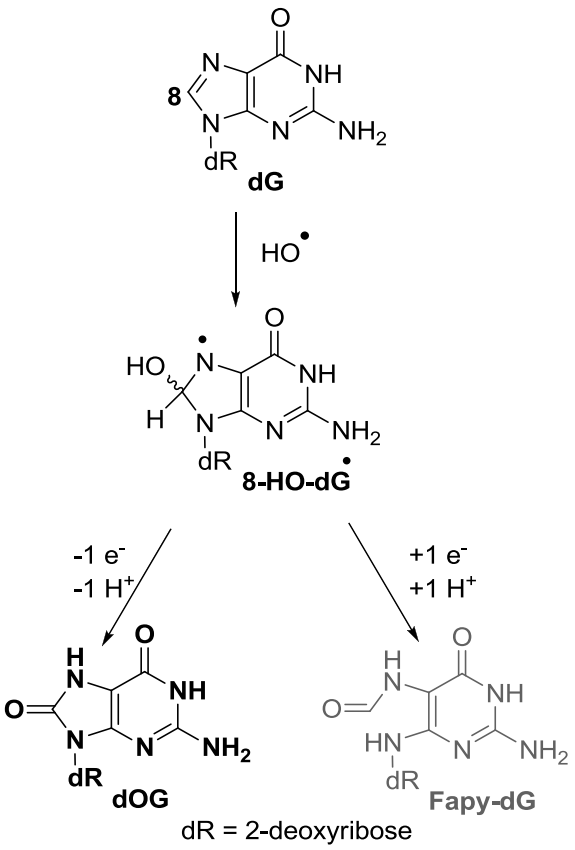


**Figure 2.7**. HO•-mediated oxidation of dG at C8 leading to dOG and Fapy-dG.

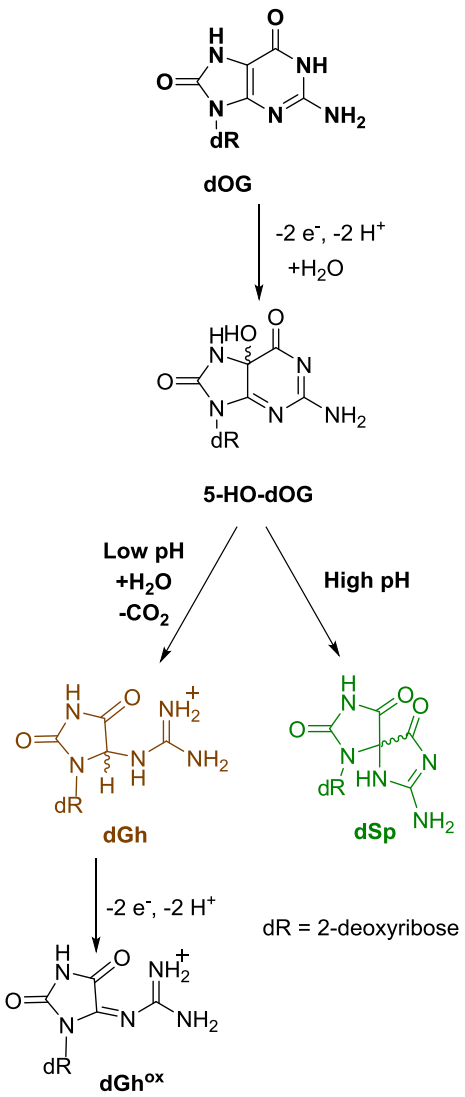


**Figure 2.8.** Proposed pathway for products derived from further oxidation of dOG.

as further oxidation of dOG to dSp was quenched with added reductant (Figures 2.2 and 2.4). These data, in which dOG was obtained in greater yield than the hydantoins under conditions with physiologically relevant reductant, further explain why the concentrations of dOG are generally much greater than hydantoins *in vivo*.[27,29]

Oxidations of dOG have detected a four-electron oxidation product dehydroguanidinohydantoin-2'-deoxyribonucleoside ($dGh^{ox}$), or formally a six-electron oxidation product of dG (Figure 2.8).[61] This compound has a short half-life and decomposes to yield oxaluric acid that further hydrolyzes to liberate oxalate and ultimately 2'-deoxyribosyl-urea.[62] These analytical conditions allow identification of oxaluric acid (unpublished result from our laboratory); however, under the current $HO^{\bullet}$-mediated oxidations, neither $dGh^{ox}$ nor oxaluric acid was detected. In these studies, low product conversion was maintained, preventing hyperoxidation of dG to $dGh^{ox}$.

The products dZ and d2Ih result from oxidation of dG followed by initial product forming chemistry occurring at C5. Previous $HO^{\bullet}$-mediated oxidations of dG detected dZ as a major product under aerobic and nonreducing conditions. The dZ was proposed to form from one-electron oxidation of dG ($dG^{\bullet+}/dG^{\bullet}(-H^{+})$, p$K_a$ ~3.9),[60] to a neutral radical that couples with $O_2/O_2^{\bullet-}$ to ultimately yield a hydroperoxy intermediate (5-HOO-dG). Next, 5-HOO-dG decomposes through a multistep process to dIz followed by hydration to dZ (Figure 2.9).[13,27,61] Additional support for the role of $O_2/O_2^{\bullet-}$ in the product defining step leading to dZ was observed in the reaction under anaerobic conditions, for which dZ was not detected (Table 2.1). Further, as the reducing agent was titrated into the reactions, the yield of dZ dramatically decreased, an observation consistent with previous report.[42]

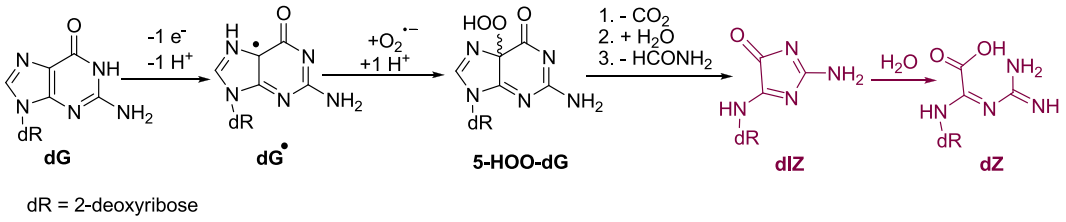


**Figure 2.9**. Proposed pathway for oxidation of dG followed by initial reaction at C5 leading to dZ.

When the oxidations were conducted under aerobic conditions with relevant concentrations of reductant (Asc or NAC), d2Ih was the major product detected (Figures 2.3, 2.4, and 2.5). In Figure 2.10 a pathway is proposed to explain this observation. Formation of $HO^{\bullet}$ via the Fe(II)-Fenton reaction or X-ray radiolysis of water (Reactions 1 – 4) affects the one-electron oxidation of dG followed by proton loss to yield $dG^{\bullet}$. Next, $dG^{\bullet}$ couples with $O_2^{\bullet-}$ to ultimately yield 5-HOO-dG[23] that is the intermediate susceptible to reduction. When reductant was not present, 5-HOO-dG decomposes to yield dIz; however, when reductant was present, the hydroperoxyl group can be reduced to the alcohol 5-HO-dG. Next, 5-HO-dG undergoes acyl migration to reduced-dSp ($dSp_{red}$) that hydrates at C8 and ring opens to yield d2Ih (Figure 2.10A). This proposed pathway provides a role for $O_2$ and reducing agent in the formation of d2Ih that was observed in the product distribution studies (Figures 2.2 and 2.4). The proposed mechanistic steps from 5-HO-dG to d2Ih were previously proposed from dG oxidations with $KHSO_5$ catalyzed by a Mn-porphyrin complex.[38,64] Because d2Ih was also observed under anaerobic conditions (Table 2.1) there must be an alternative pathway for its formation that is not $O_2$ dependent. In Figure 2.10B, such a pathway is proposed in which $HO^{\bullet}$ adds to C5 yielding $5\text{-HO-dG}^{\bullet}$ that proceeds through a second one-electron oxidation and deprotonation to yield 5-HO-dG. The acyl migration and then the hydration will yield d2Ih (Figure 2.10B). This second pathway provides a route to d2Ih under anaerobic and nonreducing reaction conditions. The alternative pathway must be a minor reaction channel to d2Ih, because added reductant significantly increases d2Ih formation supporting the pathway in Figure 2.10A.

Product formation upon oxidation of dG initially occurs on the sugar leading to

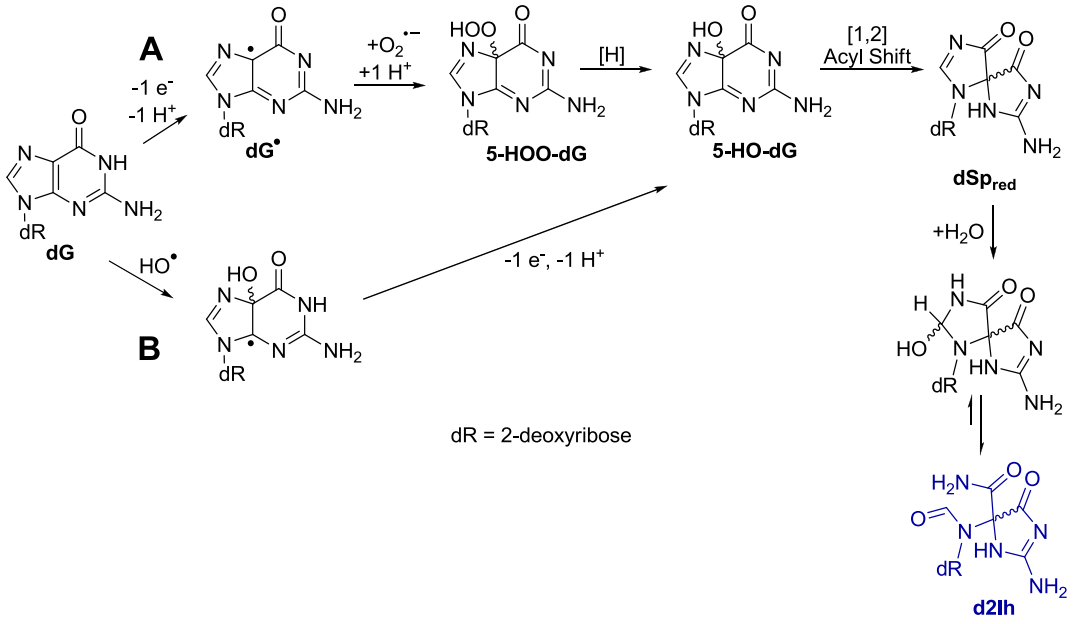


**Figure 2.10**. Proposed pathways for d2Ih product derived from C5 pathway oxidation.

base release or cyclo-dG (Figure 2.6), on C5 of the heterocyclic base leading to d2Ih and dZ (Figure 2.9 and 2.10), or on C8 of the heterocyclic base leading to Fapy-dG and dOG (Figure 2.7), in which dOG is further oxidized to dSp and dGh (Figure2.8). Inspection of the product distributions allows ranking the initial dG site of reactivity toward oxidation under each condition. The focus will be on reactions conducted under aerobic conditions with and without the addition of Asc (Tables 2.1 and 2.2). The iron-Fenton reaction without the addition of Asc focused on the sugar, C5, and C8 carbons in a ratio of 1.3:1.5:1.0, respectively, with the C5 products showing the highest yield. A comparison of the C5 and C8 product distributions show that C5 products are ~150% of the C8 products. When Asc (2 mM) was added to the mixture, the ratio of reactivity was 1.0:1.9:1.3 for the sugar, C5, and C8 carbons, respectively (Table 2.1). The addition of Asc to the iron-Fenton reaction suppressed oxidation of the sugar and initial reaction at the C5 was still greater than C8. More interestingly, C5 products were still ~150% more than the C8 products. This observation is consistent with the proposed mechanistic role of Asc in product formation, in which it reduces intermediate species that have already reacted at C5 or C8 (Figure 2.10).

The X-ray mediated oxidation of dG without Asc yielded sugar, C5, and C8 products in a 1.0:1.4:1.0 ratio, respectively (Table 2.2). Initial reactivity at C5 was the dominant pathway, and it was ~140% greater than the C8 pathway, similar to that observed for the iron-Fenton mediated oxidation of dG. When Asc was added to the mixture the ratio of reactivity at the sugar, C5, and C8 sites on dG was 1.0:1.5:1.4, respectively. Overall, Asc decreased the sugar oxidation products (Table 2.2) and the C5 and C8 products were found in nearly the same yield. The reason C5 and C8

products were observed in similar yields has to do with dZ. The presence of Asc dramatically diminished the yield of dZ in the X-ray mediated oxidations, leading to fewer C5 products, and similar yields of C5 and C8 products. These comparisons support a greater level of oxidation occurring at the heterocyclic ring of dG nucleoside compared to the sugar particularly with Asc present.

Use of a Hypercarb column allowed separation of the d2Ih and dSp diastereomers for which the absolute configurations and elution order on this HPLC column are known.[43,44] In the current studies, the *R* and *S* isomers of d2Ih were observed in a 1:2 ratio, respectively, for both oxidation reactions studied, while the *R* and *S* isomers of dSp were observed in a 1:1 ratio. Furthermore, these ratios did not change under any of the reaction conditions studied. The observation that the d2Ih isomers were not in a 1:1 ratio points to steric hindrance during the defining point of the reaction that determines product stereochemistry and was likely caused by the 2-deoxyribose sugar. In contrast to this result, the diastereomer ratio of d2Ih found from the copper-mediated Fenton oxidation was 2:1.[8] In the other d2Ih studies, the diastereomer identity and ratios were not stated.[35-38,40]

In the last study, the products resulting from base oxidation of dG in oligonucleotides of known sequence in single- (ODN1) and double-stranded (ODN2) contexts were determined, as well as products observed from λ-DNA. The product analysis was achieved using HF to hydrolyze the bases from the sugar-phosphate backbone. This approach prevented the quantification of sugar oxidation leading to base release. Because of this limitation, only base oxidation products are compared. Further, products resulting from oxidation of other nucleotides, leading to thymine glycol, for

example, were observed but were not quantified; masses consistent with guanine cross-links with thymine and cytosine were observed, but their yields are not reported due to a lack of established extinction coefficients to obtain their yields. These limitations in product analysis prevent an ideal comparison; however, we can use these data to understand context-dependent product distributions leading to C5 products (2Ih and Z) vs. C8 products (OG, Sp, and Gh) when iron-Fenton or x-ray mediated oxidations were conducted with Asc (2 mM) present under aerobic reaction conditions.

5`-TCA TCG GTC GTC GGT ATA-3` ODN1

5`-TCA TCG GTC GTC GGT ATA-3` ODN2
3`-AGT AGC CAG CAG CCA TAT-5`

The overall context-dependent trends were very similar for iron-Fenton and x-ray irradiation reactions (Figures 2.11A and B). The relative yield of Z diminished dramatically when comparing oxidations between nucleoside to ODN and DNA contexts. In the duplex contexts no Z was observed, an observation similar to previous studies that added reductant during the oxidations.[59] The OG free base was observed in all contexts and comprised the smallest relative yield in the ODN and DNA contexts and largest yield in the nucleoside studies from both iron-Fenton and x-ray oxidations. The yield of Sp and Gh showed strong context-dependent yields, in which Sp was greatest in nucleoside and single-stranded contexts and Gh was observed to be greatest in duplex contexts. This observation is consistent with previous reports.[8,52] Lastly, the relative yield of 2Ih remained nearly the same in all three contexts (~40-50%, Figures

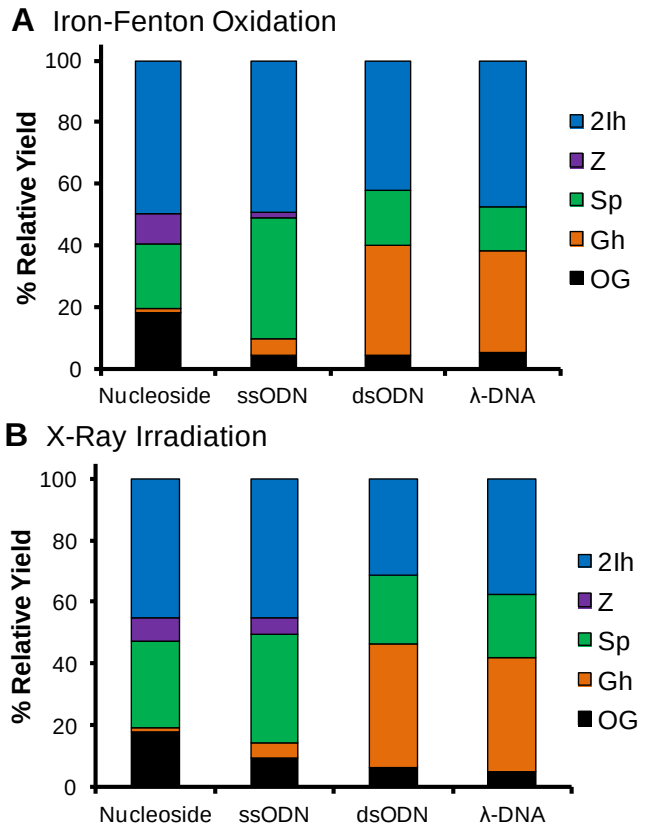


**Figure 2.11**. Context-dependent yields of dG base oxidation products from the iron-Fenton and X-ray irradiated samples. The ODN and λ-DNA distributions were obtained after HF hydrolysis of the oxidized samples. In the ODN and λ-DNA samples products were also observed from oxidation of the other nucleotides. Because of the HF hydrolysis to liberate the oxidized free bases, the extent of sugar oxidation leading to free base could not be determined. Data represent the average of three trials with an error in each value of 3 - 8%.

2.11A and B). Without complete mass balances for oxidations in the ODN and DNA contexts, it cannot be definitively stated that d2Ih is the major oxidation product of dG; nonetheless, d2Ih is clearly a major product observed from oxidation of dG in the nucleoside, single- and double-stranded ODN and λ-DNA contexts. This observation supports the possibility of d2Ih formation in the cellular context.

The current results are compared to literature studies that reported d2Ih as shown in Table 2.3. The Ball laboratory exclusively observed d2Ih when dG was exposed to the epoxidizing reagent dimethyldioxirane (DMDO), and they confirmed the structure of d2Ih via complementary NMR methods.[39,65] The Meunier laboratory observed d2Ih (M+34) when dG was oxidized with Mn-TMPyP/$KHSO_5$.[38,64] Studies in the Karlin and Rokita laboratories observed a product mass in high yield consistent with d2Ih (M+34) when an oligodeoxynucleotide was allowed to react with a dicopper(II)-complex.[40,66] In our laboratory, d2Ih was detected in high yield with the NiCR/$KHSO_5$ system, and in studies utilizing the copper-mediated Fenton oxidation of dG.[8,36] Further the Bohme laboratory conducted the lead-mediated Fenton oxidation of dG to yield d2Ih as the major product.[35] In all of the metal-catalyzed studies, the transition metal was proposed to play a role in the product-forming step leading to d2Ih. However, studies conducted in the Shafirovich laboratory observed d2Ih during $CO_3^{\bullet-}$ oxidations of dG, demonstrating that a transition metal was not required for d2Ih formation.[37] In the current report, d2Ih was the major product of "free" $HO^{\bullet}$-mediated oxidation of dG with relevant amounts of reductant under aerobic conditions. The X-ray studies demonstrate once again that d2Ih can be formed under conditions that do not require the involvement of a transition-metal catalyst.

**Table 2.3.** Comparison of the current results to other reports.

| | Initial reaction at C8 | | Initial reaction at C5 | | Initial reaction at 2-deoxyribose | |
|---|---|---|---|---|---|---|
| Products / Oxidants | dOG | dSp/dGh | dIz/dZ | d2Ih | Sugar | Reference |
| $HO^{\bullet}$ (radiolysis) | + | + | ++ | N.D. | + | 57, 58 |
| $CO_3^{\bullet-}$ | + | + | + | ++ | + | 37 |
| $Pb(II)/H_2O_2$ | + | + | + | ++ | + | 35 |
| $NiCR/KHSO_5$ | N.D. | + | N.D. | ++ | N.D. | 36 |
| DMDO | N.D. | N.D. | N.D. | ++ | N.D. | 39 |
| $Cu(I)/H_2O_2$ | + | + | + | ++ | + | 8 |
| Dicopper(II)-complex | N.D. | N.D. | N.D. | ++ | N.D. | 62 |
| $Mn\text{-}TMPyP/KHSO_5$ | N.D. | + | + | ++ | + | 59 |
| $Fe(II)\text{-}EDTA/H_2O_2$/Asc or NAC | + | + | + | ++ | + | Current study |
| X-ray/Asc or NAC | + | + | + | ++ | + | Current study |

(++) a major product, (+) a minor product, (N.D.) not detected or not reported.

**Conclusions**

The current studies monitored oxidation products from dG resulting from $HO^{\bullet}$ generated via the Fe(II)-mediated Fenton reaction or X-ray radiolysis of water. Products resulting from oxidation and initial reaction at the sugar, C5, or C8 carbons were quantified (Figures 2.2-2.5). Under aerobic conditions without reductant, the major products observed include dZ, dSp, and sugar oxidation leading to Gua. Under anaerobic reaction conditions the major product observed was dSp. When reactions were conducted with cellularly relevant (mM) amounts of reductant (Asc or NAC) and $O_2$, the major product observed in all cases was d2Ih. The isomers of d2Ih are two-electron oxidation products of dG that have not been previously detected in oxidations with $HO^{\bullet}$ generated by the Fe(II)-mediated Fenton reaction or X-ray radiolysis of $H_2O$. The high yields of d2Ih observed and the observation that this lesion is highly prone to piperidine cleavage in a DNA oligomer, unlike dOG,[67] lead to a hypothesis that oxidations in DNA imposed by electron transfer agents yield C5 oxidation products (i.e., d2Ih or dZ) and not the C8 oxidation product dOG.[68] Oxidations in the context of single- and double-stranded ODNs and λ-DNA yielded d2Ih as a product of dG oxidation in significant yield that was competitive with the yield of dOG. More importantly, the current results highlight d2Ih as a major product observed in reactions that include relevant amounts of reductant in the presence of $O_2$, suggesting that d2Ih should be investigated more closely for its biochemical properties.

**References**


1. Sies, H. (1991) Role of reactive oxygen species in biological processes, *Klin. Wochenschr. 69*, 965-968.

2. Breen, A. P., and Murphy, J. A. (1995) Reactions of oxyl radicals with DNA, *Free Radic. Biol. Med. 18*, 1033-1077.

3. Ames, B. N., Sheigenaga, M. K., and Hagen, T. M. (1995) Mitochondrial decay in aging, *Biochem. Biophys. Acta 1271*, 165-170.

4. Burrows, C. J., and Muller, J. G. (1998) Oxidative nucleobase modifications leading to strand scission, *Chem. Rev. 98*, 1109-1152.

5. Cadet, J., Douki, T., Gasparutto, D., and Ravanat, J.-L. (2003) Oxidative damage to DNA: formation, measurement and biochemical features, *Mutat. Res. 531*, 5-23.

6. MacFaul, P. A., Wayner, D. D. M., and Ingold, K. U. A. (1998) A radical account of 'oxygenated Fenton chemistry' *Acc. Chem. Res. 31*, 159-162.

7. Walling, C. (1998) Intermediates in the reactions of fenton type reagents, *Acc. Chem. Res. 31*, 155-157.

8. Fleming, A. M., Muller, J. G., Ji, I., and Burrows, C. J. (2011) Characterization of 2'-deoxyguanosine oxidation products observed in the Fenton-like system Cu(II)/$H_2O_2$/reductant in nucleoside and oligodeoxynucleotide contexts, *Org. Biomol. Chem. 9*, 3338-3348.

9. Cadet, J., Douki, T., and Ravanat, J.-L. (2008) Oxidatively generated damage to the guanine moiety of DNA: mechanistic aspect and formation in cells, *Acc. Chem. Res. 41*, 1075-1083.

10. Gimisis, T., and Cismas, C. (2006) Isolation, characterization and independent synthesis of guanine oxidation products, *Eur. J. Org. Chem.*, 1351-1378.

11. Pogozelski, W. K., and Tullius, T. D. (1998) Oxidative strand scission of nucleic acids: routes initiated by hydrogen abstraction from the sugar moiety, *Chem. Rev. 98*, 1089-1108.

12. Pratviel, G., and Meunier, B. (2006) Guanine oxidation: one- and two-electron reactions, *Chem. Eur. J. 12*, 6018-6030.

13. Steenken, S., Jovanovic, S. V., Bietti, M., and Bernhard, K. (2000) The trap depth (in DNA) of 8-oxo-7,8-dihydro-2'deoxyguanosine as derived from electron-transfer equilibria in aqueous solution, *J. Am. Chem. Soc. 122*, 2373-

2374.

14. Devasagayam, T. P., Steenken, S., Obendorf, M. S., Schulz, W., and Sies, H. (1991) Formation of 8-hydroxy(deoxy)guanosine and generation of strand breaks at guanine residues in DNA by singlet oxygen, *Biochemistry 30*, 6283-6289.

15. Belmadoui , N., Boussicault , F., Guerra , M., Ravanat , J.-L., Chatgilialoglu, C., and Cadet, J. (2010) Radiation-induced formation of purine 5′,8-cyclonucleosides in isolated and cellular DNA: High stereospecificity and modulating effect of oxygen, *Org. Biomol. Chem. 8*, 3211-3219.

16. Grey, C. E., and Adlercreutz, P. (2006) Evaluation of multiple oxidation products for monitoring effects of antioxidants in Fenton oxidation of 2'-deoxyguanosine, *J. Agric. Food Chem. 54*, 2350-2358.

17. Henle, E. S., Luo, Y., Gassmann, W., and Linn, S. (1996) Oxidative damage to DNA constituents by iron-mediated fenton reactions. The deoxyguanosine family, *J. Biol. Chem. 271*, 21177-21186.

18. Dizdaroglu, M., Rao, G., Halliwell, B., and gajewski, E. (1991) Damage to the DNA bases in mammalian chromatin by hydrogen peroxide in the presence of ferric and cupric ions, *Arch. Biochem. Biophys. 285*, 317-324.

19. Douki, T., Martini, R., Ravanat, J.-L., Turesky, R. J., and Cadet, J. (1997) Measurement of 2,6-diamino-4-hydroxy-5-formamidopyrimidine and 8-oxo-7,8-dihydroguanine in isolated DNA exposed to gamma radiation in aqueous solution, *Carcinogenesis 18*, 2385-2391.

20. Pouget, J.-P., Frelon, S., Ravanat, J.-L., Testard, I., Odin, F., and Cadet, J. (2002) Formation of modified DNA bases in cells exposed either to gamma radiation or to high-LET particles, *Radiat. Res. 157*, 589-595.

21. Gedik, C. M., and Collins, A. F. (2005) Establishing the background level of base oxidation in human lymphocyte DNA: results of an interlaboratory validation study, *FASEB J. 19*, 82-84.

22. Luo, W., Muller, J. G., Rachlin, E. M., and Burrows, C. J. (2000) Characterization of spiroiminodihydantoin as a product of one-electron oxidation of 8-oxo-7,8-dihydroguanosine, *Org. Lett. 2*, 613-616.

23. Misiaszek, R., Crean, C., Geacintov, N. E., and Shafirovich, V. (2005) Combination of nitrogen dioxide radicals with 8-oxo-7,8-dihydroguanine and guanine radicals in DNA: oxidation and nitration end-products, *J. Am. Chem. Soc. 127*, 2191-2200.

24. Niles, J. C., Wishnok, J. S., and Tannenbaum, S. R. (2004) Spiroiminodihydantoin and guanidinohydantoin are the dominant products of 8-oxoguanosine oxidation at low fluxes of peroxynitrite: mechanistic studies with $^{18}O$, *Chem. Res. Toxicol. 17*, 1510-1519.

25. Slade, P. G., Hailer, M. K., Martin, B. D., and Sugden, K. D. (2005) Guanine-specific oxidation of double-stranded DNA by Cr(VI) and ascorbic acid forms spiroiminodihydantoin and 8-oxo-2'-deoxyguanosine, *Chem. Res. Toxicol. 18*, 1140-1149.

26. Delaney, S., Neeley, W. L., Delaney, J. C., and Essigmann, J. M. (2007) The substrate specificity of MutY for hyperoxidized guanine lesions *in vivo*, *Biochemistry 46*, 1448-1455.

27. Hailer, M. K., Slade, P. G., Martin, B. D., and Sugden, K. D. (2005) Nei deficient *Escherichia coli* are sensitive to chromate and accumulate the oxidized guanine lesion spiroiminodihydantoin, *Chem. Res. Toxicol. 18*, 1378-1383.

28. Henderson, P. T., Delaney, J. C., Muller, J. G., Neeley, W. L., Tannenbaum, S. R., Burrows, C. J., and Essigmann, J. M. (2003) The Hydantoin Lesions Formed from Oxidation of 7,8-Dihydro-8-oxoguanine Are Potent Sources of Replication Errors in Vivo†, *Biochemistry 42*, 9257-9262.

29. Mangerich, A., Knutson, C. G., Parry, N. M., Muthupalani, S., Ye, W., Prestwich, E., Cui, L., McFaline, J. L., Mobley, M., Ge, Z., Taghizadeh, K., Wishnok, J. S., Wogan, G. N., Fox, J. G., Tannenbaum, S. R., and and Dedon, P. C. (2012) Infection-induced colitis in mice causes dynamic and tissue-specific changes in stress response and DNA damage leading to colon cancer, *Proc. Natl. Acad. Sci. U.S.A. 109*, E1820-E1829.

30. Cadet, J., Berger, M., Buchko, G. W., Joshi, P. C., Raoul, S., and Ravanat, J.-L. (1994) 2,2-Diamino-4-[(3,5-di-acetyl-2-deoxy-β-d-erythro-pentofuranosyl) amino]-5-(2H)-oxazolone: a novel and predominant radical oxidation product of 3′,5′-di-acetyl-2′-deoxyguanosine, *J. Am. Chem. Soc. 116*, 7403-7404.

31. Gasparutto, D., Ravanat, J.-L., Gérot, O., and Cadet, J. (1998) Characterization and chemical stability of photooxidized oligonucleotides that contain 2,2-diamino-4-[(2-deoxy-β-D-erythro-pentofuranosyl)amino]-5*(2H)*-oxazolone, *J. Am. Chem. Soc. 120*, 10283-10286.

32. Kino, K., Saito, I., and Sugiyama, H. (1998) Product analysis of GG-specific photooxidation of DNA via electron transfer: 2-aminoimidazolone as a major guanine oxidation product, *J. Am. Chem. Soc. 120*, 7373-7374.

33. Kupan, A., Saulière, A., Broussy, S., Seguy, C., Pratviel, G., and Meunier, B. (2006) Guanine oxidation by electron transfer: one- versus two-electron

oxidation mechanism, *Chem. Bio. Chem. 7*, 125-133.

34. Raoul, S., Berger, M., Buchko, G. W., Joshi, P. C., Morin, B., Weinfeld, M., and Cadet, J. J. (1996) Novel oxidation products of deoxyguanosine:oxazolone and imidazolone nucleosides, *Chem. Soc., Perkin Trans. 2*, 371-381.

35. Banu, L., Blagojevic, V., and Bohme, D. K. (2012) Lead(II)-catalyzed oxidation of guanine in solution studied with electrospray ionization mass spectrometry, *J. Phys. Chem. B. 116*, 11791–11797.

36. Ghude, P., Schallenberger, M. A., Fleming, A. M., Muller, J. G., and Burrows, C. J. (2011) Comparison of transition metal-mediated oxidation reactions of guanine in nucleoside and single-stranded oligodeoxynucleotide contexts, *Inorg. Chem. Acta 369*, 240-246.

37. Rokhlenko, Y., Geacintov, N. E., and Shafirovich, V. (2012) Lifetimes and reaction pathways of guanine radical cations and neutral guanine radicals in an oligonucleotide in aqueous solutions, *J. Am. Chem. Soc. 134*, 4955-4962.

38. Vialas, C., Claparols, C., Pratviel, G., and Meunier, B. (2000) Guanine oxidation in double-stranded DNA by Mn-TMPyP/$KHSO_5$: 5,8-dihydroxy-7,8-dihydroguanine residue as a key precursor of imidazolone and parabanic acid derivatives, *J. Am. Chem. Soc. 122*, 2157-2167.

39. Ye, W., Sangaiah, R., Degen, D. E., Gold, A., Jayaraj, K., Koshlap, K. M., Boysen, G., Williams, J., Tomer, K. B., Mocanu, V., Dicheva, N., Parker, C. E., Schaaper, R. M., and Ball, L. M. (2009) Iminohydantoin lesion induced in DNA by peracids and other epoxidizing oxidants, *J. Am. Chem. Soc. 131*, 6114-6123.

40. Li, L., Murthy, N. N., Telser, J., Zakharov, L. N., Yap, G. P. A., Rheingold, A. L., Karlin, K. D., and Rokita, S. E. (2006) Targeted guanine oxidation by a dinuclear copper(II) complex at single stranded/double stranded DNA junctions, *Inorg. Chem. 45*, 7144-7159.

41. Meister, A., and Anderson, M. E. (1983) Glutathione, *Annu. Rev. Biochem. 52*, 711-760.

42. Douki, T., Spinelli, S., Ravanat, J.-L., and Cadet, J. (1999) Hydroxyl radical-induced degradation of 2′-deoxyguanosine under reducing conditions, *J. Chem. Soc., Perkin Trans. 2*, 1875-1880.

43. Fleming, A. M., Alshykhly, O., Orendt, A. M., and Burrows, C. J. (2015) Computational studies of electronic circular dichroism spectra predict absolute configuration assignments for the guanine oxidation product 5-carboxamido-5-formamido-2-iminohydantoin, *Tetrahedron Lett. 56*, 3191-3196.

44. Fleming, A. M., Orendt, A. M., He, Y., Zhu, J., Dukor, R. K., and Burrows, C. J. (2013) Reconciliation of chemical, enzymatic, spectroscopic and computational data to assign the absolute configuration of the DNA base lesion spiroiminodihydantoin, *J. Am. Chem. Soc. 135*, 18191-18204.

45. Matter, B., Malejka-Giganti, D., Csallany, A. S., and Tretyakova, N. (2006) Quantitative analysis of the oxidative DNA lesion, 2,2-diamino-4-(2-deoxy-beta-D-erythro-pentofuranosyl)amino]-5(*2H*)-oxazolone (oxazolone), *in vitro* and *in vivo* by isotope dilution-capillary HPLC-ESI-MS/MS, *Nucleic Acids Res. 34*, 5449–5460.

46. Ye, Y., Muller, J. G., Luo, W., Mayne, C. L., Shallop, A. J., Jones, R. A., and Burrows, C. J. (2003) Formation of $^{13}$C-, $^{15}$N-, and $^{18}$O-labeled guanidinohydantoin from guanosine oxidation with singlet oxygen. Implications for structure and mechanism, *J. Am. Chem. Soc. 125*, 13926-13927.

47. Huang, H., Das, R. S., Basu, A. K., and Stone, M. P. (2011) Structure of (5 *S*)-8,5`-Cyclo-2`-deoxyguanosine in DNA, *J. Am. Chem. Soc. 133*, 20357-20368.

48. Eckenroth, B. E., Fleming, A. M., Sweasy, J. B., Burrows, C. J., and Doublié, S. (2014) Crystal structure of DNA polymerase β with DNA containing the base lesion spiroiminodihydantoin in a templating position, *Biochemistry 53*, 2075-2077.

49. Karwowski, B., Dupeyrat, F., Bardet, M., Ravanat, J.-L., Krajewski, P., and Cadet, J. (2006) Nuclear magnetic resonance studies of the 4R and 4S diastereomers of spiroiminodihydantoin 2'-deoxyribonucleosides: absolute configuration and conformational features, *Chem. Res. Toxicol. 19*, 1357-1365.

50. Extinction coefficients (ε240 nm) for dSp and d2Ih were assumed to be the same value; however, ring opening of the imidazole ring is anticipated to lead to a lower value of ε240 nm for d2Ih compared to the ring closed dSp structure. Support for this claim was taken from the TDDFT calculations we have conducted to determine the UV spectroscopic properties of d2Ih and dSp (see refs 42 and 62). In these studies, UV-vis spectra were calculated with explicit and implicit solvation using the M06-2X functional and 6-311++G(2d,2p) basis set with implicit definition of water using the PCM, and these data allow a relative comparison of the ε240 nm between dSp and d2Ih to be made. These calculations identify that d2Ih absorbs light at ~70% of dSp (Appendix A).

51. Luo, W., Muller, J. G., Rachlin, E. M., and Burrows, C. J. (2001) Characterization of hydantoin products from one-electron oxidation of 8-oxo-7,8-dihydroguanosine in a nucleoside model, *Chem. Res. Toxicol. 14*, 927-938.

52. Fleming, A. M., Muller, J. G., Dlouhy, A. C., and Burrows, C. J. (2012) Structural context effects in the oxidation of 8-oxo-7,8-dihydro-2'-

deoxyguanosine to hydantoin products: electrostatics, base stacking, and base pairing, *J. Am. Chem. Soc. 134*, 15091-15102.

53. Crespo-Hernández, C. E., and Arce, R. (2004) Formamidopyrimidines as major products in the low- and high-intensity UV irradiation of guanine derivatives, *Journal of Photochemistry and Photobiology B: Biology 73*, 167-175.

54. Greenberg, M. M. (2012) The formamidopyrimidines: purine lesions formed in competition with 8-oxopurines from oxidative stress, *Acc. Chem. Res. 45*, 588-597.

55. Frelon, S., Douki, T., Favier, A., and Cadet, J. (2002) Comparative study of base damage induced by gamma radiation and Fenton reaction in isolated DNA, *J. Chem. Soc., Perkin Trans. 1*, 2866-2870.

56. Solivio, M. J., Joy, T. J., Sallans, L., and Merino, E. J. (2010) Copper generated reactive oxygen leads to formation of lysine-DNA adducts, *J. Inorg. Biochem. 104*, 1000-1005.

57. Xiaoyun Xu, James G. Muller, Yu Ye, and Burrows, C. J. (2008) DNA-protein cross-links between guanine and lysine depend on the mechanism of oxidation for formation of C5 vs C8 guanosine adducts, *J. Am. Chem. Soc. 130*, 703-709.

58. Lee, J., Koo, N., and Min, D. B. (2004) Reactive oxygen species, aging, and antioxidative nutraceuticals, *Comp. Rev. Food Sci. Food Safety 3*, 21-33.

59. Yu, H., Niles, J. C., Wishnok, J. S., and Tannenbaum, S. R. (2004) Spirodihydantoin is a minor product of 5-hydroxyisourate in urate oxidation, *Org. Lett. 6*, 3417-3420.

60. Fleming, A. M., and and Burrows, C. J. (2013) G-quadruplex folds of the human telomere sequence alter the site reactivity and reaction pathway of guanine oxidation compared to duplex DNA, *Chem. Res. Toxicol. 26*, 593 - 607.

61. Lim, K. S., Cui, L., Taghizadeh, K., Wishnok, J. S., Chan, W., DeMott, M. S., Babu, I. R., Tannenbaum, S. R., and and Dedon, P. C. (2012) In situ analysis of 8-oxo-7,8-dihydro-2'-deoxyguanosine oxidation reveals sequence- and agent-specific damage spectra, *J. Am. Chem. Soc. 134*, 18053-18064.

62. Neeley, W. L., and Essigmann, J. M. (2006) Mechanisms of formation, genotoxicity, and mutation of guanine oxidation products, *Chem. Res. Toxicol. 19*, 491-505.

63. Cui, L., Ye, W., Prestwich, E. G., Wishnok, J. S., Taghizadeh, K., Dedon, P. C., and Tannenbaum, S. R. (2013) Comparative analysis of four oxidized guanine lesions from reactions of DNA with peroxynitrite, singlet oxygen, and γ-

radiation, *Chem. Res. Toxicol. 26*, 195-202.

64. Tomaszewska, A., Mourgues, S., Guga, P., Nawrot, B., and Pratviel, G. (2012) A single nuclease-resistant linkage in DNA as a versatile tool for the characterization of DNA lesions: application to the guanine oxidative lesion "G+34" generated by metalloporphyrin/$KHSO_5$ reagent, *Chem. Res. Toxicol. 25*, 2505-2512.

65. Ye, W., Sangaiah, R., Degen, D. E., Gold, A., Jayaraj, K., Koshlap, K. M., Boysen, G., Williams, J., Tomer, K. B., and Ball, L. M. (2006) A 2-iminohydantoin from the oxidation of guanine, *Chem. Res. Toxicol. 19*, 506-510.

66. Li, L., Karlin, K. D., and Rokita, S. E. (2005) Changing selectivity of DNA oxidation from deoxyribose to guanine by ligand design and a new binuclear copper complex, *J. Am. Chem. Soc. 127*, 520-521.

67. Fleming, A. M., Alshykhly, O., Zhu, J., Muller, J. G., and Burrows, C. J. (2015) Rates of chemical cleavage of DNA and RNA oligomers containing guanine oxidation products, *Chem. Res. Toxicol. 28*, 1292-1300.

68. Kanvah, S., Joseph, J., Schuster, G. B., Barnett, R. N., Cleveland, C. L., and Landman, U. (2010) Oxidation of DNA: damage to nucleobases, *Acc. Chem. Res. 43*, 280-287.

# CHAPTER 3

# THE GUANINE OXIDATION PRODUCT 5-CARBOXAMIDO-5-FORMAMIDO-2-IMINOHYDANTOIN INDUCES MUTATIONS WHEN BYPASSED BY DNA POLYMERASES AND IS A SUBSTRATE FOR BASE EXCISION REPAIR*

## Introduction

DNA damage has been implicated in aging, carcinogenesis, and neurological disorders.[1] Reactive oxygen species (ROS) represent one of the key threats that affect damage to the genome yielding strand breaks and base lesions. Base lesions have the ability to stall or cause replicative polymerases to incorporate the incorrect nucleotide that can lead to mutations.[2,3] To avoid mutations, biology has a repair system, of which the base excision repair (BER) pathway is one approach to maintain the integrity of the genome.[3,4] Mutation profiles observed in a number of cancers have identified critical mutations at guanine nucleotides.[5]

The heterocyclic base of 2'-deoxyguanosine (G) is the most susceptible to

*Partially reproduced with permission from "Alshykhly, O. R., Fleming, A. M., and Burrows, C. J. (2015) The guanine oxidation product 5-carboxamido-5-formamido-2-iminohydantoin induces mutations when bypassed by DNA polymerases and is a substrate for base excision repair, *Chem. Res. Toxicol.*, DOI:10.1021/acs.chemrestox.1025b00302".

oxidative damage because it has the lowest redox potential among the four DNA bases.[6] Oxidation of G by two electrons yields 8-oxo-7,8-dihydro-2'-deoxyguanosine (OG).[7,8] The four-electron oxidation of G yields two diastereomers of spiroiminodihydantoin-2'-deoxyribonucleoside (Sp), two diastereomers of 5-guanidinohydantoin-2'-deoxyribonucleoside (Gh), and 2,5-diaminoimidazolone-2'-deoxyribonucleoside (Iz) that hydrolyzes to 2,2,4-triamino-*2H*-oxazol-5-one-2'-deoxyribonucleoside (Z) and other products.[7,9-19] Lastly, a second two-electron oxidation product resulting from G oxidation is the diastereomeric pair 5-carboxamido-5-formamido-2-iminohydantoin-2'-deoxyribonucleoside (2Ih, Figure 3.1).[20-28] In eukaryotic and prokaryotic models, many of these lesions have been detected;[29-33] however, 2Ih has not yet been the subject of such an investigation.

Lesions in templating strands of DNA can induce misinsertions of nucleotides opposite the lesion that are determined by the polymerase active site and the base pairing properties of the lesion. Previous studies have demonstrated that DNA polymerases can synthesize past OG and incorporate dATP or dCTP opposite the lesion, that upon further replication causes G•C → T•A transversion mutations in the absence of repair.[34-36] When Sp or Gh are in the template strand, they show preference for incorporation of dATP or dGTP, in which dGTP is more efficiently incorporated opposite Gh than Sp. These polymerase studies identify both lesions as inducing either G•C → C•G or G•C → T•A transversion mutations.[34,37-41] Three common classes of DNA polymerases include those that are replicative, those involved in the DNA damage response whose role is to bypass damaged nucleotides, and PCR polymerases used in sequencing applications. Ideally, mutations are avoided by the action of multiple repair

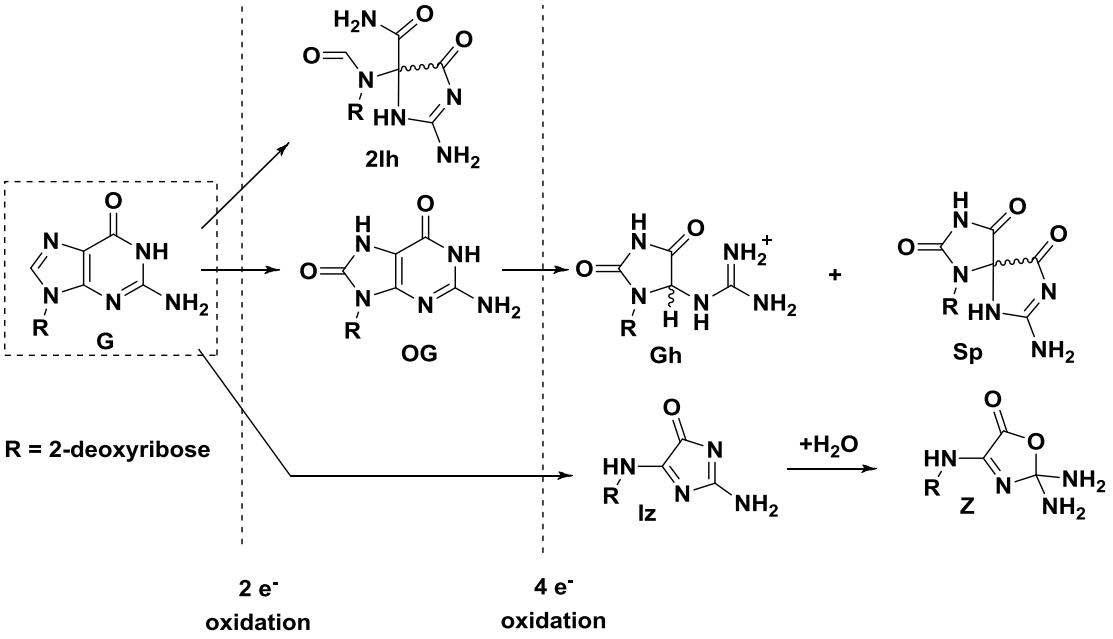


**Figure 3.1.** Products observed from the oxidation of 2`-deoxyguanosine.

enzymes that remove the damage before polymerase bypass can occur.

The base excision repair (BER) pathway is one mechanism responsible for removal of damaged DNA nucleotides. The first step in the BER process employs a DNA glycosylase to recognize and remove the damaged base. The repair process is then completed by the actions of an endonuclease yielding a gap at the damage site, followed by polymerase filling of the gap, and finally a ligase seals the nick to furnish a repaired strand.[42] The ability to repair OG has been found in bacterial and mammalian cells.[3] In *E. coli*, MutM (i.e., Fpg) can remove OG from an OG•C base pair, while MutY removes A from an OG•A base pair.[3,43-45] In mammalian cells, OGG1 acts on the OG•C lesion while MUTYH acts on the A in an OG•A base pair.[46] Endonuclease VIII (Nei) and endonuclease III (Nth) in prokaryotes have the ability to repair oxidized pyrimidines,[3,43,44] while the oxidized purines such as Z, Gh, and Sp are substrates for these glycosylases with reduced activity.[47,48] A "Nei-like" glycosylase in humans (NEIL1) has been identified and characterized.[49] NEIL1, like Fpg and Nei, is a bifunctional repair enzyme (glycosylase/lyase) that catalyzes *N*-glycosidic bond hydrolysis and β-,δ-elimination reactions to affect strand scission.[2,3,42] NEIL1 was originally found to cleave Fapy-G, Fapy-A, thymine glycol (Tg), 5-hydroxycytosine (5-OHC), and 5-hydroxyuracil (5-OHU);[50-52] however, the best substrates found so far for NEIL1 are the diastereomers of Gh and Sp. Furthermore, the efficient removal of Sp or Gh is not dependent on the base opposite in dsDNA.[47,53-55] Gh and Sp have also been found to be substrates for Fpg.[56,57] As new lesions to DNA are found, their ability to be repaired by BER DNA glycosylases should be assessed to determine if the lesion will persist in DNA and cause problems during polymerase activity.

To date, the ability of 2Ih to cause mutations via incorrect polymerase activity or to evade the BER pathway has not been evaluated. In this study, we investigated polymerase activity toward (*R*)-2Ih or (*S*)-2Ih in the template strand using the three polymerases Klenow fragment (Kf) exo$^-$ (replicative), DPO4 (translesion synthesis), and Hemo KlenTaq (PCR). Next, we investigated the excision of (*R*)-2Ih and (*S*)-2Ih lesions with the BER DNA glycosylases Fpg, Nth, and human NEIL1. These polymerase studies identify the diastereomers of 2Ih to induce mutations when bypassed by all three polymerases studied, and the 2Ih isomers are substrates for Fpg and NEIL1, but are poorly acted on by Nth.

**Experimental** (representative data are provided in Appendix B)

*Materials and methods*

All chemicals were obtained from commercially available sources and used without further purification. All oligodeoxynucleotides (ODNs) were synthesized by the DNA/peptide core facility at the University of Utah and then cleaved, deprotected, and purified following standard protocols.[58] NiCR was synthesized by a literature protocol by Dr. James G. Muller (University of Utah).[59]

*Synthesis of oligonucleotides containing 2Ih or Sp*

The 2Ih-containing ODNs were synthesized by oxidizing ODNs 1 (18 mer) and 3 (15 mer) when X and Y = G (Table 3.1), respectively, in the presence of the nickel(II) complex NiCR as catalyst with $KHSO_5$ as oxidant yielding 2Ih at the only G site via a method previously described by our laboratory.[22,60] Briefly, 10 μM ODN in 20 mM

**Table 3.1.** Oligodeoxynucleotide sequences used in the polymerase and repair enzyme studies.

| |
|---|
| ODN1 5’-AA**X** CCA CCT ACA CAC CTC-3’ |
| ODN2 3’-GGT GGA TGT GTG GAG-5’ ( primer ) |
| ODN3 5’-AAT CCA C**Y**A CAC CTC-3’ |
| ODN4 3’- TTA GGT GNT GTG GAG-5’ |
| **X** or **Y** = G, OG, (*S*-2Ih, *R*-2Ih, *S*-Sp, or *R*-Sp), **N** = A, C, G, or T |

$NaP_i$ buffer (pH 7.4) and 100 mM NaCl were incubated with 5 μM NiCR at 37 °C for 20 min prior to the addition of 100 μM $KHSO_5$, and the reaction was allowed to progress for 30 min. The reaction was quenched by adding 50 mM HEPES (pH 8). The Sp-containing ODNs were used as a standard to compare how polymerases and BER enzymes react with 2Ih-containing ODNS. The Sp-containing ODNs were synthesized by oxidizing ODNs 1 and 3, in which X and Y = OG. To 10 μM ODN in 20 mM $NaP_i$ buffer (pH 7.4) and 100 mM NaCl was added 100 μM $Na_2IrCl_6$ at 37 °C for 30 min. The 2Ih- and the Sp-containing ODN diastereomers were separated and purified by an analytical ion-exchange HPLC column in which mobile phase A = 10% $CH_3CN$ and 90% $ddH_2O$, and B = 1.5 M NaOAc (pH 7) in 10% $CH_3CN$/90% $ddH_2O$ running at 1 mL/min while monitoring the absorbance at 260 nm. The absolute configurations for the diastereomers of 2Ih and Sp have previously been determined, as well as their elution order in an ODN on the ion-exchange HPLC column used in the present studies.[60,61] These ODNs were further purified by HPLC to obtain > 95% purity before use. The ODNs with 2Ih or Sp were characterized by either ESI-MS for ODNs 1 (G: calcd 5357.5, found 5356.9; (*S*)-2Ih or (*R*)-2Ih): calcd 5391.5, found 5391.0 and 5391.1, respectively; a mixture of the Sp diastereomers: calcd 5389.5, found 5389.6) or MALDI-MS for ODNs 3 (G: calcd 4463.8, found 4464.2; mixture of 2Ih diastereomers: calcd 4497.8, found 4498.2; mixture of Sp diastereomers: calcd 4495.8, found 4496.6).

*Thermal denaturation studies ($T_m$) and CD measurements*

ODNs 3 and 4 (Y = G, (*S*)-2Ih, or (*R*)-2Ih, and N = A, C, G, or T, Table 1) were annealed in a ratio of 2:1, respectively, at 10 μM duplex in analysis buffer (20 mM $NaP_i$ (pH 7.4) and 100 mM NaCl), followed by heating to 90 °C for 5 min and then allowing

to cool slowly to room temperature (~3 h). The samples were kept at 4 °C prior to their analysis. The $T_m$ analysis was conducted by monitoring the absorbance at 260 nm while heating the samples from 15 to 80 °C ramped at 1 °C per min and then cooling down to 15 °C via the same rate. The CD spectra for these samples (5 μM) were obtained on a JACSO 815 CD spectrophotometer. The wavelength scanned ranged from 200 to 320 nm while maintaining the temperature at 20 °C.

*ODN labeling*

For the polymerase studies, ODN 2 (primer, Table 3.1) was radiolabeled at the 5'-end using T4-polynucleotide kinase and [γ-$^{32}$P]-ATP at 37 °C for 30 min following literature methods.[58] Unreacted [γ-$^{32}$P]-ATP and enzyme were removed using a Microspin G-25 column (GE Health Sciences) following the manufacturer's protocol. The primer was annealed to the template ODN 1 (X = (*S*)-2Ih, (*R*)-2Ih, (*S*)-Sp, or (*R*)-Sp) in 100 μL of buffer solution (10 mM Tris-HCl, 5 mM $MgCl_2$, and 7.5 mM DTT, pH 7.5) with a molar ratio 2:1 template:primer. In the BER studies, ODNs 3 (Y = (*S*)-2Ih, (*R*)-2Ih, (*S*)-Sp, or (*R*)-Sp) were labeled at the 5'-end following the same procedure prescribed above, and then were annealed with 20% excess complementary strand ODN 4 (N = A, C, G, or T) in annealing buffer (10 mM EDTA, 150 mM NaCl, and 20 mM Tris-HCl at pH 7.6).

*Polymerase studies*

Single nucleotide insertion or full primer extension reactions were conducted using the DNA polymerases Kf exo$^-$, DPO4, or Hemo KlenTaq. The polymerization

was initiated by mixing a solution containing the labeled template/primer ODNs (final concentration = 50 nM), 10 μM of each dNTP (for the single nucleotide insertion studies), or a mixture of the four dNTPs (for the full primer extension studies), and polymerase (0.2 unit of Kf exo$^-$, 0.5 unit of DPO4, or 0.5 unit Hemo KlenTaq). Reaction mixtures were incubated at 37 °C for 30 min, then quenched with 5 μL of termination solution (95% formamide, 0.1% bromophenol blue, and 0.1% xylene cyanol) and heated to 90 °C for 5 min. These samples were applied to a 20% polyacrylamide gel in the presence of 7 M urea, electrophoresed at 45 W for 2 h, and then put on a phosphor screen for 18 h. The screen was imaged by phosphorimager autoradiography, and the band intensities were quantified using ImagQuant software.

*Glycosylase studies*

Single-turnover experiments where [Enz] > [DNA] were conducted by mixing 50 nM of labeled ssODN or dsODN and 500 nM enzyme (Fpg, NEIL1, or Nth) in assay buffer (20 mM Tris-HCl, pH 7.5, 10 mM EDTA, 0.1 mg/mL BSA, and 150 mM NaCl) at 37 °C for 20 min. In order to measure the glycosylase activity, these samples were quenched by adding 5 μL of 0.5 N NaOH and heating to 90 °C for 2 min. The samples were analyzed by gel electrophoresis as described for the polymerase assays. The Fpg and Nth were from commercial sources, while NEIL1 was a kind gift from Dr. Sheila David (University of California-Davis).

*Density functional theory calculations*

All density functional theory (DFT) energy minimization calculations were conducted using the Gaussian 09 software package.[62] Each structure was geometrically optimized using the B3LYP functional[63,64] and 6-31G basis set,[65,66] while implicitly defining the solvent as water with the polarizable continuum model (PCM).[67,68] Scans of the dihedral angles provided lowest energy conformations for the 2Ih diastereomers.

**Results and discussion**

*Synthesis of 2Ih in oligodeoxynucleotides*

The modified nucleoside containing 2Ih is not available in the form of a phosphoramidite, nor is there a suitable precursor to this lesion other than guanine. Therefore, the only available synthetic route to 2Ih incorporation into a specific site in an oligodeoxynucleotide is oxidation of an oligomer that contains only one G. This imposes a limitation on the number of sequence contexts that can be studied. Additionally, the yield of 2Ih is ~10% under ideal conditions, requiring HPLC purification before biochemical studies can be performed. Although 2Ih is formed from a variety of reactive oxygen species including hydroxyl radical formed by iron and copper Fenton-like reactions,[21,28] we have found that nickel(II)-catalyzed decomposition of monoperoxysulfate is a high yielding method for conversion of G to 2Ih.[22] The square-planar coordination compound NiCR, formed by Schiff base condensation of 2,6-diacetylpyridine with 1,5,9-triazanonane, is a convenient catalyst for this reaction.[22]

*Polymerase studies*

To investigate how polymerases would process 2Ih in a template strand, a series of standing start and full extension assays were conducted with the replicative polymerase Kf exo$^-$, DNA damage response polymerase DPO4, and the PCR polymerase Hemo KlenTaq. The template ODN 1 (18 mer; X = G, (*S*)-2Ih, (*R*)-2Ih, (*S*)-Sp, or (*R*)-Sp) was annealed with the 5'-labeled primer ODN 2 (15 mer) for the single nucleotide insertion and full primer extension experiments. In this study, the concentration of dNTPs was initially studied at near physiological concentrations (10 μM) for Kf exo$^-$ and DPO4,[69] and Hemo KlenTaq was studied with the standard 100 μM dNTP concentrations. However, DPO4 had activity too low to be reliably quantified at physiological dNTPs, and therefore, the dNTP concentrations were increased threefold.

The control experiment with a template G led to the expected result with Kf exo$^-$ in which dCTP was inserted opposite; however, when dTTP was the only possible nucleotide, it was inserted in 39% yield, likely due to a feasible G•T wobble base pair. The (*R*)-2Ih-containing template showed insertion of dGTP (40%) more than dATP (14%); similarly (*S*)-2Ih-containing templates showed insertion of dGTP (19%) more than dATP (7%, Figure 3.2A). In these assays, dTTP or dCTP were not observed to be inserted opposite either diastereomer of 2Ih, and for this reason, only dGTP and dATP insertion data are shown in Figure 3.2A. Next, all dNTPs were added to the reaction mixture to determine if full primer extension could occur. The control study was conducted with a template that has unmodified G and showed 95% full extension. When (*R*)-2Ih was in the template a 30% full extension was observed,

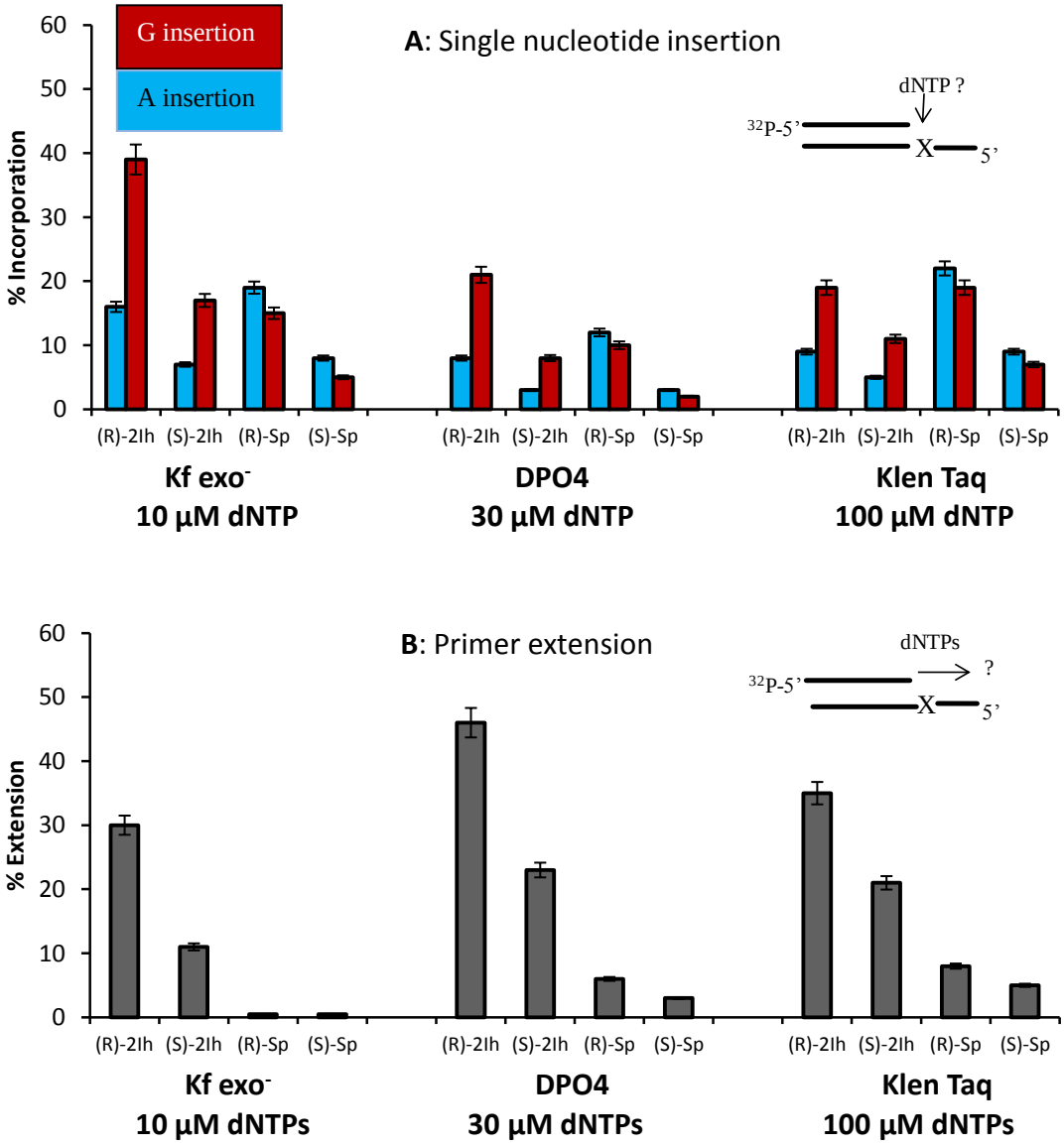


**Figure 3.2.** Comparison of the relative amount of nucleotide insertion opposite X (X = (*R*)-2Ih, (*S*)-2Ih, (*R*)-Sp, or (*S*)-Sp) by Kf exo$^-$, DPO4, and Hemo KlenTaq polymerases. (A) Single nucleotide insertion, the dCTP and dTTP insertions were studied but they were not incorporated and data for these studies are provided in Appendix B. (B) Full extension of the primer in the presence of all four nucleotides.

while a template (*S*)-2Ih led to only 11% full extension (Figure 3.2B). These studies with the replicative polymerase Kf exo⁻ demonstrate that when either diastereomer of 2Ih was in the template, dGTP insertion was threefold greater than dATP insertion. Additionally, higher yields of dNTP insertion were observed for the *R* isomer relative to the *S* isomer of 2Ih. Lastly, bypass of (*R*)-2Ih was threefold greater than bypass of (*S*)-2Ih when all dNTPs were present.

A comparison was then made between the 2Ih data and the diastereomers of Sp in the template strand (Figure 3.2A). First, it should be noted that the geometric configurations for the *R* isomers of 2Ih and Sp or *S* isomers of 2Ih and Sp are essentially the same; the only difference is that in 2Ih, the five-membered ring attached to the sugar is ring opened compared to Sp (Figure 3.3) and the oxidation state of what was C8 of G is reduced in 2Ih compared to Sp.[60,61] When (*R*)- or (*S*)-Sp were in the template, dATP (*R* = 19% and *S* = 8%) was inserted more often than dGTP (*R* = 15% and *S* = 5%). For template Sp, dATP vs. dGTP were selected in nearly equal amounts. Next, when all dNTPs were added to the mixture, primer extension past Sp was not observed with physiologically relevant amounts of dNTPs (Figure 3.2B). A comparison of 2Ih with Sp identifies the diastereomers of 2Ih to show a much stronger preference for base pairing with G over A (3:1) compared to the ~1:1 preference opposite Sp. Furthermore, 2Ih is more easily bypassed than Sp under identical conditions.

The lesion bypass polymerase DPO4 was then analyzed for nucleotide insertion opposite 2Ih. Insertion of dGTP opposite (*R*)-2Ih was observed in a yield of 7%, (*S*)-2Ih at a 3% yield and no dATP insertion was observed at physiological concentrations of dNTPs. When the dNTP concentrations were increased to 30 μM, the single nucleotide

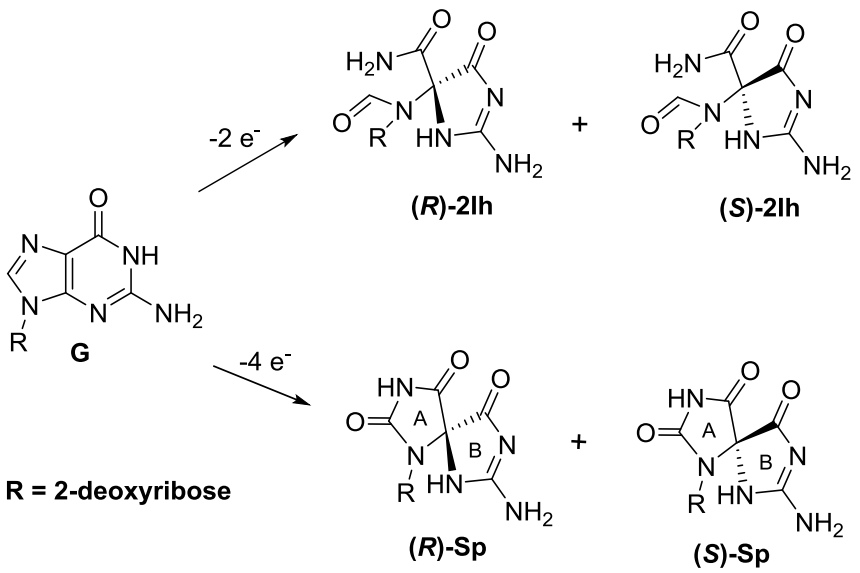


**Figure 3.3.** Comparison of the geometric configurations for the diastereomers of 2Ih and Sp that are products resulting from the oxidation of G.

insertion opposite (*R*)-2Ih and (*S*)-2Ih yielded more dGTP (*R* = 25% and *S* = 9%) than dATP (*R* = 6% and *S* = 2%) opposite the lesion (Figure 3.2A). No insertion of dCTP or dTTP opposite the 2Ih diastereomers was observed with DPO4. When all four nucleotides were added to the reaction mixture, DPO4 was able to provide full extension in a yield of 49% and 23% for (*R*)-2Ih and (*S*)-2Ih, respectively (Figure 3.2B). These results demonstrate that (*R*)-2Ih is more easily bypassed by DPO4 than (*S*)-2Ih, and dGTP is inserted nearly five times more than dATP opposite either diastereomer.

Comparisons were then made between DPO4 activities with template 2Ih vs. Sp (Figure 3.2). Insertions opposite the Sp diastereomers were not observed with 10 μM dNTPs; however, increasing the dNTP concentrations to 30 μM produced insertion opposite the Sp isomers. Specifically, insertion opposite (*R*)-Sp and (*S*)-Sp gave dATP (*R* = 12% and *S* = 4%) and dGTP (*R* = 10% and *S* = 3%) in nearly equal yields. When all four dNTPs were added to the mixture, (*R*)-Sp was extended by 10% and (*S*)-Sp was extended by 8%. This observation demonstrates that DPO4 shows similar activity with the Sp diastereomers; in contrast, DPO4 accommodated the *R* diastereomer of 2Ih better than the *S* isomer leading to more efficient bypass, and both 2Ih isomers yielded dGTP insertion fivefold more than dATP.

In the last study, the PCR polymerase Hemo KlenTaq was allowed to insert dNTPs opposite a template (*R*)- or (*S*)-2Ih diastereomer. At the typical 100 μM dNTP concentration used in PCR amplification, template (*R*)-2Ih or (*S*)-2Ih gave more dGTP (*R* = 17% and *S* = 11%) insertion than dATP insertion (*R* = 10% and *S* = 7%). When all four dNTPs were added to the mixture, the (*R*)-2Ih was extended with a 34% yield and

(*S*)-2Ih was extended in a 21% yield (Figure 3.2). These observations demonstrate when 2Ih is present in DNA to be PCR amplified by Hemo KlenTaq, these strands will be poorly extended to full length amplicons, and they will have twofold more G•C → C•G than G•C → T•A transversion mutations. The (*R*)-2Ih isomer showed less inhibition for Hemo KlenTaq bypass than (*S*)-2Ih. The (*R*)-Sp and (*S*)-Sp diastereomers were shown to yield insertion for dATP (20% and 9%) or dGTP (17% and 7%) by Hemo KlenTaq with full primer extension of 8% and 5% observed for (*R*)- and (*S*)-Sp, respectively (Figure 3.2).

These results illustrate how three polymerases select dNTPs when either of the 2-Ih diastereomers were in the template strand. The incorporation efficiencies were found to be polymerase dependent. All three polymerases studied incorporated dGTP opposite 2Ih more than dATP; in contrast, when Sp was in the template, there was a nearly identical level of insertion of dGTP vs. dATP opposite. Because 2Ih and Sp have similar structures in the B ring (Figure 3.3), the large contrast in dNTP insertion opposite them was unexpected. Thus, selection of dNTPs opposite 2Ih or Sp must be determined by other features than their similar B-ring structures or similarity in the geometric arrangement of atoms for the diastereomers (Figure 3.3). Full extension of the primer with either 2Ih diastereomer in the template could be extended with all three polymerases, but not with high efficiency like that observed for a template G. According to this, 2Ih lesions can inhibit the replication by polymerases during *in vitro* DNA synthesis. These results identify that 2Ih lesions in DNA can predominantly induce G•C → C•G transversion mutations and to a lesser degree cause G•C → T•A transversion mutations. The Sp lesions showed a higher inhibition and cause greater

blocking for polymerases compared to 2Ih. The Sp lesions cause nearly equal amounts of G•C → C•G and G•C → T•A transversion mutations, a result consistent with previous studies.[37,38]

*DNA glycosylase activity toward the diastereomers of 2Ih*

DNA glycosylase activity was measured using ODN 3 (Y = (*R*)-2Ih, (*S*)-2Ih, (*R*)-Sp, and (*S*)-Sp) for a ssODN context with NEIL1, and ODN 3 (Y = (*R*)-2Ih, (*S*)-2Ih, (*R*)-Sp, and (*S*)-Sp) annealed with ODN 4 (N = A, C, G, or T) as a dsODN context with the NEIL1, Fpg, or Nth enzymes. Repair activity was analyzed by PAGE after the reactions were run for 20 min and quenched with NaOH (0.2 M) and heat (90 °C for 2 min). NEIL1 successfully cleaved 2Ih-containing dsODNs and showed a 50% yield for (*R*)-2Ih•C and a 25% yield for (*S*)-2Ih•C (Figure 3.4A and B). These reactivities were compared to Sp-containing dsODN that gave > 95% cleavage for (*R*)-Sp•C and 45% for (*S*)-Sp•C. From this comparison, the activity of NEIL1 toward 2Ih-containing dsODNs was half that observed with Sp. Therefore, 2Ih is a substrate for NEIL1, but not as good as Sp in this context. Next, NEIL1 activity toward (*R*)-2Ih and (*S*)-2Ih-containing dsODNs with different bases (A, C, G, or T) opposite showed the repair efficiency to be independent of the base-pair partner (Figure 3.4A and B). When Fpg was assayed for cleavage of (*R*)-2Ih- and (*S*)-2Ih-containing dsODNs, 35% and 20% product formation was observed, respectively (Figure 3.4A and B). The cleavage activity of Fpg toward (*R*)-2Ih and (*S*)-2Ih was a little lower than observed for (*R*)-Sp•C (40%) and (*S*)-Sp•C (25%). When the base pair partners were changed, Fpg showed a similar activity toward (*R*)-2Ih and (*S*)-2Ih opposite any of the four nucleotides. The 2Ih lesions were shown to

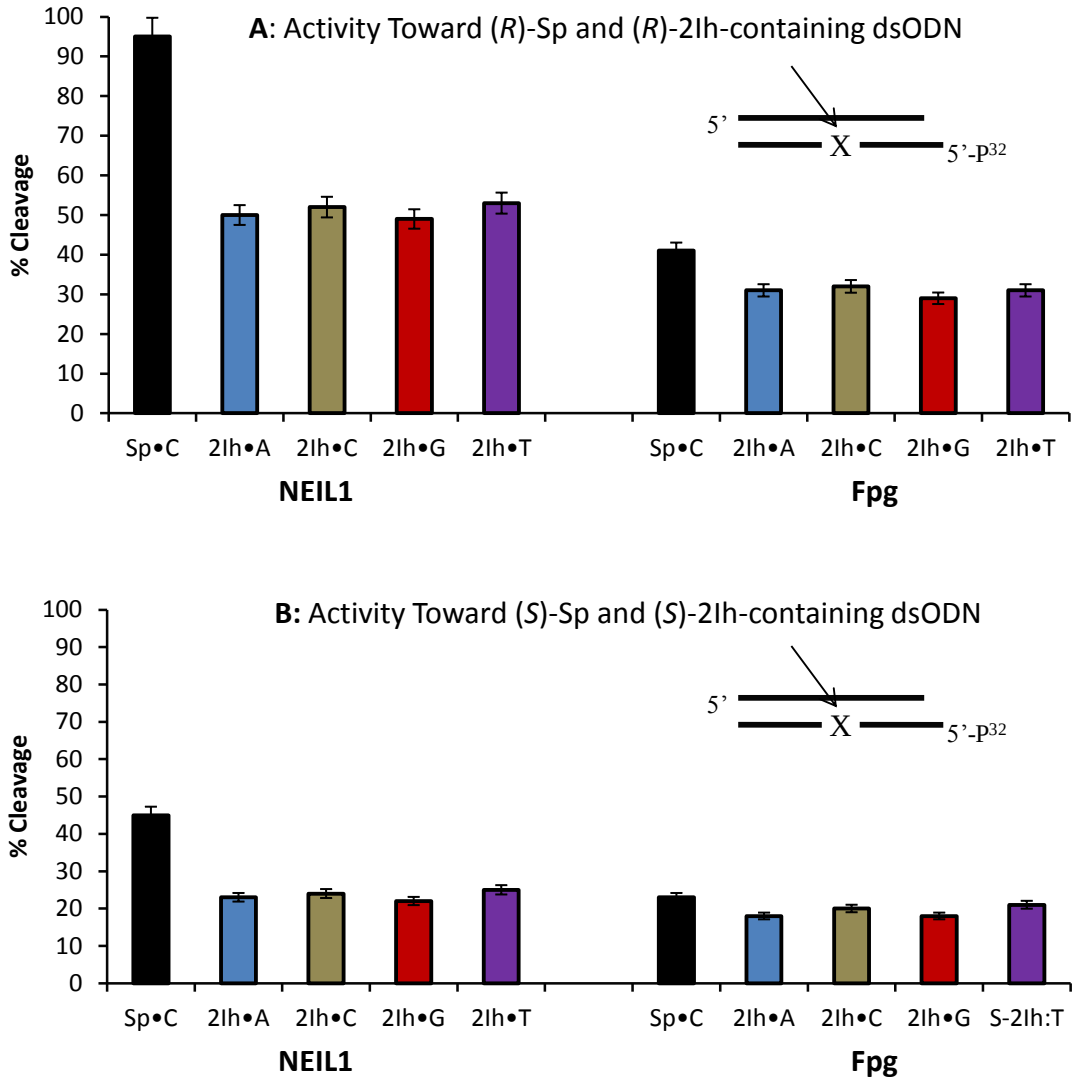


**Figure 3.4.** Comparison of NEIL1 or Fpg DNA glycosylase activity toward dsODNs containing X (X = 2Ih or Sp lesions). (A) Studies when (*R*)-2Ih was base paired with A, C, G, or T and compared to (*R*)-Sp•C, and (B) studies when (*S*)-2Ih base paired with A, C, G, or T was compared to (*S*)-Sp•C.

be substrates for Fpg with similar cleavage efficiency as observe for Sp. Finally, Nth was able to cleave the dsODNs with (*R*)-2Ih (15%), (*S*)-2Ih (10%), (*R*)-Sp (16%), (*S*)-Sp (11%). Compared to Fpg and NEIL1, Nth showed the lowest activity toward 2Ih and Sp lesions, the latter result is consistent with literature reports.[47] The DNA glycosylase activity toward 2Ih-containing dsODNs, both the *R* or *S* isomers were found to give activity in the order of NEIL1> Fpg> Nth. NEIL1 was able to cleave the 2Ih-containing ssODN to 50% yield for (*R*)-2Ih and 20% yield for *S*-2Ih (Figure 3.5). The Sp-containing ssODNs containing either *R* or *S* isomers were better substrates than 2Ih-containing ssODNs, and (*R*)-Sp cleavage was 70% while 25% cleavage was observed for (*S*)-Sp. When DNA lesions cause polymerases to miscode the original message, they cause a mutation if not repaired.[3,70] The ability of NEIL1 to initiate repair of the 2Ih lesions in ssODN and dsODNs suggests that cells can defend against them. NEIL1 showed a higher cleavage activity toward Sp in agreement with previous studies.[53-55] The 2Ih lesions are viable candidate substrates for cleavage by NEIL1. Fpg was able to cleave both 2Ih and Sp in dsODN with slightly lower efficiency compared to NEIL1 (Figure 3.4A and B). Again, the Sp lesion cleavage by Fpg was in agreement with previous studies.[56,57] The 2Ih lesion is a potential substrate for Fpg to act upon, similarly to other modified purines[71] including the initially identified substrates Fapy-G and OG.[43,72,73]

Nth has shown good activity toward several modified pyrimidine bases,[74-78] and very low activity toward modified purines such as Z, Gh, and Sp.[47,48] In this study, Nth has the lowest activity among the glycosylases to remove 2Ih and Sp. The results showed that the *R* isomer of either Sp or 2Ih was always a better substrate for BER

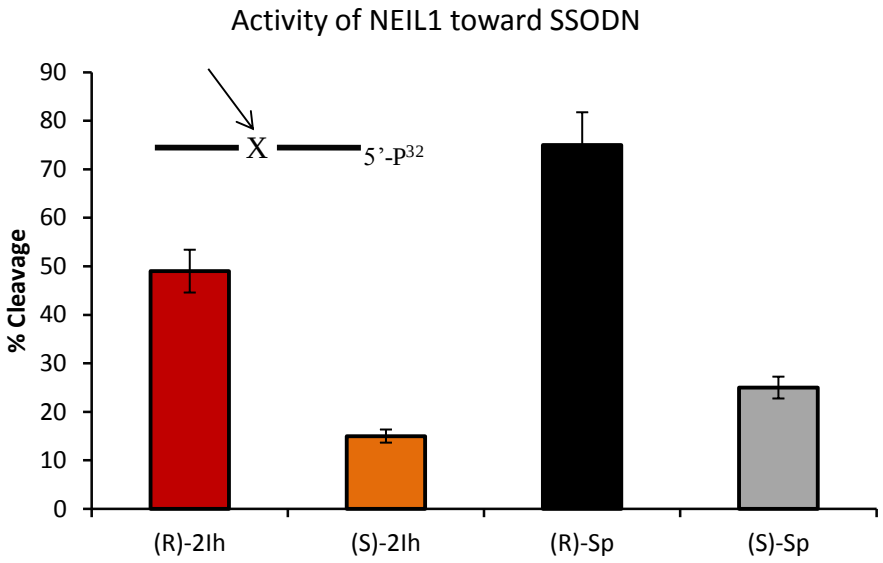


**Figure 3.5.** Glycosylase activity of NEIL1 toward ssODNs containing X (X = (*R*)-2Ih, (*S*)-2Ih, (*R*)-Sp, and (*S*)-Sp).

glycosylases than the *S* isomer. The preference of (*R*)-Sp over (*S*)-Sp for NEIL1 is not in agreement with what was previously reported in our laboratory.[53,54] This difference may indicate that DNA glycosylase activity is dependent on the configuration of lesions as well as the sequence context. The length of the ODN in our previous studies was 30 nucleotides with a context of 5'-CXT-3' (X = (*R*)-Sp or (*S*)-Sp), while the present ODN was 15 nucleotides with the context of 5'-CXA-3' (X = (*R*)-Sp or (*S*)-Sp). Further studies with different sequence contexts and different lengths of ODN would address the importance of sequence length and context for repair activity by NEIL1.

*$T_m$ and CD analysis of 2Ih in dsODNs*

Next, experiments were conducted to address the favorability of dGTP insertion opposite 2Ih in a template strand by a DNA polymerase. As a first test, the halfway points through the melting transition ($T_m$) for duplexes containing 2Ih and their CD spectra were measured. The duplex ODN comprised of the 15-mer ODN 3 with (*R*)-2Ih or (*S*)-2Ih opposite all four canonical nucleotides in ODN 4 (N = A, C, G, or T) allowed $T_m$ and CD spectra of these dsODNs in comparison to a control dsODN containing a G•C base pair. The $T_m$ of ODN with a G•C base pair was 58.5 °C (Figure 3.6). The $T_m$ of ODNs with (*R*)-2Ih•G and (*S*)-2Ih•G base pairs were 11.0 and 9.5 °C less than the G•C base pair, respectively. The (*R*)-2Ih•A and (*S*)-2Ih•A base pairs showed a $T_m$ of 16.5 and 16.0 °C lower than the G•C base pair, respectively. The 2Ih•A base pairs gave $T_m$ values 6.5 °C less than the 2Ih•G base pair. The $T_m$ of dsODNs when 2Ih was base paired opposite C or T was relatively lower than the 2Ih•G or 2Ih•A base pairs, and was as follows: (*R*)-2Ih•C was 39.0 °C, (*S*)-2Ih•C was 39.5 °C, while (*R*)-2Ih•T and (*S*)-

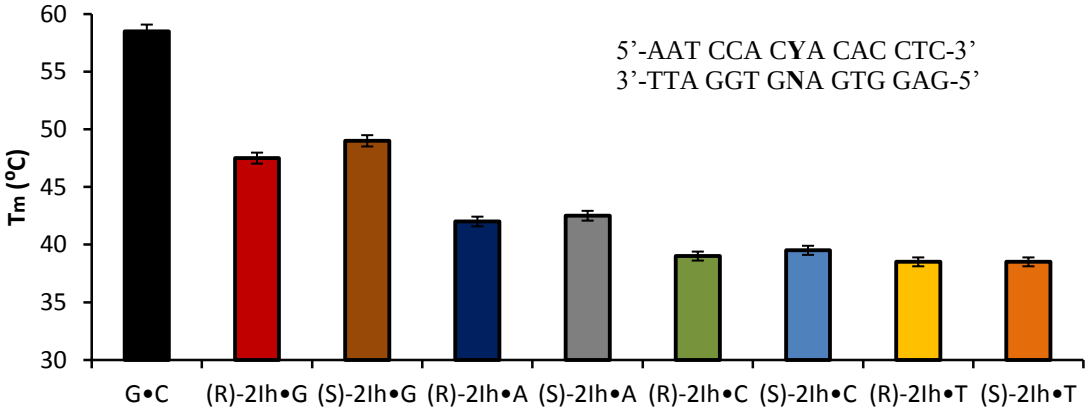


**Figure 3.6.** $T_m$ analysis data for the 15 mers dsODN, when Y = (*R*)-2Ih or (*S*)-2Ih and N = A, C, G, or T.

2Ih•T were 38.5 °C (Figure 3.6). From these results, the thermal stability of duplexes containing 2Ih was significantly reduced compared to duplexes with unmodified G. The thermal stability for all duplexes followed a trend decreasing from 2Ih•G > 2Ih•A > 2Ih•C ~ 2Ih•T. These results indicate that 2Ih-containing ODN duplexes with G opposite are the most stable. This adds one line of evidence why dGTP was the preferred nucleotide inserted opposite the 2Ih lesions. Further reasoning for dGTP selection opposite the 2Ih lesions may include hydrogen bonding and base stacking. These properties will be determined when a high-resolution structure is solved of a duplex with the 2Ih base pairs.

The CD spectra for dsODNs with a G•C base pair as a control and (*R*)-2Ih or (*S*)-2Ih when base paired with A, C, G, or T were measured. These CD spectra showed no significant difference in the $\lambda_{max}$ (277 nm) and $\lambda_{min}$ (240 nm, Figure 3.7) between the control duplex and those bearing the 2Ih lesions. These results highlight that 2Ih does not significantly distort the structure of a 15-mer duplex. Previous studies also demonstrated that the Sp diastereomers did not significantly distort the CD spectra for a short duplex.[79] These studies support the structural hypothesis that 2Ih and Sp only lead to local disruption of the duplex structure. In the case of Sp, molecular dynamic simulations found that Sp distorted two base pairs 5' and 3' to the lesion,[80] 2Ih most likely has a similar impact on the duplex structure.

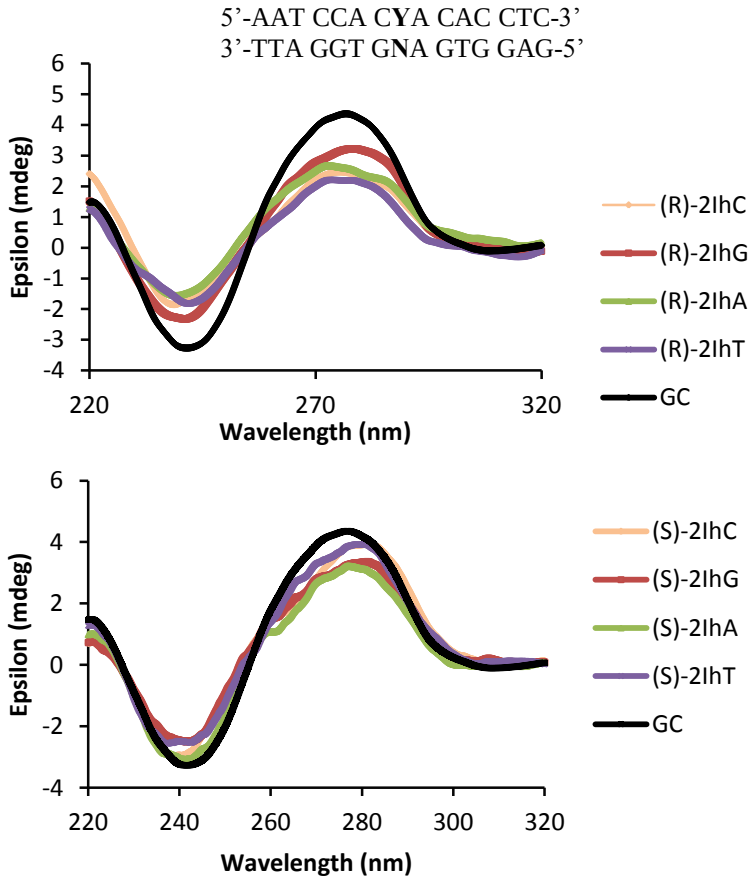


**Figure 3.7.** CD analysis data for the 15 mers dsODN, when Y = (*R*)-2Ih or (*S*)-2Ih and N = A, C, G, T.

*Determination of energetically preferred conformations for the 2Ih diastereomers by DFT calculations*

These computational studies and their interpretation were conducted by Dr. Aaron Fleming. Inspection of the 2Ih nucleosides identifies three rotatable bonds that could lead to energetically favorable conformations (Figure 3.3). A series of DFT calculations were conducted to scan the dihedral angles of these bonds to identify the lowest energy conformations for the two diastereomers. To allow these calculations to finish in a reasonable amount of time, scans of the energy vs. bond angle were conducted for the C1',N9 bond and the C4,C5 bond when they were locked (Figure 3.8), while letting the N9,C8 bond to freely rotate during each calculation. The bond angles were scanned in 18° increments for each bond (400 total calculations) in the diastereomers utilizing the B3LYP functional and 6-31G basis set while implicitly defining the solvent as water with the PCM model. Lastly, methyl groups were placed on the 3' and 5' alcohols to prevent these groups from acting as H-bond donors. The energy minimization calculations identified distinct conformations, and these lowest energy conformations from the scans were resubmitted to geometric optimization calculations in which all bonds were allowed to freely rotate. These final structures are the ones reported in Figure 3.9.

The computational geometric optimizations identified two low energy conformations for (*R*)-2Ih that differed in energy by 2.5 kcal/mol and one low energy conformation for (*S*)-2Ih. A few key structural features were identified from these energy minimization calculations. The lowest energy structures were all observed to have H-bonds (distance ~1.6 – 2.0 Å) between the base and sugar, a feature that was not

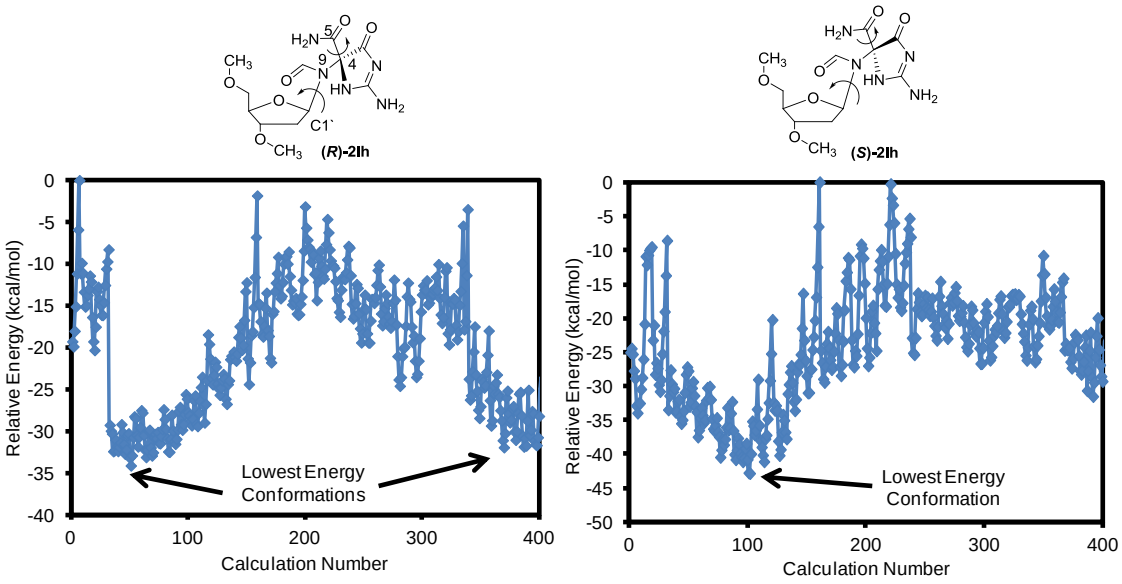


**Figure 3.8**. DFT dihedral scans for the 2Ih diastereomers to identify the lowest energy conformations. Relative energy vs. calculation number for the *R* (left) and *S* (right) diastereomers of 2Ih are provided. The energies were obtained using the B3LYP-6-31G functional and basis set while implicitly defining the solvent as water with the PCM model.

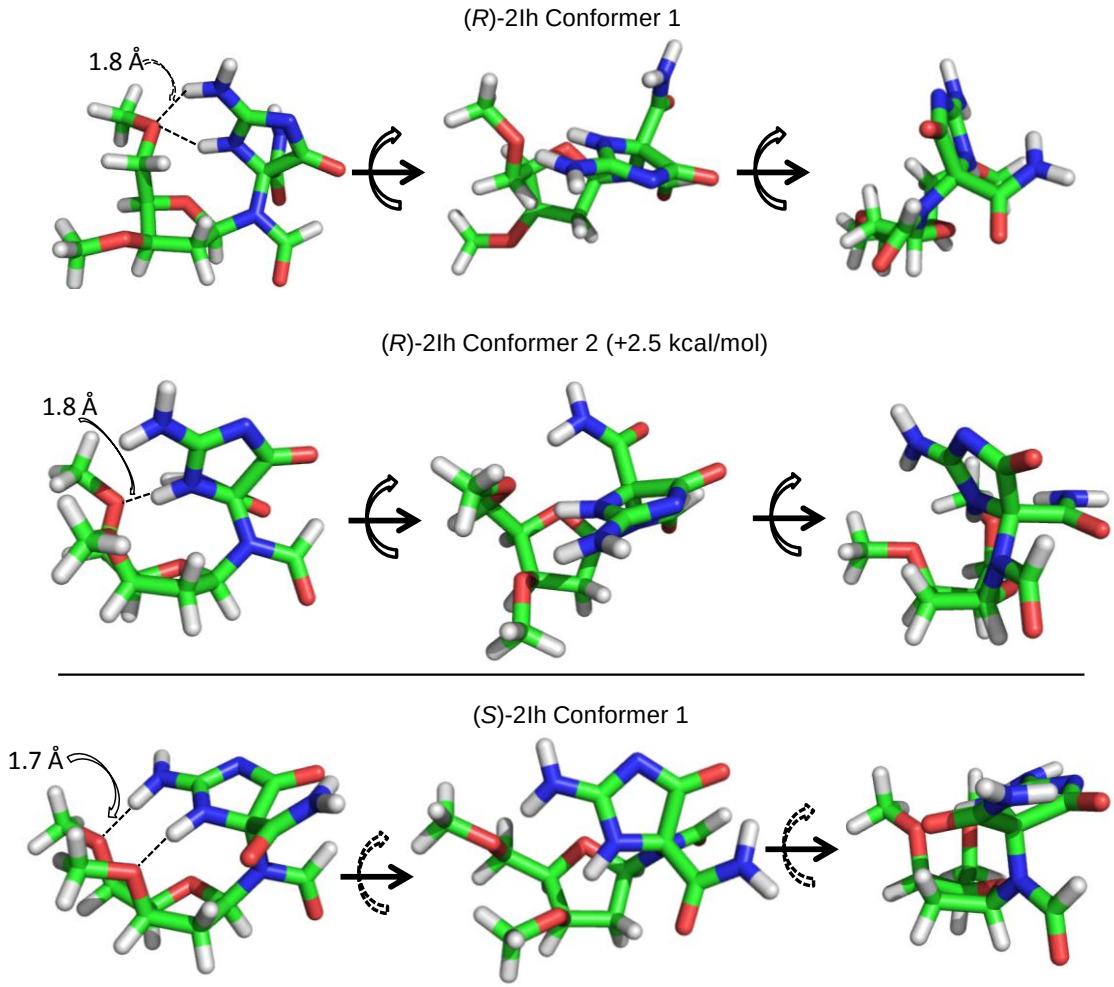


**Figure 3.9.** The lowest energy conformations for the 2Ih diastereomers identified by DFT dihedral scan calculations.

observed in the higher energy structures. Specifically, the lowest energy (*R*)-2Ih conformer has two H-bonds (N3-*O*5', and $N^2$-*O*5'), while the second lowest energy conformation has one H-bond (N3-*O*5', Figure 3.9). The lowest energy (*S*)-2Ih conformation has two H-bonds (N3,*O*3', and $N^2$,*O*5', Figure 3.9) between the base and Sugar. The ability to H-bond between the base and the sugar is a feature that has not been observed for the diastereomers of Sp.[81] These structures provide initial clues to the stereochemical dependency of the polymerase and BER assays previously described. The polymerase studies consistently found the *R* diastereomer of 2Ih to yield twofold greater insertion of dNTPs and bypass relative to the *S* isomer (Figure 3.2 and 3.3). Further, this stereochemical dependency is independent of the polymerase studied suggesting that polymerase activity is dependent on the lesion. The selection of dGTP vs. dATP was nearly the same for the two diastereomers of 2Ih. Polymerase activity on lesion-containing DNA templates will be most efficient if the lesion has complementary H-bonds with an incoming dNTP and the lesion does not distort the polymerase active site preventing the ability to catalyze further polymerization of dNTPs. The 2Ih diastereomers are not planar, and based on the calculations the closed ring is poorly positioned to select a dNTP based on H-bonding potential. Therefore, selection of dGTP or dATP could be due to H-bonds to the amide or formamide groups. Alternatively, if selection is based on dNTP size, slightly larger dGTP would be favored over dATP. Confirmation of nucleotide selection will be best answered when an X-ray crystal structure is solved for 2Ih in the active site of a polymerase. In contrast to the 2Ih results, the Sp diastereomers yielded nearly equal amounts of dATP and dGTP insertion (Figure 3.2), an observation that identifies dNTP selection to not be entirely

sterochemically dependent.

Lesion bypass for distorting lesions, such as the 2Ih diastereomers, will show the greatest yield for the isomer that is most accommodating for dNTP insertion after processing of the lesion. On the basis of the DFT scans, the *R* isomer of 2Ih has a greater degree of flexibility, likely allowing greater bypass. In contrast, the *S* isomer of 2Ih adopts one conformation that is stabilized by two internal H-bonds leading to a potentially more rigid structure that could be more challenging for polymerases to bypass (Figure 3.8 and 3.9). Further, this structure provides a nonplanar base for the next dNTP to $\pi$ stack with, leading to lower bypass efficiency. In contrast, the Sp diastereomers with two fused rings are more poorly bypassed by polymerases than 2Ih (Figure 3.2). This observation results from the propeller shape of the Sp base, a feature that has previously been described in the literature.[80]

Lesion selection and cleavage rate by BER enzymes will be dependent on a number of factors. First, lesion recognition by the DNA glycosylase, and the ability for the active-site nucleophilic lysine residue (Fpg = Lys57 and NEIL = Lys53)[82,83] to initiate *N*-glycosydic bond hydrolysis and strand scission are lesion structure dependent. Again, the DFT calculations identified (*R*)-2Ih to adopt more conformations than (*S*)-2Ih. This greater degree of flexibility may allow the *R* isomer to be more easily processed than the *S* isomer. This claim is consistent with the experimental results in which (*R*)-2Ih was more efficiently acted on by Fpg and NEIL1 than (*S*)-2Ih (Figure 3.4 and 3.5). Experiments that evaluate the stereochemical dependency of 2Ih to be repaired and cause mutations *in vivo* will ultimately determine if these structure based arguments hold in the cell. A similar set of comparative studies have been conducted for the Sp

diastereomers that found the *in vitro* work to provide some explanations for the *in vivo* studies.[37,40]

These comparative studies between 2Ih and Sp as substrates for polymerases and BER DNA glycosylase removal have identified properties of 2Ih that might be characteristic of this lesion in the cell. First, the diastereomers of 2Ih will lead to twofold greater G•C → C•G transversion mutations than G•C → T•A; in contrast, the Sp diastereomers gave nearly equal amounts of G•C → C•G and G•C → T•A transversion mutations. Further, the *R* diastereomer of 2Ih was most easily bypassed by polymerases leading to a greater degree of mutations in the cell. On the basis of these studies, 2Ih will not be as efficiently removed by DNA glycosylases compared to Sp. This feature supports a hypothesis that 2Ih is a highly mutagenic lesion in DNA.

**Conclusions**

This study demonstrates that the G-oxidation lesion 2Ih when bypassed by DNA polymerases induces misinsertion of dGTP and to a lesser extent dATP during replication *in vitro* and leads to a significant block for DNA elongation. The insertion of dGTP or dATP opposite 2Ih leads to G•C → C•G and G•C → T•A transversion mutations. Transversion mutations at G similar to those identified in these studies for 2Ih have been characterized in a number of cancers and diseases.[5] These studies also verify that 2Ih is a substrate for the BER DNA glycosylases. The NEIL1 DNA glycosylase showed activity toward 2Ih in ssODN and dsODNs. Curiously, NEIL1 was able to remove 2Ih in dsODNs regardless of which base was in the opposite strand. Lastly, Fpg and Nth were able to remove 2Ih in dsODNs with lower efficiency

compared to NEIL1. Fpg was similar to NEIL1 with removal of 2Ih being independent of the base opposite. These results suggest that polymerases maintain a low degree of activity when 2Ih is in the template strand and DNA glycosylases can initiate the BER process to avoid mutations derived from this lesion.

In comparison to its close analog Sp, 2Ih shows greater differences between the (*R*) and (*S*) diastereomers when being processed by either polymerases or BER glycosylases. Additionally, the extent of lesion bypass was significantly greater for both 2Ih diastereomers compared to Sp but particularly high for (*R*)-2Ih, while the extent of repair was lower for 2Ih compared to Sp. These results suggest that 2-Ih, particularly the (*R*) diastereomer, could accumulate in the genome, inducing G•C → C•G and, to a lesser extent, G•C → T•A transversion mutations.

The present work paints an initial picture of the potential mutational profile of the 2Ih lesions. We recently showed that 2Ih is formed *in vitro* from ionizing radiation and Fenton-catalyzed oxidation to a similar extent as OG,[21,28] suggesting that it is a significant lesion *in vivo*. While the OG lesion is very readily bypassed, it also benefits from an efficient repair system for both the OG:C and OG:A base pairs in DNA.[3] OG has been widely studied in various contexts in DNA and RNA, and these studies benefit from the synthetic availability of the OG phosphoramidite. Until a better synthesis to oligomers containing 2Ih in specific sequence contexts is available, further biochemical studies of 2Ih remain challenging.

**References**


1. Beckman, K. B., and Ames, B. N. (1997) Oxidative decay of DNA, *J. Biol. Chem. 272*, 19633-19636.

2. Wallace, S., Murphy, D., and Sweasy, J. (2012) Base excision repair and cancer, *Cancer Lett. 327*, 73-89.

3. David, S. S., O'Shea, V. L., and Kundu, S. (2007) Base-excision repair of oxidative DNA damage, *Nature 447*, 941-950.

4. Modrich, P., and Lahue, R. (1996) Mismatch repair in replication fidelity, genetic recombination, and cancer biology, *Annu. Rev. Biochem. 65*, 101-133.

5. Pfeifer, G., and Besaratinia, A. (2009) Mutational spectra of human cancer, *Hum. Genet. 125*, 493-506.

6. Steenken, S., and Jovanovic, S. V. (1997) How easily oxidizable is DNA? One-electron reduction potentials of adenosine and guanosine radicals in aqueous solution, *J. Am. Chem. Soc. 119*, 617-618.

7. Angelov, D., Spassky, A., Berger, M., and Cadet, J. (1997) High-intensity UV laser photolysis of DNA and purine 2'-deoxyribonucleosides: formation of 8-oxopurine damage and oligonucleotide strand cleavage as revealed by HPLC and gel electrophoresis studies, *J. Am. Chem. Soc. 119*, 11373-11380

.

8. Douki, T., Martini, R., Ravanat, J.-L., Turesky, R. J., and Cadet, J. (1997) Measurement of 2,6-diamino-4-hydroxy-5-formamidopyrimidine and 8-oxo-7,8-dihydroguanine in isolated DNA exposed to gamma radiation in aqueous solution, *Carcinogenesis 18*, 2385-2391.

9. Crean, C., Geacintov, N. E., and Shafirovich, V. (2005) Oxidation of guanine and 8-oxo-7,8-dihydroguanine by carbonate radical anions: insight from oxygen-18 labeling experiments, *Ang. Chem. Int. Ed. 44*, 5057-5060.

10. Cui, L., Ye, W., Prestwich, E. G., Wishnok, J. S., Taghizadeh, K., Dedon, P. C., and Tannenbaum, S. R. (2013) Comparative analysis of four oxidized guanine lesions from reactions of DNA with peroxynitrite, singlet oxygen, and γ-radiation, *Chem. Res. Toxicol. 26*, 195-202.

11. Fleming, A. M., Muller, J. G., Dlouhy, A. C., and Burrows, C. J. (2012) Structural context effects in the oxidation of 8-oxo-7,8-dihydro-2'-deoxyguanosine to hydantoin products: electrostatics, base stacking, and base pairing, *J. Am. Chem. Soc. 134*, 15091-15102.

12. Gremaud, J. N., Martin, B. D., and Sugden, K. D. (2010) Influence of substrate

complexity on the diastereoselective formation of spiroiminodihydantoin and guanidinohydantoin from chromate oxidation, *Chem. Res. Toxicol. 23*, 379-385.

13. Joffe, A., Geacintov, N. E., and Shafirovich, V. (2003) DNA lesions derived from the site selective oxidation of guanine by carbonate radical anions, *Chem. Res. Toxicol. 16*, 1528-1538.

14. Luo, W., Muller, J. G., and Burrows, C. J. (2001) The pH-dependent role of superoxide in riboflavin-catalyzed photooxidation of 8-oxo-7,8-dihydroguanosine, *Org. Lett. 3*, 2801-2804.

15. Luo, W., Muller, J. G., Rachlin, E. M., and Burrows, C. J. (2000) Characterization of spiroiminodihydantoin as a product of one-electron oxidation of 8-oxo-7,8-dihydroguanosine, *Org. Lett. 2*, 613-616.

16. Luo, W., Muller, J. G., Rachlin, E. M., and Burrows, C. J. (2001) Characterization of hydantoin products from one-electron oxidation of 8-oxo-7,8-dihydroguanosine in a nucleoside model, *Chem. Res. Toxicol. 14*, 927-938.

17. Niles, J. C., Wishnok, J. S., and Tannenbaum, S. R. (2004) Spiroiminodihydantoin and guanidinohydantoin are the dominant products of 8-oxoguanosine oxidation at low fluxes of peroxynitrite: mechanistic studies with $^{18}O$, *Chem. Res. Toxicol. 17*, 1510-1519.

18. Sugden, K. D., Campo, C. K., and Martin, B. D. (2001) Direct oxidation of guanine and 7,8-dihydro-8-oxoguanine in DNA by a high-valent chromium complex: a possible mechanism for chromate genotoxicity, *Chem. Res. Toxicol. 14*, 1315-1322.

19. Suzuki, T., Friesen, M. D., and Ohshima, H. (2003) Identification of products formed by reaction of 3',5'-di-*O*-acetyl-2'-deoxyguanosine with hypochlorous acid or a myeloperoxidase−$H_2O_2$−$Cl^-$ System, *Chem. Res. Toxicol. 16*, 382-389.

20. Banu, L., Blagojevic, V., and Bohme, D. K. (2012) Lead(II)-catalyzed oxidation of guanine in solution studied with electrospray ionization mass spectrometry, *J. Phys. Chem. B. 116*, 11791–11797.

21. Fleming, A. M., Muller, J. G., Ji, I., and Burrows, C. J. (2011) Characterization of 2'-deoxyguanosine oxidation products observed in the Fenton-like system Cu(II)/$H_2O_2$/reductant in nucleoside and oligodeoxynucleotide contexts, *Org. Biomol. Chem. 9*, 3338-3348.

22. Ghude, P., Schallenberger, M. A., Fleming, A. M., Muller, J. G., and Burrows, C. J. (2011) Comparison of transition metal-mediated oxidation reactions of guanine in nucleoside and single-stranded oligodeoxynucleotide contexts, *Inorg. Chem. Acta 369*, 240-246.

23. Li, L., Murthy, N. N., Telser, J., Zakharov, L. N., Yap, G. P., Rheingold, A. L., Karlin, K. D., and Rokita, S. E. (2006) Targeted guanine oxidation by a dinuclear copper(II) complex at single stranded/double stranded DNA junctions, *Inorg. Chem. 45*, 7144-7159.

24. Rokhlenko, Y., Geacintov, N. E., and Shafirovich, V. (2012) Lifetimes and reaction pathways of guanine radical cations and neutral guanine radicals in an oligonucleotide in aqueous solutions, *J. Am. Chem. Soc. 134*, 4955-4962.

25. Tomaszewska, A., Mourgues, S., Guga, P., Nawrot, B., and Pratviel, G. (2012) A single nuclease-resistant linkage in DNA as a versatile tool for the characterization of DNA lesions: application to the guanine oxidative lesion "G+34" generated by metalloporphyrin/$KHSO_5$ reagent, *Chem. Res. Toxicol. 25*, 2505-2512.

26. Vialas, C., Claparols, C., Pratviel, G., and Meunier, B. (2000) Guanine oxidation in double-stranded DNA by Mn-TMPyP/$KHSO_5$: 5,8-dihydroxy-7,8-dihydroguanine residue as a key precursor of imidazolone and parabanic acid derivatives, *J. Am. Chem. Soc. 122*, 2157-2167.

27. Ye, W., Sangaiah, R., Degen, D. E., Gold, A., Jayaraj, K., Koshlap, K. M., Boysen, G., Williams, J., Tomer, K. B., Mocanu, V., Dicheva, N., Parker, C. E., Schaaper, R. M., and Ball, L. M. (2009) Iminohydantoin lesion induced in DNA by peracids and other epoxidizing oxidants, *J. Am. Chem. Soc. 131*, 6114-6123.

28. Alshykhly, O. R., Fleming, A. M., and Burrows, C. J. (2015) 5-Carboxamido-5-formamido-2-iminohydantoin, in addition to 8-oxo-7,8-dihydroguanine, is the major product of the iron-Fenton or X-ray radiation-induced oxidation of guanine under aerobic reducing conditions in nucleoside and DNA contexts, *J. Org. Chem. 80*, 6996-7007.

29. Gedik, C. M., and Collins, A. F. (2005) Establishing the background level of base oxidation in human lymphocyte DNA: results of an interlaboratory validation study, *FASEB J. 19*, 82-84.

30. Hailer, M. K., Slade, P. G., Martin, B. D., and Sugden, K. D. (2005) Nei deficient *Escherichia coli* are sensitive to chromate and accumulate the oxidized guanine lesion spiroiminodihydantoin, *Chem. Res. Toxicol. 18*, 1378-1383.

31. Mangerich, A., Knutson, C. G., Parry, N. M., Muthupalani, S., Ye, W., Prestwich, E., Cui, L., McFaline, J. L., Mobley, M., Ge, Z., Taghizadeh, K., Wishnok, J. S., Wogan, G. N., Fox, J. G., Tannenbaum, S. R., and and Dedon, P. C. (2012) Infection-induced colitis in mice causes dynamic and tissue-specific changes in stress response and DNA damage leading to colon cancer, *Proc. Natl. Acad. Sci. U.S.A. 109*, E1820-E1829.

32. Matter, B., Malejka-Giganti, D., Csallany, A. S., and Tretyakova, N. (2006) Quantitative analysis of the oxidative DNA lesion, 2,2-diamino-4-(2-deoxy-beta-D-erythro-pentofuranosyl)amino]-5(*2H*)-oxazolone (oxazolone), *in vitro* and *in vivo* by isotope dilution-capillary HPLC-ESI-MS/MS, *Nucleic Acids Res. 34*, 5449–5460.

33. Pouget, J.-P., Frelon, S., Ravanat, J.-L., Testard, I., Odin, F., and Cadet, J. (2002) Formation of modified DNA bases in cells exposed either to gamma radiation or to high-LET particles, *Radiat. Res. 157*, 589-595.

34. Duarte, V., Muller, J. G., and Burrows, C. J. (1999) Insertion of dGMP and dAMP during *in vitro* DNA synthesis opposite an oxidized form of 7,8-dihydro-8-oxoguanine, *Nucleic Acids Res. 27*, 496-502.

35. Lowe, L. G., and Guengerich, F. P. (1996) Steady-state and pre-steady-state kinetic analysis of dNTP insertion opposite 8-oxo-7,8-dihydroguanine by *Escherichia coli* Polymerases I exo$^-$ and II exo$^-$ *Biochemistry 35*, 9840-9849.

36. Shibutani, S., Takeshita, M., and Grollman, A. P. (1991) Insertion of specific bases during DNA synthesis past the oxidation-damaged base 8-oxodG, *Nature 349*, 431-434.

37. Kornyushyna, O., Berges, A. M., Muller, J. G., and Burrows, C. J. (2002) *In vitro* nucleotide misinsertion opposite the oxidized guanosine lesions spiroiminodihydantoin and guanidinohydantoin and DNA synthesis past the lesions using *Escherichia coli* DNA polymerase I (Klenow fragment), *Biochemistry 41*, 15304-15314.

38. Kornyushyna, O., and Burrows, C. J. (2003) Effect of the oxidized guanosine lesions spiroiminodihydantoin and guanidinohydantoin on proofreading by *Escherichia coli* DNA polymerase I (Klenow fragment) in different sequence contexts, *Biochemistry 42*, 13008-13018.

39. Neeley, W. L., and Essigmann, J. M. (2006) Mechanisms of formation, genotoxicity, and mutation of guanine oxidation products, *Chem. Res. Toxicol. 19*, 491-505.

40. Henderson, P. T., Delaney, J. C., Muller, J. G., Neeley, W. L., Tannenbaum, S. R., Burrows, C. J., and Essigmann, J. M. (2003) The hydantoin lesions formed from oxidation of 7,8-dihydro-8-oxoguanine are potent sources of replication errors *in vivo*, *Biochemistry 42*, 9257−9262.

41. Neeley, W., Delaney, S., Alekseyev, Y., Jarosz, D., Delaney, J., Walker, G., and Essigmann, J. (2007) DNA polymerase V allows bypass of toxic guanine oxidation products *in vivo*, *J. Biol. Chem. 282*, 12741-12748.

42. Wilson III, D. M., and Bohr, V. A. (2007) The mechanics of base excision repair, and its relationship to aging and disease, *DNA Repair 6*, 544-559.

43. Michaels, M. L., Tchou, J., Grollman, A. P., and Miller, J. H. (1992) A repair system for 8-oxo-7,8-dihydrodeoxyguanine, *Biochemistry 31*, 10964-10968.

44. David, S. S., and Williams, S. D. (1998) Chemistry of glycosylases and endonucleases involved in base-excision repair, *Chem. Rev. 98*, 1221-1262.

45. Delaney, S., Neeley, W. L., Delaney, J. C., and Essigmann, J. M. (2007) The substrate specificity of MutY for hyperoxidized guanine lesions *in vivo*, *Biochemistry 46*, 1448-1455.

46. Barnes, D. E., and Lindahl, T. (2004) Repair and genetic consequences of endogenous DNA base damage in mammalian cells, *Annu. Rev. Genet. 38*, 445-476.

47. Zhou, J., Liu, M., Fleming, A. M., Burrows, C. J., and Wallace, S. S. (2013) Neil3 and NEIL1 DNA glycosylases remove oxidative damages from quadruplex DNA and exhibit preferences for lesions in the telomeric sequence context, *J. Biol. Chem. 288*, 27263-27272.

48. Duarte, V., Gasparutto, D., Jaquinod, M., and Cadet, J. (2000) *In vitro* DNA synthesis opposite oxazolone and repair of this DNA damage using modified oligonucleotides, *Nucleic Acids Res. 28*, 1555-1563.

49. Doublié, S., Bandaru, V., Bond, J. P., and Wallace, S. S. (2004) The crystal structure of human endonuclease VIII-like 1 (NEIL1) reveals a zincless finger motif required for glycosylase activity, *Proc. Natl. Acad. Sci. U. S. A. 101*, 10284-10289.

50. Nakano, T., Katafuchi, A., Shimizu, R., Terato, H., Suzuki, T., Tauchi, H., Makino, K., Skorvaga, M., Van Houten, B., and Ide, H. (2005) Repair activity of base and nucleotide excision repair enzymes for guanine lesions induced by nitrosative stress, *Nucleic Acids Res. 33*, 2181-2191.

51. Hazra, T. K., Izumi, T., Boldogh, I., Imhoff, B., Kow, Y. W., Jaruga, P., Dizdaroglu, M., and Mitra, S. (2002) Identification and characterization of a human DNA glycosylase for repair of modified bases in oxidatively damaged DNA, *Proc. Natl. Acad. Sci. 99*, 3523-3528.

52. Bandaru, V., Sunkara, S., Wallace, S. S., and Bond, J. P. (2002) A novel human DNA glycosylase that removes oxidative DNA damage and is homologous to *Escherichia coli* endonuclease VIII, *DNA Repair 1*, 517-529.

53. Zhao, X., Krishnamurthy, N., Burrows, C. J., and David, S. S. (2010) Mutation

versus repair: NEIL1 removal of hydantoin lesions in single-stranded, bulge, bubble, and duplex DNA contexts, *Biochemistry 49*, 1658-1666.

54. Krishnamurthy, N., Zhao, X., Burrows, C. J., and David, S. S. (2008) Superior removal of hydantoin lesions relative to other oxidized bases by the human DNA glycosylase hNEIL1, *Biochemistry 47*, 7137-7146.

55. Hailer, M. K., Slade, P. G., Martin, B. D., Rosenquist, T. A., and Sugden, K. D. (2005) Recognition of the oxidized lesions spiroiminodihydantoin and guanidinohydantoin in DNA by the mammalian base excision repair glycosylases NEIL1 and NEIL2, *DNA Repair 4*, 41-50.

56. Leipold, M. D., Muller, J. G., Burrows, C. J., and David, S. S. (2000) Removal of hydantoin products of 8-oxoguanine oxidation by the *Escherichia coli* DNA repair enzyme, FPG, *Biochemistry 39*, 14984-14992.

57. Krishnamurthy, N., Muller, J. G., Burrows, C. J., and David, S. S. (2007) Unusual structural features of hydantoin lesions translate into efficient recognition by *Escherichia coli* Fpg, *Biochemistry 46*, 9355-9365.

58. Fleming, A. M., Alshykhly, O., Zhu, J., Muller, J. G., and Burrows, C. J. (2015) Rates of chemical cleavage of DNA and RNA oligomers containing guanine oxidation products, *Chem. Res. Toxicol. 28*, 1292-1300.

59. Karn, J. L., and Busch, D. H. (1966) Nickel (II) complexes of the tetradentate macrocycle 2,12-dimethyl-3,7,11,17-tetraazabicyclo (11.3.1) heptadeca-1 (17),2,11,13,15-pentaene, *Nature 211*, 160-162.

60. Fleming, A. M., Alshykhly, O., Orendt, A. M., and Burrows, C. J. (2015) Computational studies of electronic circular dichroism spectra predict absolute configuration assignments for the guanine oxidation product 5-carboxamido-5-formamido-2-iminohydantoin, *Tetrahedron Lett. 56*, 3191-3196.

61. Fleming, A. M., Orendt, A. M., He, Y., Zhu, J., Dukor, R. K., and and Burrows. (2013) Reconciliation of chemical, enzymatic, spectroscopic and computational data to assign the absolute configuration of the DNA base lesion spiroiminodihydantoin, *J. Am. Chem. Soc. 135*, 18191 - 18204.

62. Frisch, G. W. et al., *Gaussian 09 Revision C.01*, Gaussian, Wallingford, CT (2010).

63. Becke, A. D. (1993) Density-functional thermochemistry. III. The role of exact exchange, *J. Chem. Phys. 98*, 5648-5652.

64. Lee, C., Yang, W., and Parr, R. G. (1988) Development of the Colle-Salvetti correlation-energy formula into a functional of the electron density, *Phys. Rev. B*

*37*, 785-789.

65. Krishnan, R., Binkley, J. S., Seeger, R., and Pople, J. A. (1980) Self-consistent molecular orbital methods. XX. A basis set for correlated wave functions, *J. Chem. Phys. 72*, 650-654.

66. Frisch, M. J., Pople, J. A., and Binkley, J. S. (1984) Self-consistent molecular orbital methods 25. Supplementary functions for Gaussian basis sets, *J. Chem. Phys. 80*, 3265-3269.

67. Scalmani, G., and Frisch, M. J. (2010) Continuous surface charge polarizable continuum models of solvation. I. General formalism, *J. Chem. Phys. 132*, 114110.

68. Tomasi, J., Mennucci, B., and Cammi, R. (2005) Quantum mechanical continuum solvation models, *Chem. Rev. 105*, 2999-3093.

69. Traut, T. (1994) Physiological concentrations of purines and pyrimidines, *Mol. Cell. Biochem. 140*, 1-22.

70. Wallace, S. (2014) Base excision repair: a critical player in many games, *DNA Repair 19*, 14-26.

71. Tchou, J., Bodepudi, V., Shibutani, S., Antoshechkin, I., Miller, J., Grollman, A. P., and Johnson, F. (1994) Substrate specificity of Fpg protein. Recognition and cleavage of oxidatively damaged DNA, *J. Biol. Chem. 269*, 15318-15324.

72. Chetsanga, C. J., and Lindahl, T. (1979) Release of 7-methylguanine residues whose imidazole rings have been opened from damaged DNA by a DNA glycosylase from *Escherichia coli*, *Nucleic Acids Res. 6*, 3673-3684.

73. Tchou, J., Kasai, H., Shibutani, S., Chung, M. H., Laval, J., Grollman, A. P., and Nishimura, S. (1991) 8-oxoguanine (8-hydroxyguanine) DNA glycosylase and its substrate specificity, *Proc. Natl. Acad. Sci. U. S. A. 88*, 4690-4694.

74. Boiteux, S., O'Connor, T. R., Lederer, F., Gouyette, A., and Laval, J. (1990) Homogeneous *Escherichia coli* FPG protein. A DNA glycosylase which excises imidazole ring-opened purines and nicks DNA at apurinic/apyrimidinic sites, *J. Biol. Chem. 265*, 3916-3922.

75. Wang, D., and Essigmann, J. M. (1997) Kinetics of oxidized cytosine repair by endonuclease III of *Escherichia coli*, *Biochemistry 36*, 8628-8633.

76. Hatahet, Z., Kow, Y. W., Purmal, A. A., Cunningham, R. P., and Wallace, S. S. (1994) New substrates for old enzymes. 5-Hydroxy-2'-deoxycytidine and 5-hydroxy-2'-deoxyuridine are substrates for *Escherichia coli* endonuclease III and

formamidopyrimidine DNA N-glycosylase, while 5-hydroxy-2'-deoxyuridine is a substrate for uracil DNA N-glycosylase, *J. Biol. Chem. 269*, 18814-18820.

77. Breimer, L. H., and Lindahl, T. (1984) DNA glycosylase activities for thymine residues damaged by ring saturation, fragmentation, or ring contraction are functions of endonuclease III in *Escherichia coli*, *J. Biol. Chem. 259*, 5543-5548.

78. Boorstein, R. J., Hilbert, T. P., Cadet, J., Cunningham, R. P., and Teebor, G. W. (1989) UV-induced pyrimidine hydrates in DNA are repaired by bacterial and mammalian DNA glycosylase activities, *Biochemistry 28*, 6164-6170.

79. Khutsishvili, I., Zhang, N., Marky, L., Crean, C., Patel, D., Geacintov, N., and Shafirovich, V. (2013) Thermodynamic profiles and nuclear magnetic resonance studies of oligonucleotide duplexes containing single diastereomeric spiroiminodihydantoin lesions, *Biochemistry 52*, 1354-1363.

80. Jia, L., Shafirovich, V., Shapiro, R., Geacintov, N., and Broyde, S. (2005) Structural and thermodynamic features of spiroiminodihydantoin damaged DNA duplexes, *Biochemistry 44*, 13342-13353.

81. Jia, L., Shafirovich, V., Shapiro, R., Geacintov, N., and Broyde, S. (2005) Spiroiminodihydantoin lesions derived from guanine oxidation: structures, energetics, and functional implications, *Biochemistry 44*, 6043-6051.

82. Sidorkina, O. M., and Laval, J. (1998) Role of lysine-57 in the catalytic activities of Escherichia coli formamidopyrimidine-DNA glycosylase (Fpg protein), *Nucleic Acids Res. 26*, 5351-5357.

83. Hazra, T. K., Das, A., Das, S., Choudhury, S., Kow, Y. W., and Roy, R. (2007) Oxidative DNA damage repair in mammalian cells: a new perspective, *DNA Repair 6*, 470-480.

# CHAPTER 4

# pH-DEPENDENT STABILITY FOR THE *N*-GLYCOSIDIC BOND OF 5-CARBOXAMIDO-5-FORMAMIDO-2-IMINOHYDANTOIN

## Introduction

The deoxynucleosides of DNA consist of nucleobases and deoxyribose rings linked together by the *N*-glycosidic bond. For many DNA lesions, changes in the structure of the heterocyclic base may lead to the destabilization and cleavage of the *N*-glycosidic bond to give an abasic site (depurination or depyrimidination).[1] Approximately 2,000–10,000 DNA abasic sites are estimated to form in each human cell every day due to hydrolytic depurination.[2,3] Depurination and depyrimidination is greatly accelerated under acidic conditions and at high temperature.[3-6] Moreover, cleavage of the *N*-glycosidic bond is part of the base excision repair (BER) pathway. DNA glycosylases can recognize damaged bases and excise them by hydrolyzing the *N*-glycosidic bond between the nucleobase and the sugar moiety,[7] leading to abasic sites. Abasic sites in DNA are mutagenic, contribute to cellular aging, and are observed in a number of cancers.[8-10]

The DNA lesion 5-carboxamido-5-formamido-2-iminohydantoin deoxyribonucleoside (d2Ih) is formed upon oxidation of 2'-deoxyguanosine (dG) via

metal-catalyzed, X-ray radiation, and carbonate radical oxidations.[11-19] Additionally, d2Ih exists as a pair of diastereomers, and the absolute configurations for these lesions were determined in our laboratory in which the first eluting peak from a Hypercarb HPLC column is the *S* isomer and the second eluting peak is the *R* isomer.[20] In our previous study, the two diastereomers of d2Ih nucleoside were shown to give the enantiomers of the 2Ih free base if left for 48 h at 37 °C in water. This indicated that the d2Ih lesions have an unstable *N*-glycosidic (C1' –N9) bond between the modified base and sugar susceptible to spontaneous hydrolytic cleavage. Several other damaged bases such as 2,6-diamino-4-hydroxy-5-formamidopyrimidine-2'-deoxyribonucleoside (Fapy-dG) and imidazolone deoxyribonucleoside (dIz) have been found to undergo hydrolysis of the *N*-glycosidic bond and release the free bases.[21,22] Because of these observations, we decided to investigate the stability of the (*R*)-d2Ih and (*S*)-d2Ih *N*-glycosidic bonds over the pH range 4.4 – 8.4. Also at physiological pH 7.4, we investigated the effect of biologically relevant nucleophiles to promote cleavage of the *N*-glycosidic bond. Specifically, spermine (Spm) was studied because it is present in nearly every prokaryotic and eukaryotic cell type in millimolar concentrations.[23] Further, Spm plays a role in gene regulation and proliferation in cells because of its ability to interact with DNA, RNA, and protein.[24] In this study, we found that the *N*-glycosidic bonds of (*R*)-d2Ih and (*S*)-d2Ih are not stable and may be cleaved faster at low pH and in the presence of Spm.

## Experimental

### *Materials*

All chemicals were obtained from commercially available sources and used without further purification.

### *The (R)-d2Ih and (S)-d2Ih nucleoside formation*

The two diastereomers of d2Ih were prepared from oxidation of 3 mM dG in $NaP_i$ buffer (75 mM pH 7.4) in a solution of copper acetate (1 mM) and ascorbic acid (2 mM) by adding $H_2O_2$ (10 mM) at 22 °C for 60 min via a method previously reported by our laboratory.[12] The reaction mixture was injected on a reversed-phase HPLC (RP-HPLC) column. The two diastereomers of d2Ih eluted with the void volume; therefore, we collected the void volume, lyophilized it to dryness, and reinjected it on a Hypercarb column to separate the isomers. The RP-HPLC utilized the following solvents: A = 10 mM $NH_4OAc$ (pH 7.0) in $ddH_2O$ and B = $CH_3CN$. The flow rate was 1 mL/min while monitoring the absorbance at 240 nm. The method was initiated at 1% B for 3 min after which it was increased to 10% over 10 min via a linear gradient and held for 4 min. Next, B was increased to 65% over 10 min and held for 10 min, at which point the run was terminated. The void volume from the previous run was resuspended in $ddH_2O$ and was injected in the Hypercarb column (150 X 4.6 mm, 5 μm). The diastereomers of d2Ih were individually collected during this separation in which (*S*)-d2Ih and (*R*)-d2Ih2 had retention times of 3 and 5 min, respectively (Figure 4.1A). The Hypercarb HPLC method utilized the following solvent system: A = 0.1% acetic acid in $ddH_2O$, and B = methanol, running at a flow rate of 1 mL/min while the absorbance was monitored at

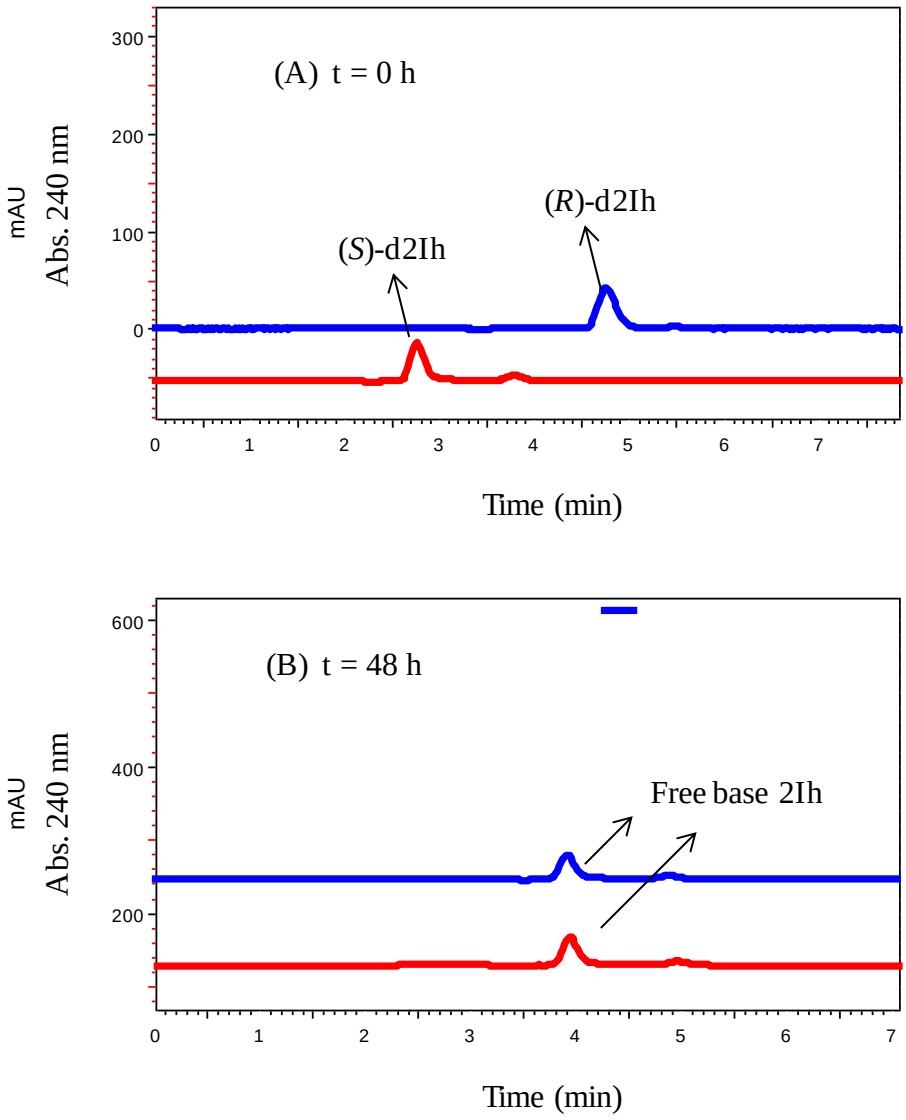


**Figure 4.1.** HPLC chromatograms to monitor the *N*-glycosidic bond hydrolysis of the 2-deoxyribonucleosides of (*R*)-d2Ih (blue) and (*S*)-d2Ih (red) to yield the free base of 2Ih. (A) The beginning of the reaction (t = 0 h) and (B) after incubation in buffer for 48 h.

240 nm. The method was initiated at 0% B and held isocratic for 20 min followed by a linear increase in B to 75% over 20 min.

*The 2Ih free base formation*

The 2Ih free base enantiomers of the two deoxyribonucleoside diastereomers were prepared by incubating the individually purified nucleosides in buffer solution using either sodium acetate or sodium phosphate (75 mM) with pH values of 4.4, 5.4, 6.4, 7.4, and 8.4 at 37 °C and time-point measurements were conducted at 0, 6, 12, 18, 24, 30, 36, 42, and 48 h. The 2Ih free bases were detected using a Hypercarb HPLC column running the previously described method, in which the retention time was 4 min for both free bases (Figure 4.1B). To study the effect of Spm on inducing the free base formation at the physiological pH 7.4, the individually purified 2Ih diastereomers were incubated in buffer solution at pH 7.4 in the absence and presence of 0.5 mM of Spm at 37 °C and time-point measurements were made at 0, 6, 12, 18, 24, 30, 36, 42, and 48 h.

*Product quantification*

Products were quantified by their absorbance intensity at 240 nm followed by normalization of these intensities using each compound's extinction coefficient at 240 nm. The values for $\varepsilon_{240nm}$ ($ddH_2O$) are 2,290 L. $mol^{-1}$. $cm^{-1}$ for the 2`-deoxyribonucleosides of (*R*)-d2Ih and (*S*)-d2Ih and their free base 2Ih.[19]

**Results and discussion**

The hydrolysis reaction was followed by HPLC analysis to monitor the disappearance of the intact nucleoside and the appearance of the free bases. The *N*-glycosidic bond hydrolysis reaction is first-order.[25-27] Plots of the ln[nucleoside] vs. reaction time provided a linear trend in the data that was fit by equation 4.1, where the slope provides the rate constant (*K*). The half-life ($t_{1/2}$) of each reaction was calculated from equation 4.2.

$$\ln[\text{nucleoside}] = -Kt \qquad \text{Eqn. 4.1}$$

$$t_{1/2} = 0.693/K \qquad \text{Eqn.4.2}$$

*Glycosidic bond hydrolysis at different pH values (4.4 - 8.4)*

By monitoring the time-course for cleavage of the d2Ih *N*-glycosidic bond by HPLC, rate profiles were determined (Figure 4.2). Additionally, the pH dependency in the hydrolysis rate was determined from pH 4.4 to 8.4. The *N*-glycosidic bond hydrolysis at pH 8.4 for both (*R*)-d2Ih and (*S*)-d2Ih gave rate constants of 49 x $10^{-3}$ $h^{-1}$ and 50 x $10^{-3}$ $h^{-1}$, respectively (Figure 4.2, and Table 4.1). At pH 7.4, the rates were found to be 50 x $10^{-3}$ $h^{-1}$ and 52 x $10^{-3}$ $h^{-1}$ for (*R*)-d2Ih and (*S*)-d2Ih, respectively, values that were similar to those determined at pH 8.4. The hydrolysis at pH 6.4 was slightly faster and gave a rate constants of 58 x $10^{-3}$ $h^{-1}$ and 59 x $10^{-3}$ $h^{-1}$ for (*R*)-d2Ih and (*S*)-d2Ih, respectively (Table 4.1). Decreasing the pH to 5.4 significantly increased the rate of hydrolysis to 79 x $10^{-3}$ $h^{-1}$ and 82 x $10^{-3}$ $h^{-1}$ for (*R*)-d2Ih and (*S*)-d2Ih, respectively (Table 4.1). The most rapid hydrolysis was at pH 4.4 with a rate constant of 103 x $10^{-3}$

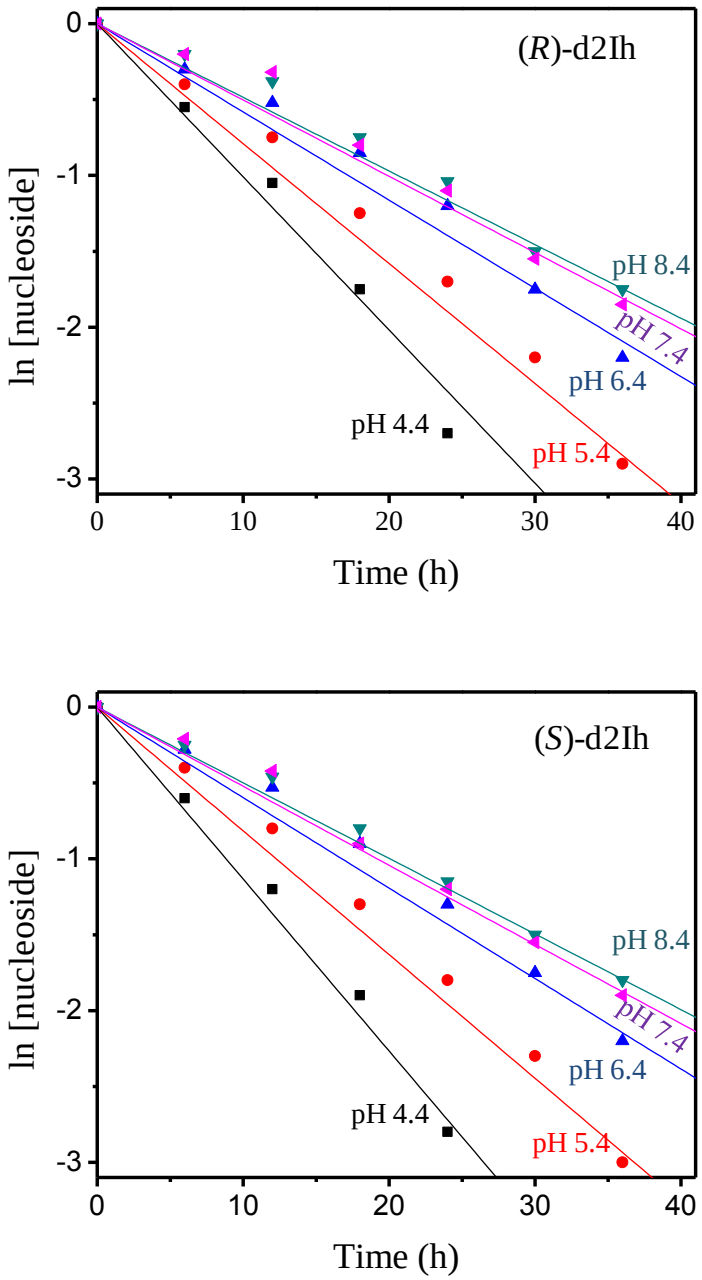


**Figure 4.2.** ln[nucleoside] vs. time for *N*-glycosidic hydrolysis at pH 4.4, 5.4, 6.4, 7.4, and 8.4 Plots for (*R*)-d2Ih and(*S*)-d2Ih are shown. The reaction yields were monitored by the free base 2Ih formation by HPLC. Based on triplicate trials, the errors were ± 5 - 10% of each value.

**Table 4.1.** Rate constants and half-lives for the (*S*)-d2Ih and (*R*)-d2Ih *N*-glycosidic bond hydrolysis at different pH values from 4.4 - 8.4, and in the absence[a] or presence[b] of Spm at pH 7.4.

| | **(*S*)-d2Ih** | | **(*R*)-d2Ih** | |
|---|---|---|---|---|
| **pH** | ***k* x $10^{-3}$ ($h^{-1}$)** | **$t_{1/2}$ (h)** | ***k* x $10^{-3}$ ($h^{-1}$)** | **$t_{1/2}$ (h)** |
| **4.4** | 107 ± 3 | 6.3 | 103 ± 2 | 6.8 |
| **5.4** | 82 ± 5 | 8.5 | 79 ± 4 | 8.8 |
| **6.4** | 59 ± 4 | 11.6 | 58 ± 3 | 11.9 |
| **7.4 (- Spm)[a]** | 52 ± 4 | 13.3 | 50 ± 5 | 13.8 |
| **8.4** | 50 ± 5 | 13.9 | 49 ± 4 | 14.2 |
| **7.4 (+ Spm)[b]** | 380 ± 10 | 1.8 | 380 ± 8 | 1.8 |

$h^{-1}$ and 107 x $10^{-3}$ $h^{-1}$, for (*R*)-d2Ih and (*S*)-d2Ih, respectively. No significant pH-dependent difference has been found for the hydrolysis rate between (*R*)-d2Ih and (*S*)-d2Ih. These results showed that the d2Ih lesion spontaneously hydrolyzed to give the free bases in a pH-dependent fashion. Furthermore, if these reactions occurred in the DNA context, the products would be release of the 2Ih free base enantiomers and an abasic site in the DNA.

The half-life ($t_{1/2}$) for 2Ih *N*-glycosidic bond hydrolysis was calculated at each pH from the rate constants (eqn. 4.2). The $t_{1/2}$ values for the (*R*)-2Ih were 14.2 h at pH 8.4, 13.8 h at pH 7.4, 11.9 h at pH 6.4, 8.8 h at pH 5.4, and 6.8 h at pH 4.4, while the $t_{1/2}$ values for the (*S*)-2Ih were 13.9 h at pH 8.4, 13.3 h at pH 7.4, 11.6 h at pH 6.4, 8.5 h at pH 5.4, and 6.3 h at pH 4.4 (Table 4.1). These results demonstrate that rates and half-lives for hydrolysis of the *N*-glycosidic bond in the d2Ih diastereomers were not stereochemically dependent; however, the reactions show a sharp increase in the rate when the pH was < 5.4.

*Glycosidic bond hydrolysis in the presence of Spm*

The glycosidic bond hydrolysis in the presence and absence of Spm at pH 7.4 was conducted to study the effect of a nucleophile on the reaction. In the presence of Spm (0.5 mM), hydrolysis was significantly faster than hydrolysis in the absence of Spm (Figure 4.3) with a rate constant of 380 x $10^{-3}$ $h^{-1}$ for both (*R*)-d2Ih and (*S*)-d2Ih (Table 4.1). The $t_{1/2}$ values of both (*R*)-2Ih and (*S*)-2Ih were 1.8 h. These results showed that *N*-glycosidic bond hydrolysis of d2Ih can be enhanced by a factor of nearly sevenfold in the presence of Spm relative to reactions without Spm present.

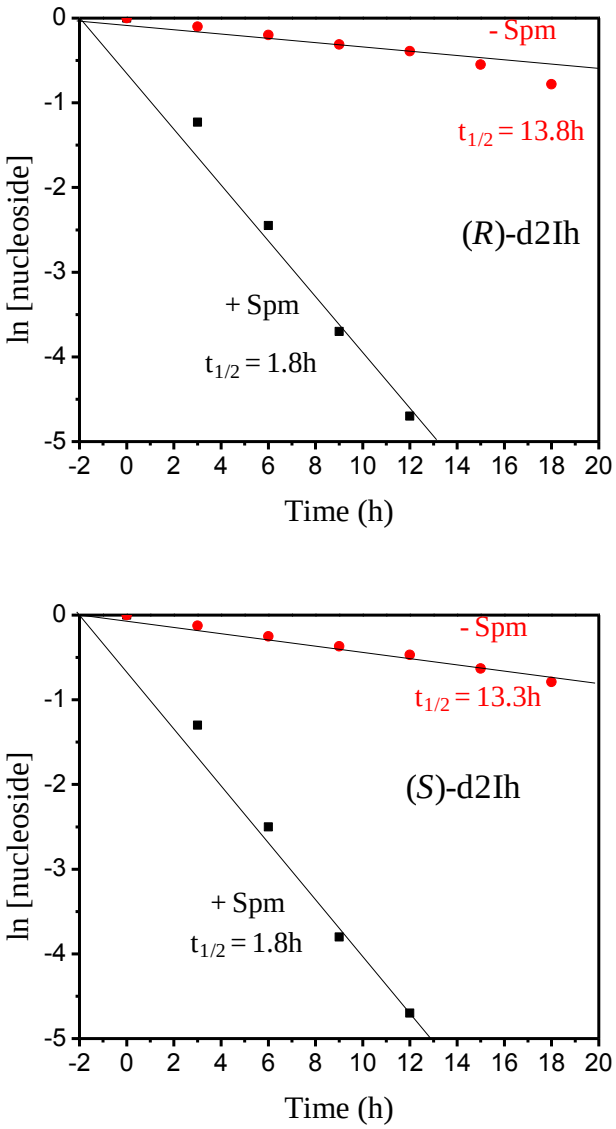


**Figure 4.3.** ln[nucleoside] vs. time for *N*-glycosidic bond hydrolysis at pH 7.4 in presence or absence of Spm. The top panal shows data for the (*R*)-d2Ih lesion and the bottom panel shows data for the (*S*)-d2Ih lesion. The reaction yields were monitored by HPLC to quantify the formation of 2Ih free base. Based on triplicate trials, the errors were 5-12% for each reported value.

In the past, several studies have analyzed nonenzymatic nucleoside glycosidic bond hydrolysis and identified the influence of environmental and chemical agents such as pH, metal cations, and alkylating compounds on the reaction rate.[2,28-30] Those results showed that both protonation and cationic alkylation largely activate purine bases making the leaving group more electron deficient, thus facilitating nucleophilic substitution at the anomeric carbon of the deoxyribose.[31,32] The effect of a protonated glycosidic nitrogen on the hydrolysis and cleavage of the *N*-glycosidic bond was calculated, and showed that there was a strong activation of the hydrolytic cleavage.[33,34] Using these studies as a guide, we propose the following mechanism for hydrolysis of the *N*-glycosidic bond in d2Ih (Figure 4.4).[35] This proposed mechanism provides a role for pH and Spm in the hydrolysis reaction of the d2Ih *N*-glycosidic bond that was observed for product formation. The protonation of N9 in d2Ih facilities hydrolysis of the glycosidic bond. Further, this identifies a plausible pH-dependent pathway consistent with our experimental results. The rupture of the *N*-glycosidic bond results in an accumulation of positive charge on O4' at the sugar ring in the transition state (Figure 4.4). The attack of Spm as a strong nucleophile compared to water on the oxocarbenium ion makes the hydrolysis much faster, also consistent with our results (Figure 4.2 and 4.3).

Previous studies showed that some damaged bases can easily hydrolyze to give an abasic site. For example, Fapy-dG has an opened imidazole ring similar to the opened ring in d2Ih, and several studies showed that the opened ring on Fapy-dG may induce lability toward hydrolysis of the *N*-glycosidic bond to release the Fapy-G free base.[21,36,37] Another study has also concluded that the dG oxidation product dIz lesion

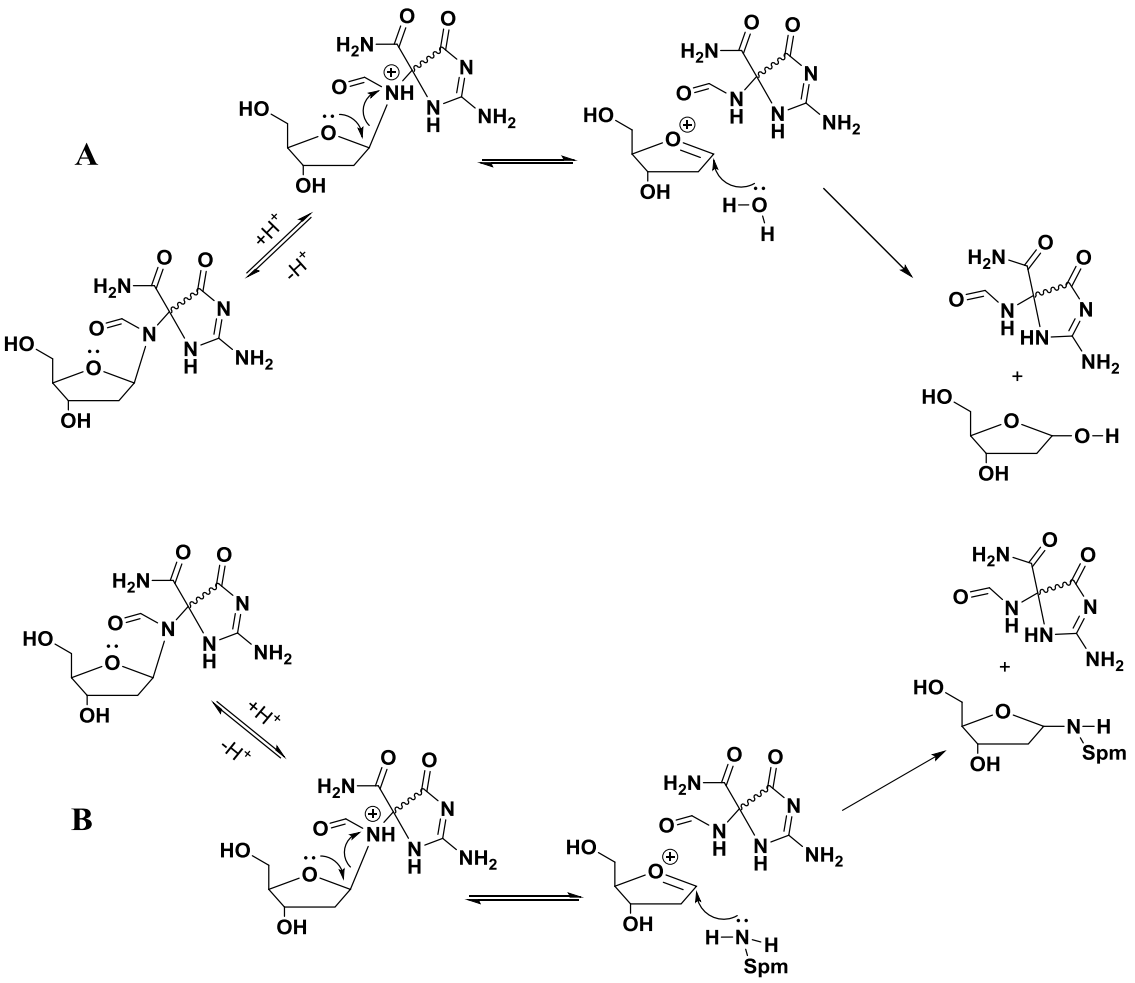


**Figure 4.4.** Proposed pathway for d2Ih *N*-glycosidic bond cleavage. (A) Proposed mechanism in the absence of Spm and (B) in the presence of Spm.

can rearrange within a few hours to give the oxazolone (dZ) lesion as the dominant species.[22] Additionally a decarboxylation can occur on the dZ lesion giving the guanidinoformimine (dGf) intermediate. Finally, 1′-amino-ribose was detected as the hydrolysis product of the dGf compound. The aminoriboside hydrolyzes thereafter to form an abasic site.[22] The present study can add additional evidence that structural changes to purine residues may lead to destabilization of the *N*-glycosidic bonds, and subsequently lead to cleavage of the C1' –N9 bond. In the physiological context of the cell, this type of DNA hydrolysis leads to abasic site formation that induces backbone damage in addition to the base damage. Abasic site formation is mutagenic.[8,38,39]

DNA base damage such as 2Ih will either persist in DNA or may cause an instability of the *N*-glycosidic bond if left unrepaired, leading to hydrolysis to give an abasic site. If the 2Ih lesion persists in DNA, it will lead to G•C → C•G and G•C → T•A transversion mutations, as has been discussed in Chapter 3. However, if the 2Ih damage leads to formation of the abasic site, a different mutation can occur. The abasic site follows the "A-rule", in which the noncoding lesion such as the abasic site is base paired with an adenine nucleotide and leads to G•C → T•A transversion mutations.[40,41] The DNA damage does not stop at this point, and additional damage may occur. The abasic site can be found as the cyclic acetal that exists in equilibrium with a small amount of the ring-opened aldehyde form (Figure 4.5). The acidic α-proton adjacent to the carbonyl residue in the aldehydic form can then be lost via elimination of the 3'-phosphate group to form a DNA strand break.[42,43] DNA strand breaks have been found to form from an abasic site with $t_{1/2}$ ~200 h at pH 7.4 and 37 °C.[42,43] A further study needs to be conducted to determine the rate of the 2Ih glycosidic bond hydrolysis in

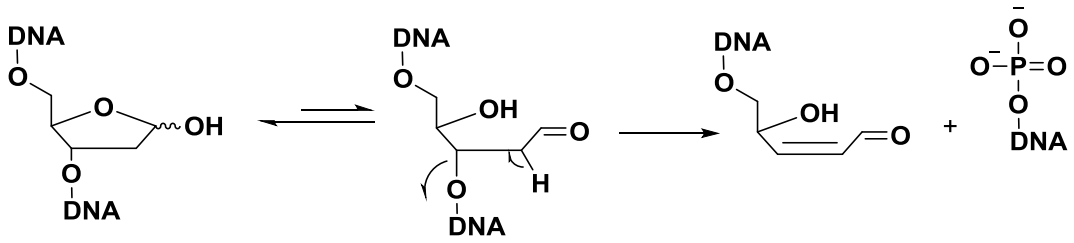


**Figure 4.5.** Proposed pathway for the conversion of an abasic site to a strand break in DNA.[42,43]

DNA. The 2Ih glycosidic bond hydrolysis in ssODN was tested in Chapter 3 (polymerases and glycosylases studies) and it was found that only 10% of it gave the abasic site after 48 h incubation on polymerase or glycosylase buffer.

## Conclusions

The present study determined the *N*-glycosidic bond stability of (*R*)-d2Ih and (*S*)-d2Ih lesions at varying pH and the effect of rate enhancement when a nucleophile such as Spm was present. The hydrolysis rate constant and $t_{1/2}$ values have been estimated by monitoring the nucleoside *N*-glycosidic bond cleavage reaction. The rate of cleavage was slow at pH 6.4, 7.4, and 8.4, while the rate was twice as fast at pH 5.4 and 4.4. The addition of Spm to the reaction at pH 7.4 increased the hydrolysis seven-fold. This type of hydrolysis in DNA will lead to formation of an abasic site, and eventually this abasic site may be converted to a DNA strand break.

**References**


1. Cavalieri, E., Saeed, M., Zahid, M., Cassada, D., Snow, D., Miljkovic, M., and Rogan, E. (2012) Mechanism of DNA depurination by carcinogens in relation to cancer initiation, *IUBMB Life 64*, 169-179.

2. Lindahl, T. (1993) Instability and decay of the primary structure of DNA, *Nature 362*, 709-715.

3. Lindahl, T., and Nyberg, B. (1972) Rate of depurination of native deoxyribonucleic acid, *Biochemistry 11*, 3610-3618.

4. Lindahl, T., and Karlstrom, O. (1973) Heat-induced depyrimidination of deoxyribonucleic acid in neutral solution, *Biochemistry 12*, 5151-5154.

5. Greer, S., and Zamenhof, S. (1962) Studies on depurination of DNA by heat, *J. Mol. Biol. 4*, 123-141.

6. Shapiro, R., and Danzig, M. (1972) Acidic hydrolysis of deoxycytidine and deoxyuridine derivatives. General mechanism of deoxyribonucleoside hydrolysis, *Biochemistry 11*, 23-29.

7. Stivers, J. T., and Jiang, Y. L. (2003) A mechanistic perspective on the chemistry of DNA repair glycosylases, *Chem. Rev. 103*, 2729-2760.

8. Loeb, L. A., and Preston, B. D. (1986) Mutagenesis by apurinic/apyrimidinic sites, *Annu. Rev. Genet. 20*, 201-230.

9. Schaaper, R. M., and Loeb, L. A. (1981) Depurination causes mutations in SOS-induced cells, *Proc. Natl. Acad. Sci. U. S. A. 78*, 1773-1777.

10. Schaaper, R. M., Glickman, B. W., and Loeb, L. A. (1982) Role of depurination in mutagenesis by chemical carcinogens, *Cancer Res. 42*, 3480-3485.

11. Banu, L., Blagojevic, V., and Bohme, D. K. (2012) Lead(II)-catalyzed oxidation of guanine in solution studied with electrospray ionization mass spectrometry, *J. Phys. Chem. B. 116*, 11791–11797.

12. Fleming, A. M., Muller, J. G., Ji, I., and Burrows, C. J. (2011) Characterization of 2'-deoxyguanosine oxidation products observed in the Fenton-like system Cu(II)/$H_2O_2$/reductant in nucleoside and oligodeoxynucleotide contexts, *Org. Biomol. Chem. 9*, 3338-3348.

13. Ghude, P., Schallenberger, M. A., Fleming, A. M., Muller, J. G., and Burrows, C. J. (2011) Comparison of transition metal-mediated oxidation reactions of guanine in nucleoside and single-stranded oligodeoxynucleotide contexts, *Inorg.*

*Chem. Acta 369*, 240-246.

14. Li, L., Murthy, N. N., Telser, J., Zakharov, L. N., Yap, G. P., Rheingold, A. L., Karlin, K. D., and Rokita, S. E. (2006) Targeted guanine oxidation by a dinuclear copper(II) complex at single stranded/double stranded DNA junctions, *Inorg. Chem. 45*, 7144-7159.

15. Rokhlenko, Y., Geacintov, N. E., and Shafirovich, V. (2012) Lifetimes and reaction pathways of guanine radical cations and neutral guanine radicals in an oligonucleotide in aqueous solutions, *J. Am. Chem. Soc. 134*, 4955-4962.

16. Tomaszewska, A., Mourgues, S., Guga, P., Nawrot, B., and Pratviel, G. (2012) A single nuclease-resistant linkage in DNA as a versatile tool for the characterization of DNA lesions: application to the guanine oxidative lesion "G+34" generated by metalloporphyrin/$KHSO_5$ reagent, *Chem. Res. Toxicol. 25*, 2505-2512.

17. Vialas, C., Claparols, C., Pratviel, G., and Meunier, B. (2000) Guanine oxidation in double-stranded DNA by Mn-TMPyP/$KHSO_5$: 5,8-dihydroxy-7,8-dihydroguanine residue as a key precursor of imidazolone and parabanic acid derivatives, *J. Am. Chem. Soc. 122*, 2157-2167.

18. Ye, W., Sangaiah, R., Degen, D. E., Gold, A., Jayaraj, K., Koshlap, K. M., Boysen, G., Williams, J., Tomer, K. B., Mocanu, V., Dicheva, N., Parker, C. E., Schaaper, R. M., and Ball, L. M. (2009) Iminohydantoin lesion induced in DNA by peracids and other epoxidizing oxidants, *J. Am. Chem. Soc. 131*, 6114-6123.

19. Alshykhly, O. R., Fleming, A. M., and Burrows, C. J. (2015) 5-Carboxamido-5-formamido-2-iminohydantoin, in addition to 8-oxo-7,8-dihydroguanine, is the major product of the iron-Fenton or X-ray radiation-induced oxidation of guanine under aerobic reducing conditions in nucleoside and DNA contexts, *J. Org. Chem.*, ASAP.

20. Fleming, A. M., Alshykhly, O., Orendt, A. M., and Burrows, C. J. (2015) Computational studies of electronic circular dichroism spectra predict absolute configuration assignments for the guanine oxidation product 5-carboxamido-5-formamido-2-iminohydantoin, *Tetrahedron Lett. 56*, 3191-3196.

21. Saladino, R., Crestini, C., Mincione, E., Costanzo, G., Di Mauro, E., and Negri, R. (1997) Mechanism of degradation of 2′-deoxycytidine by formamide: Implications for chemical DNA sequencing procedures, *Bioorg. Med. Chem. 5*, 2041-2048.

22. Stathis, D., Lischke, U., Koch, S. C., Deiml, C. A., and Carell, T. (2012) Discovery and mutagenicity of a guanidinoformimine lesion as a new intermediate of the oxidative deoxyguanosine degradation pathway, *J. Am.*

*Chem. Soc. 134*, 4925-4930.

23. Igarashi, K., and Kashiwagi, K. (2000) Polyamines: mysterious modulators of cellular functions, *Biochem. Biophys. Res. Commun. 271*, 559-564.

24. Igarashi, K., and Kashiwagi, K. (2010) Modulation of cellular function by polyamines, *Int. J. Biochem. Cell. Biol. 42*, 39-51.

25. Das, R. S., Samaraweera, M., Morton, M., Gascón, J. A., and Basu, A. K. (2012) Stability of *N*-glycosidic bond of (5′S)-8,5′-Cyclo-2′-deoxyguanosine, *Chem. Res. Toxicol. 25*, 2451-2461.

26. Stockbridge, R., Schroeder, G., and Wolfenden, R. (2010) The rate of spontaneous cleavage of the glycosidic bond of adenosine, *Bioorg. Chem. 38*, 224-228.

27. Suzuki, T., Ohsumi, S., and Makino, K. (1994) Mechanistic studies on depurination and apurinic site chain breakage in oligodeoxyribonucleotides, *Nucleic Acids Res. 22*, 4997-5003.

28. Lönnberg, H., and Lehikoinen, P. (1982) Mechanisms for solvolytic decompositions of nucleoside analogues. X. Acicic hydrolysis of 6-substituted 9-(β-D-ribofuranosyl)purines, *Nucleic Acids Res. 10*, 4339-4349.

29. Arpalahti, J., Käppi, R., Hovinen, J., Lönnberg, H., and Chattopadhyaya, J. (1989) The effect of metal ion complex formation on acidic depurination of 2′-deoxyadenosine and 2′-deoxyguanosine, *Tetrahedron 45*, 3945-3954.

30. Laayoun, A., Décout, J.-L., and Lhomme, J. (1994) Hydrolysis of 2′-deoxypurine nucleosides. The effect of substitution at the C-8 position, *Tetrahedron Lett. 35*, 4989-4990.

31. Jang, Y. H., Goddard, W. A., Noyes, K. T., Sowers, L. C., Hwang, S., and Chung, D. S. (2002) First principles calculations of the tautomers and pKa values of 8-oxoguanine: implications for mutagenicity and repair, *Chem. Res. Toxicol. 15*, 1023-1035.

32. Osakabe, T., Fujii, Y., Hata, M., Tsuda, M., Neya, S., and Hoshino, T. (2004) Quantum chemical study on base excision mechanism of 8-oxoguanine DNA glycosylase: substrate-assisted catalysis of the N-glycosidic linkage cleavage reaction, *Chem. Bio. Inf. J. 4*, 73-92.

33. Cysewski, P., Bira, D., and Bialkowski, K. (2004) An ab initio quantum chemistry study on N-glycosidic bond stabilities of hydroxyl radical modified guanosine analogs, *J. Mol. Struct.: THEOCHEM 678*, 77-81.

34. Sebera, J., Trantirek, L., Tanaka, Y., Nencka, R., Fukal, J., and Sychrovsky, V. (2014) The activation of N-glycosidic bond cleavage performed by base-excision repair enzyme hOGG1; theoretical study of the role of Lys 249 residue in activation of G, OxoG and FapyG, *RSC Adv. 4*, 44043-44051.

35. Jian, Y., Lin, G., Chomicz, L., and Li, L. (2015) Reactivity of damaged pyrimidines: formation of a Schiff base intermediate at the glycosidic bond of saturated dihydrouridine, *J. Am. Chem. Soc. 137*, 3318-3329.

36. Raoul, S., Bardet, M., and Cadet, J. (1995) Gamma irradiation of 2'-deoxyadenosine in oxygen-free aqueous solutions: identification and conformational features of formamidopyrimidine nucleoside derivatives, *Chem. Res. Toxicol. 8*, 924-933.

37. Jiang, Y. L., Wiederholt, C. J., Patro, J. N., Haraguchi, K., and Greenberg, M. M. (2005) Synthesis of oligonucleotides containing fapy·dG (N6-(2-deoxy-α,β-d-erythropentofuranosyl)-2,6-diamino-4-hydroxy-5-formamidopyrimidine) using a 5‘-dimethoxytrityl dinucleotide phosphoramidite, *J. Org. Chem. 70*, 141-149.

38. Evans, A. R., Limp-Foster, M., and Kelley, M. R. (2000) Going APE over ref-1, *Mutat. Res. 461*, 83-108.

39. Chakravarti, D., Mailander, P., Li, K., Higginbotham, S., Zhang, H., Gross, M., Meza, J., Cavalieri, E., and Rogan, E. (2001) Evidence that a burst of DNA depurination in SENCAR mouse skin induces error-prone repair and forms mutations in the H-ras gene, *Oncogene 20*, 7945-7953.

40. Shibutani, S., Takeshita, M., and Grollman, A. P. (1997) Translesional synthesis on DNA templates containing a single abasic site: a mechanistic study of the "A rule", *J. Biol. Chem. 272*, 13916-13922.

41. Goodman, M., Cai, H., Bloom, L., and Eritja, R. (1994) Nucleotide insertion and primer extension at abasic template sites in different sequence contexts, *Ann. N. Y. Acad. Sci. 726*, 132-142.

42. Lindahl, T., and Andersson, A. (1972) Rate of chain breakage at apurinic sites in double-stranded deoxyribonucleic acid, *Biochemistry 11*, 3618-3623.

43. Crine, P., and Verly, W. (1976) A study of DNA spontaneous degradation, *Biochim. Biophys. Acta. 442*, 50-57.

# CHAPTER 5

## SUMMARY AND FUTURE DIRECTIONS

The current studies monitored the formation of d2Ih from the oxidation of dG using $HO^{\bullet}$ generated via the Fe(II)-mediated Fenton reaction or X-ray radiolysis of water. When reactions were conducted with cellularly relevant (mM) amounts of reductant (Asc or NAC) and $O_2$, the major oxidation product observed in all cases was d2Ih. Oxidations in the context of single- and double-stranded ODNs and λ-DNA yielded 2Ih as a product of G oxidation in significant yield that was comparable to the yield of OG. The lesion 2Ih when bypassed by DNA polymerases induces misinsertion of dGTP and to a lesser extent dATP during replication *in vitro* and leads to a significant blockage for DNA elongation. The insertion of dGTP or dATP opposite 2Ih leads to G•C → C•G and G•C → T•A transversion mutations. These studies also verify that 2Ih is a substrate for BER enzymes. The NEIL1 DNA glycosylase showed activity toward 2Ih in ssODN and dsODNs. Fpg and Nth were able to remove 2Ih in dsODNs with lower efficiency compared to NEIL1. The last part of this study determined the *N*-glycosidic bond stability of (*R*)-d2Ih and (*S*)-d2Ih lesions at varying pH and the effect of a nucleophile such as Spm on the stability. The rate of cleavage was slow at pH 6.4, 7.4, and 8.4, while the rate was twice as fast at pH 5.4 and 4.4. The addition of Spm to

the reaction at pH 7.4 increased the hydrolysis rate approximately seven times. Hydrolysis of the *N*-glycosidic bond of d2Ih in DNA will lead to formation of an abasic site, and eventually this abasic site may be converted to a DNA strand break.

These interesting findings concerning 2Ih point to further investigations about 2Ih formation and its mutational profile *in vivo*. Therefore, the next step will be the detection of 2Ih *in vivo*. Genomic DNA can be extracted from stressed cells and purified following standard procedures. The extracted DNA can be digested with nucleases to obtain the DNA nucleosides that can be tested and quantified by LC-ESI-MS/MS. The 2Ih base appears to be a pathway-specific lesion and holds promise as a potential biomarker for oxidizing agents *in vivo*. One thing we have to keep in mind is that according to our results in Chapter 4, which indicate the high instability of the *N*-glycosidic bond in 2Ih, it is possible that 2Ih will not be easy to detect among DNA lesions *in vivo*.

The mutagenic potential of 2Ih and the mutation type and frequency *in vivo* can be determined using the restriction endonuclease and postlabeling (REAP) assay that was used before to test the mutagenic potential for the Gh and Sp lesions.[1,2] A viral genome vector such as a ss-phage DNA can be constructed as shown in Figure 5.1. A 2Ih-containing ssODN can be synthesized as described in Chapter 3 by oxidation of a ssODN with NiCR/$KHSO_5$ and will be inserted into that vector. Because a 2Ih lesion in DNA may inhibit replication as we learned from Chapter 3, a relative number of progeny phage onto a lawn of generic bacteria after transfection will cause formation of plaques. The comparison of plaque numbers obtained after replication of damaged

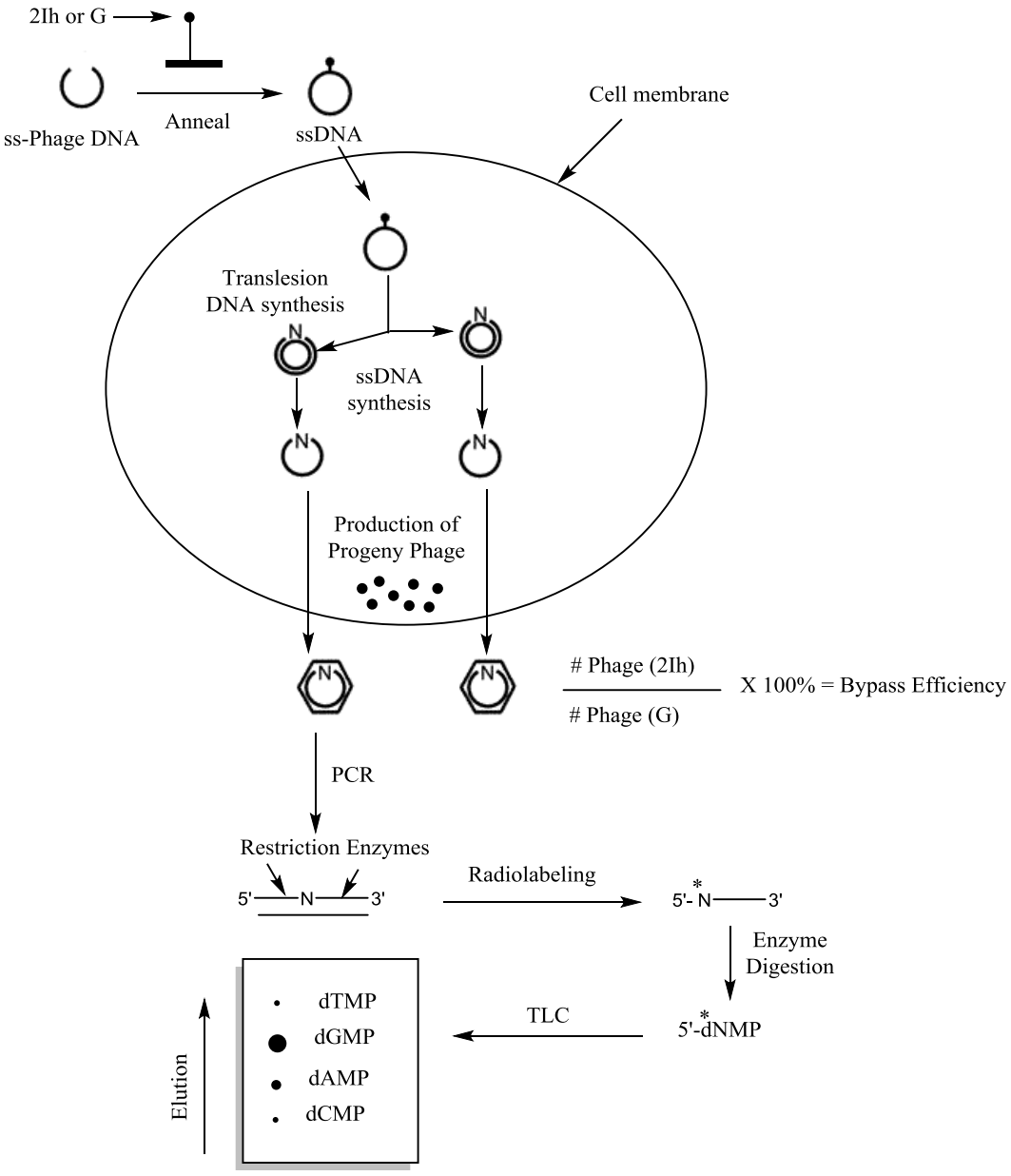


**Figure 5.1.** Strategy for determination of *in vivo* translesion DNA polymerase bypass of 2Ih lesion in a bacteriophage DNA, and the detection of mutations using the REAP assay.

phage genome with those who carry only G as a control gives a measure of the efficiency of polymerase bypass relative to a G control. This work can demonstrate if a 2Ih lesion can be readily bypassed during *in vivo* replication. A 2Ih lesion plasmid will be tranfected into a repair-proficient *E. coli* strain, and PCR amplification of the region of progeny phage genome that have the 2Ih lesion will be performed. This will be followed by using restriction endonucleases, radiolabeling, digesting, and separating the radioactive 5'-dNMPs on a thin layer chromatography (TLC) plate. This can give the mutation frequency and the type at the 2Ih lesion site (Figure 5.1).

Additional work to investigate the structural reason why dGTP was preferentially inserted opposite 2Ih could be determined by X-ray crystallography. In this work, we will use the RB69 DNA polymerase to examine how replicative DNA polymerases distinguish between dATP or dGTP incorporated opposite 2Ih. The crystal structure of the replicative RB69 DNA polymerase in complex with 2Ih-containing DNA, which can be synthesized as described in Chapter 3, would be determined. This structure will constitute the first crystallographic structure of 2Ih, and could explain the propensity of DNA polymerases to incorporate a dGTP opposite 2Ih more frequently than dATP when bypass occurs.

## References

1. Henderson, P., Delaney, J., Gu, F., Tannenbaum, S., and Essigmann, J. (2002) Oxidation of 7,8-dihydro-8-oxoguanine affords lesions that are potent sources of replication errors *in vivo*, *Biochemistry 41*, 914-921.

2. Henderson, P., Delaney, J., Muller, J., Neeley, W., Tannenbaum, S., Burrows, C., and Essigmann, J. (2003) The hydantoin lesions formed from oxidation of 7,8-dihydro-8-oxoguanine are potent sources of replication errors *in vivo*, *Biochemistry 42*, 9257-9262.

# APPENDIX A

# MASS SPECTROMETRY DATA FOR dG OXIDATION PRODUCTS

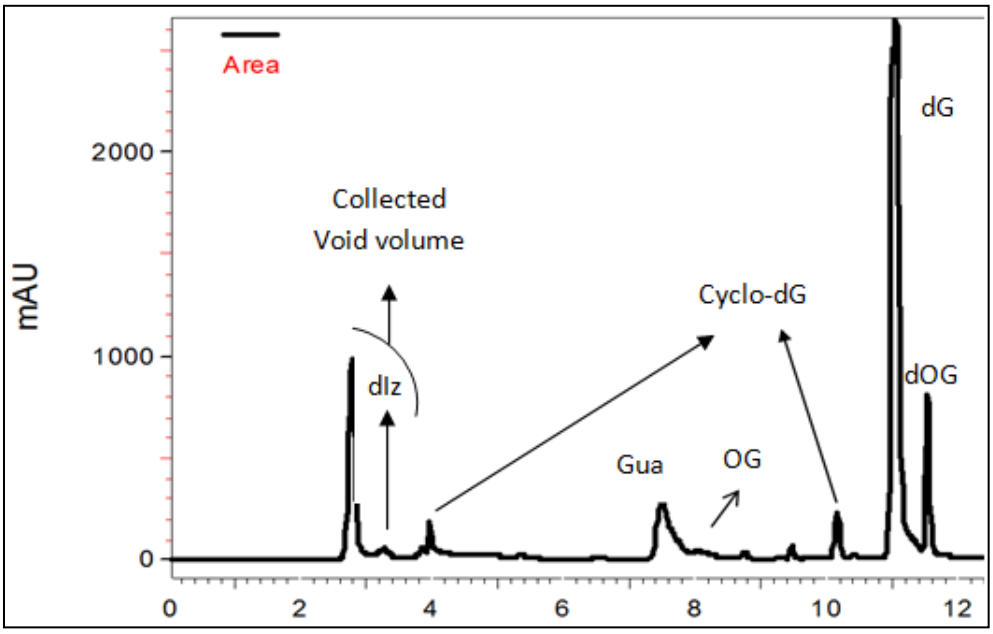


RP-HPLC analysis.

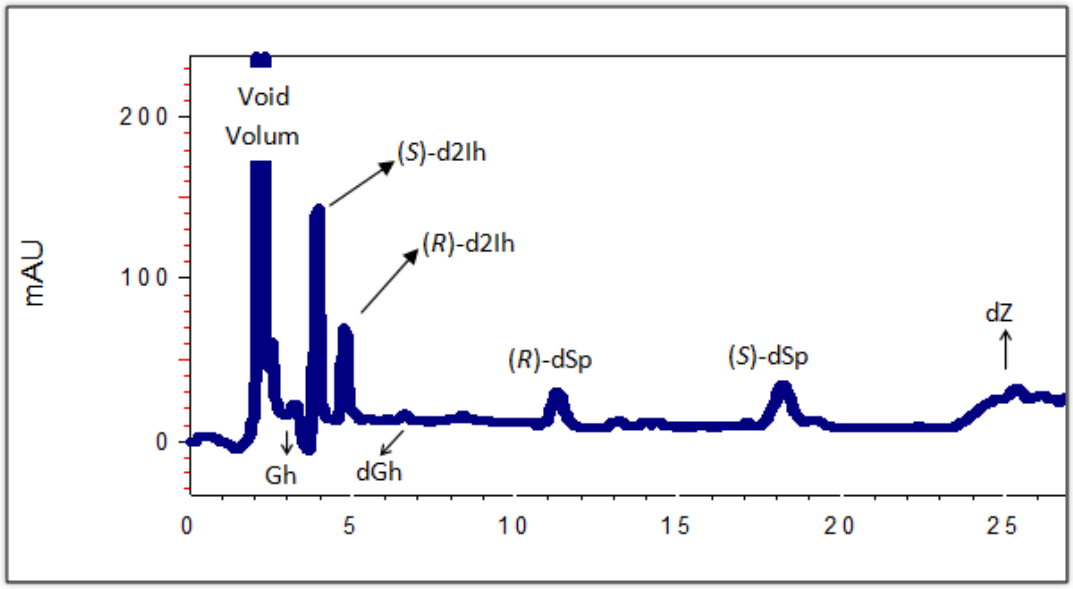


Hypercarb column analysis.

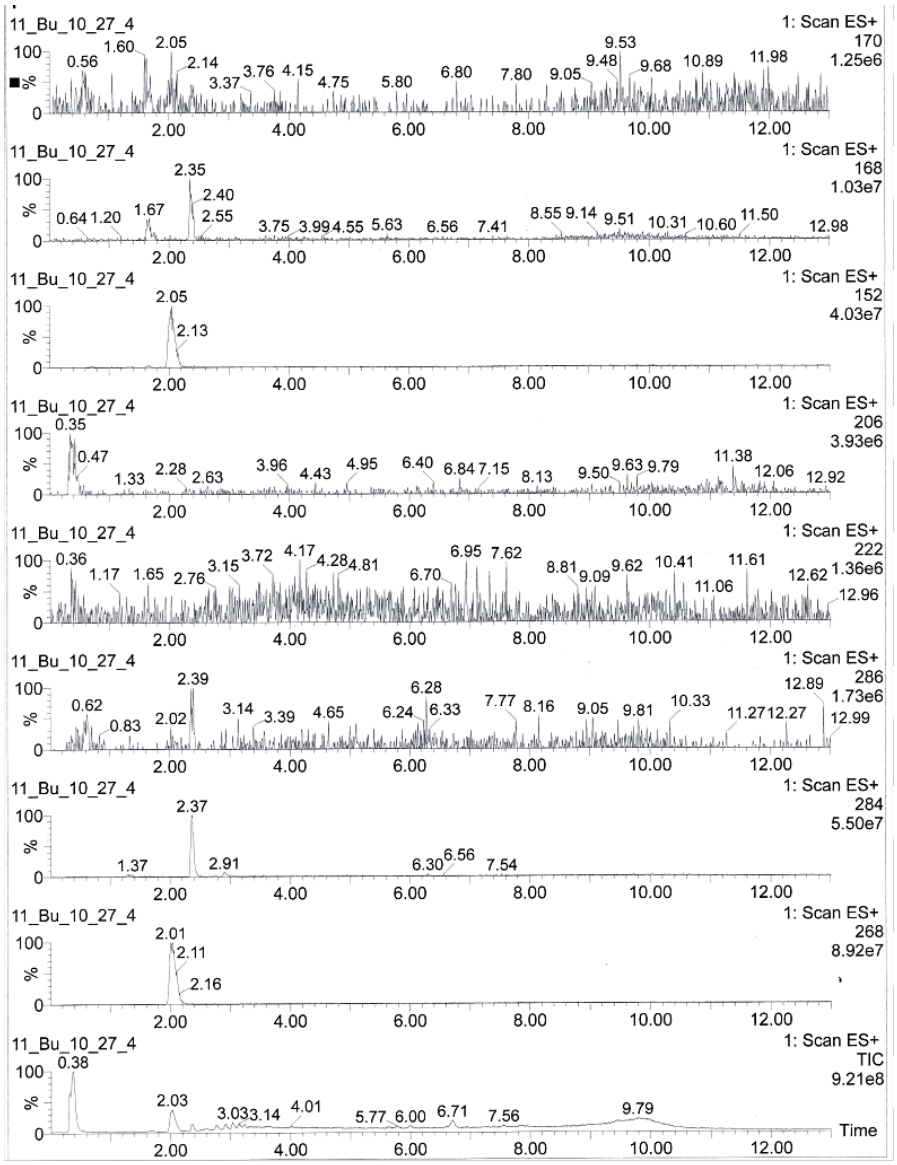


UPLC-ESI$^{+}$-MS analysis (RP-HPLC column) for dG-oxidation products, Panels: A: dG; B: dOG; C: Fapy-dG; D: guanine propenoate; E: guanine propenal; F: Gua ; G: OG; H: Fapy-Gua; I = TIC spectrum.

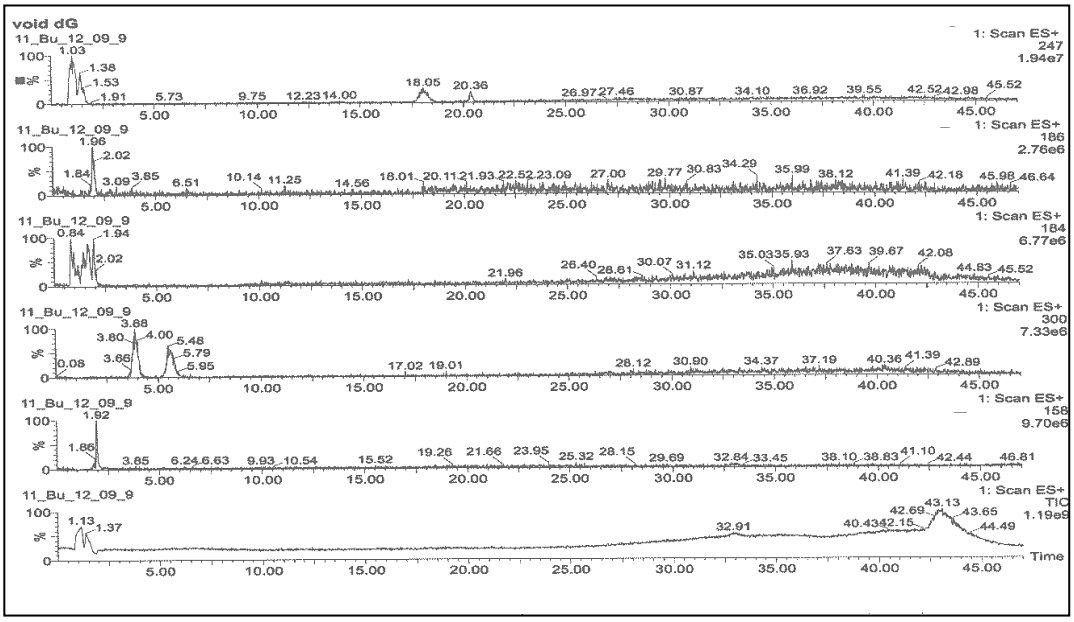


UPLC-ESI$^{+}$-MS analysis (Hypercarb column, 100 X 2.1 mm) for dG-oxidation products, panels: A: dZ; B: 2Ih; C : Sp; D: dSp; E: Gh; F = TIC spectrum.

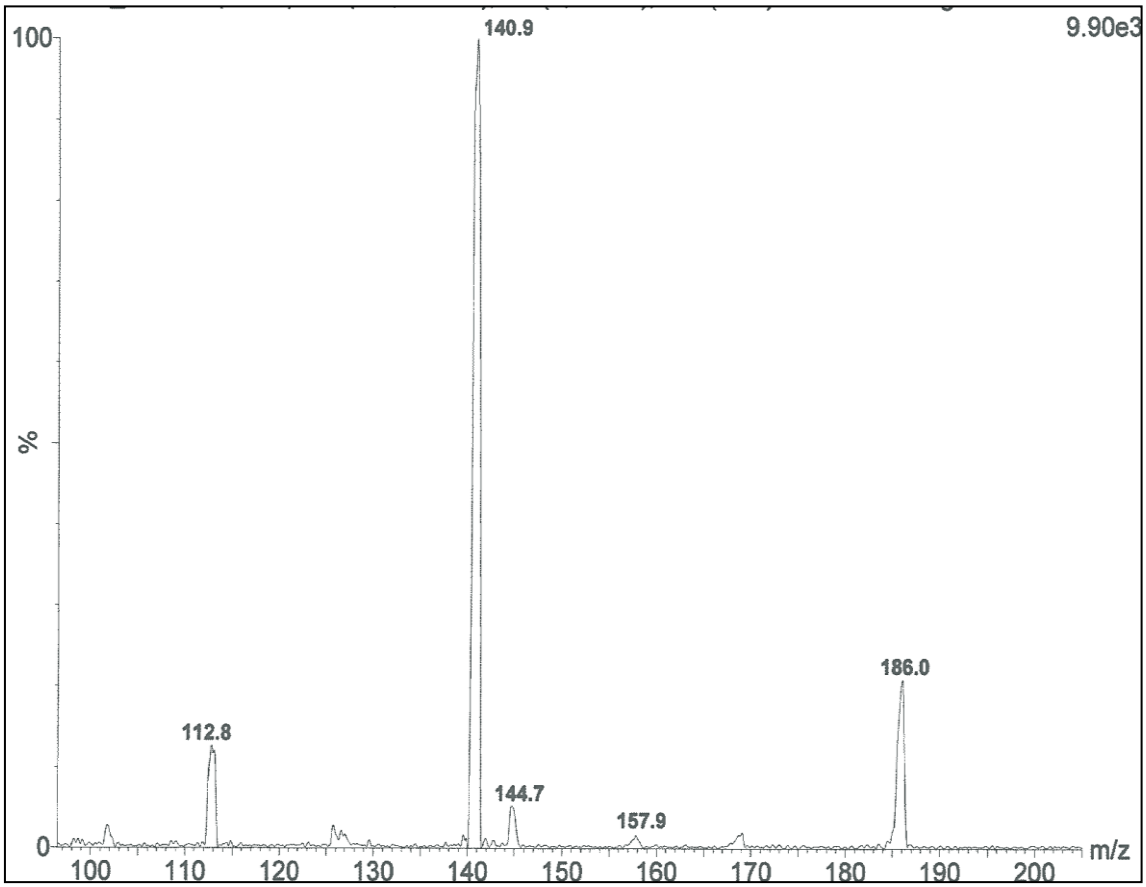


$ESI^+$-MS/MS free base fragmentation data for 2Ih free base mass $(M+H)^+$ = 186.

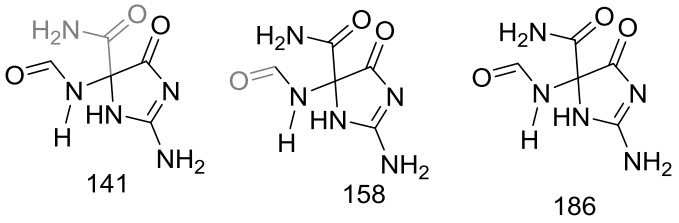

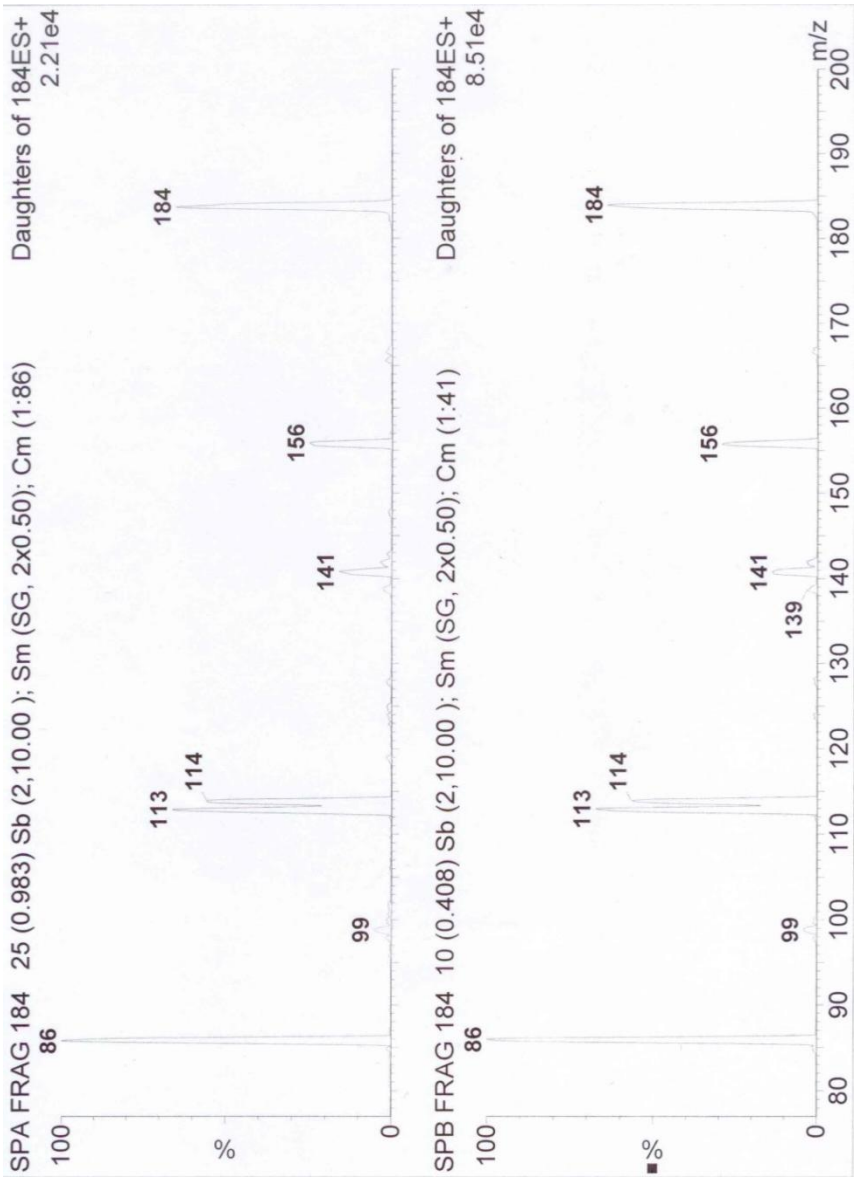


$ESI^{+}$-MS/MS free base fragmentation data for Sp free base mass $(M+H)^{+}$ = 184.

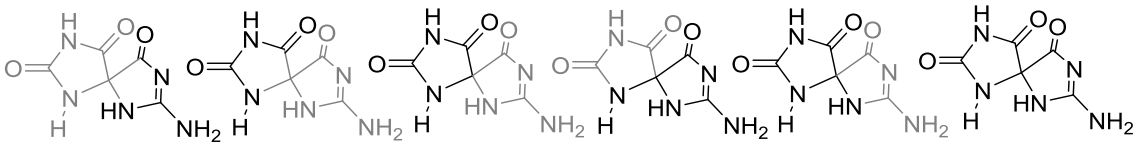

86 86 99 113 114 184

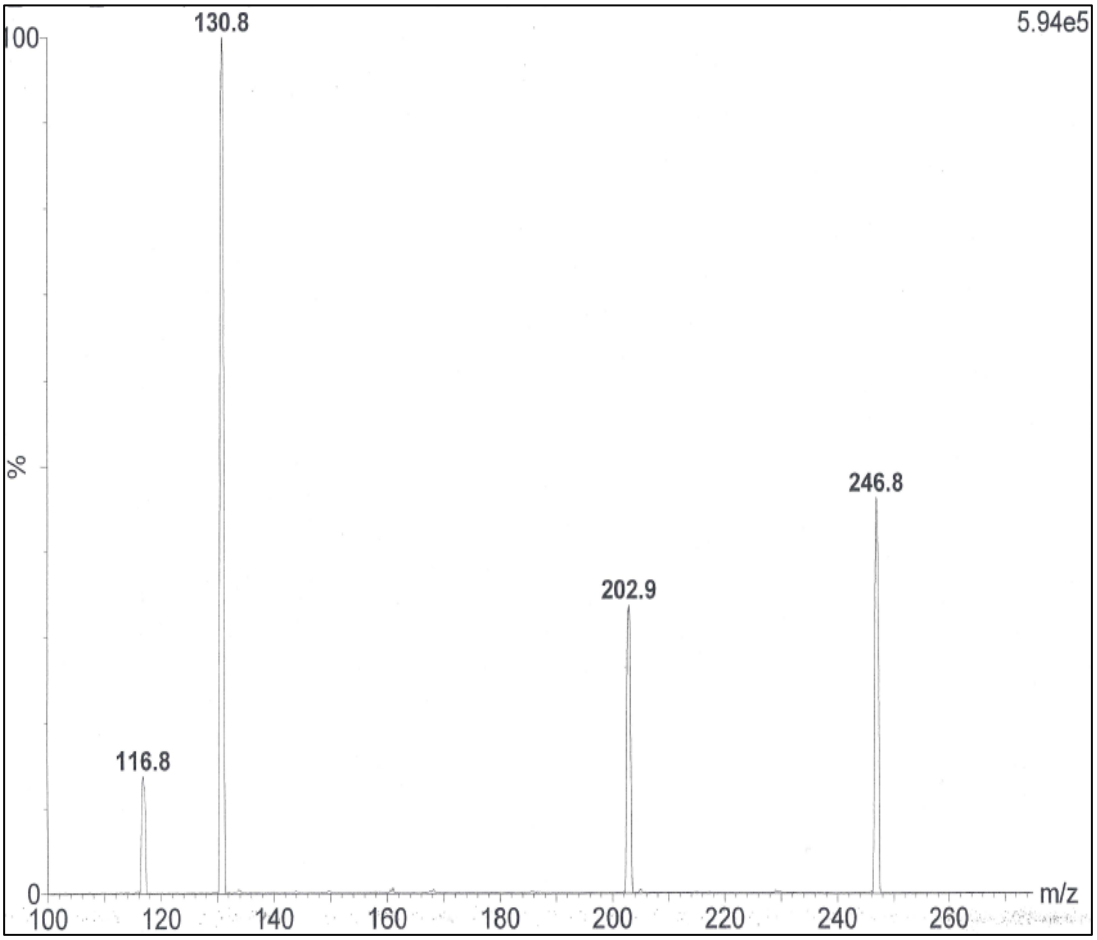


ESI$^+$-MS/MS for dZ nucleoside $(M+H)^+$ = 247.

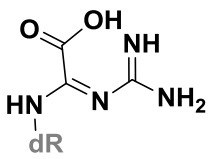


131

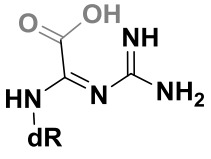


203

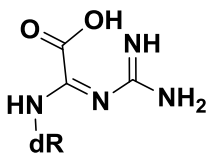


247

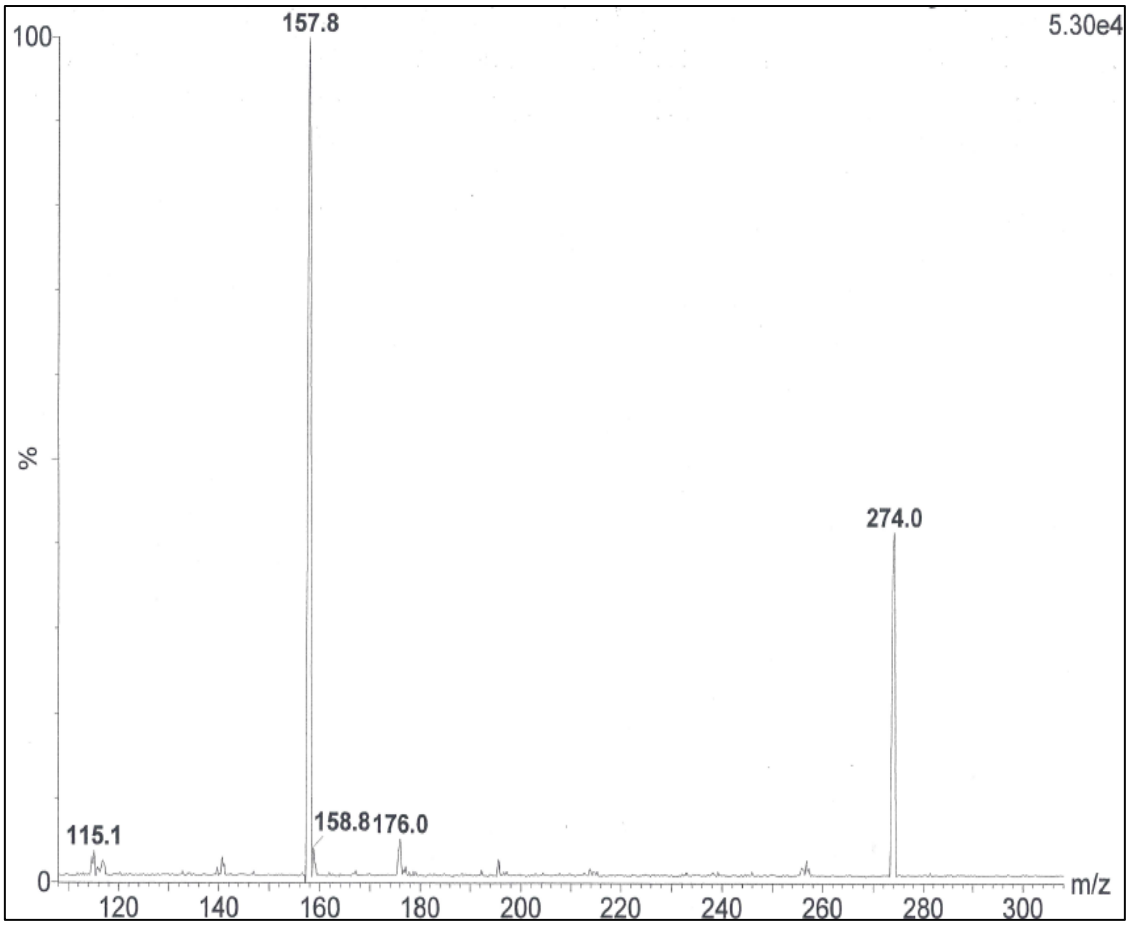


$ESI^{+}$-MS for dGh. The calculated mass $(M+H)^{+}$ = 274.3.

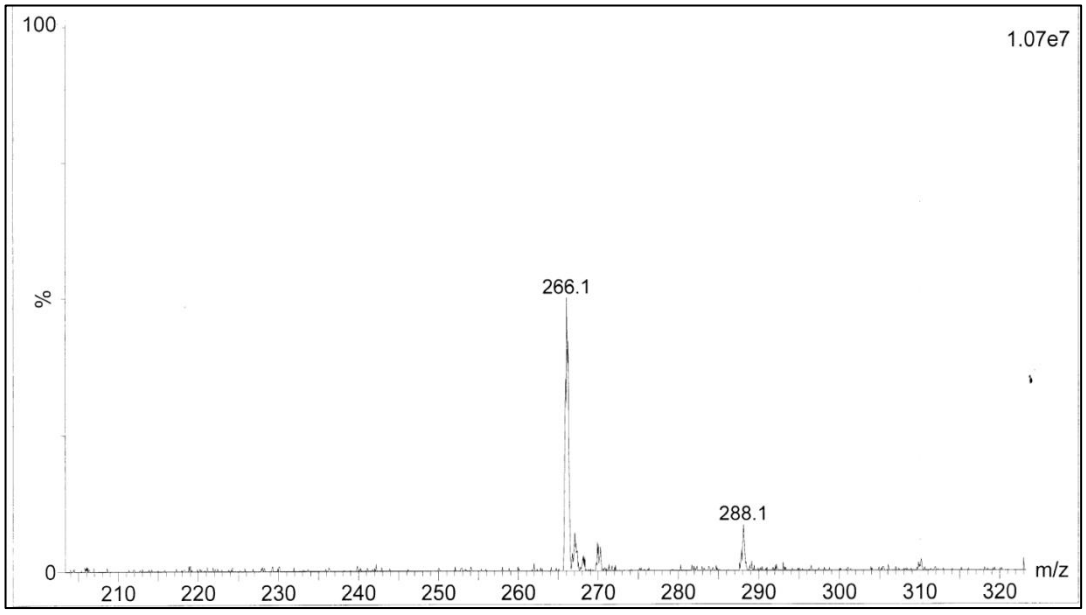


$ESI^{+}$-MS for 5',8-Cyclo-dG. The calculated mass $(M+H)^{+}$= 266.2.

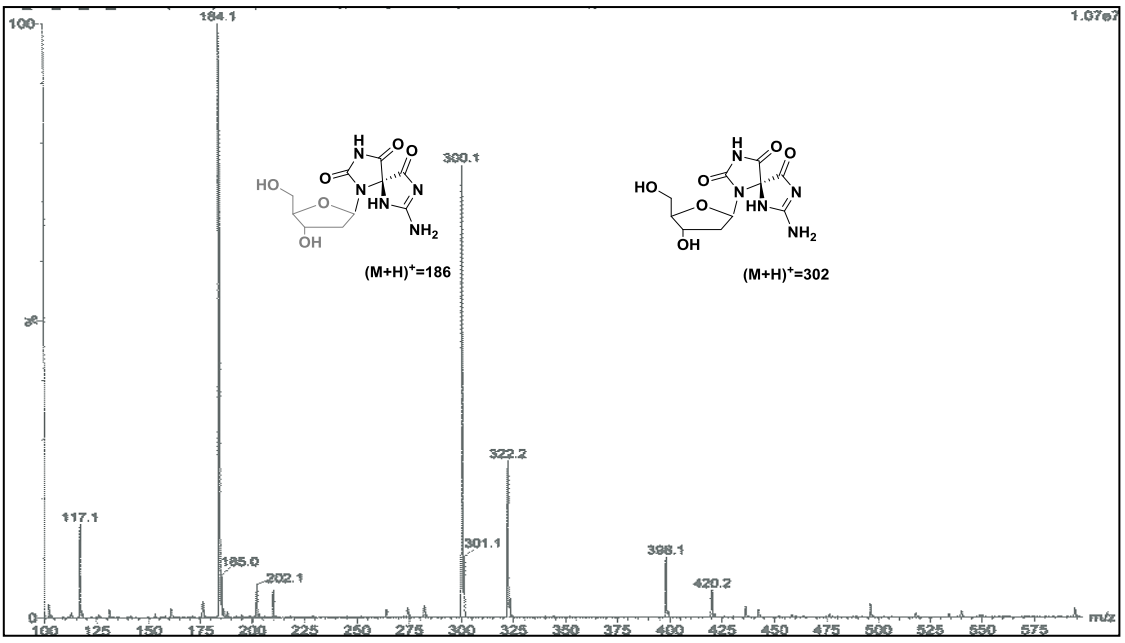


UPLC-ESI$^+$-MS for dSp nucleoside. The calculated mass $(M+H)^+$ = 300.2 and the calculated mass of the free base Sp $(M+H)^+$ = 184.1.

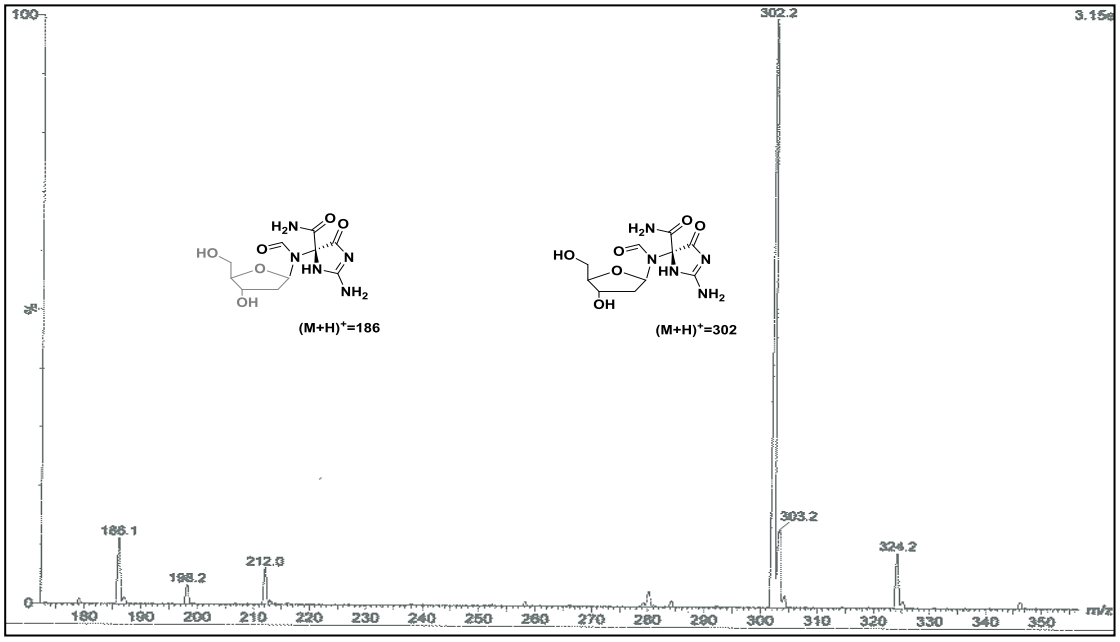


UPLC-ESI$^+$-MS for d2Ih nucleoside. The calculated mass $(M+H)^+$ = 302.3 and the calculated mass of the free base 2Ih $(M+H)^+$ = 186.2.

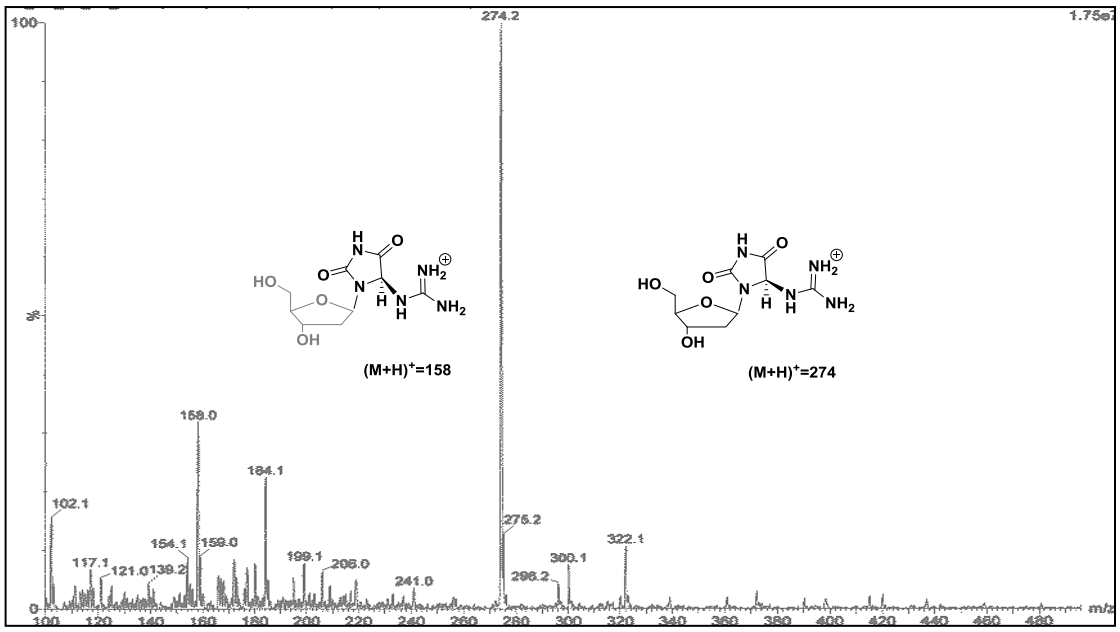


UPLC-ESI$^+$-MS for dGh nucleoside. The calculated mass $(M+H)^+$ = 274.3 and the calculated mass of the free base Gh $(M+H)^+$ = 158.1.

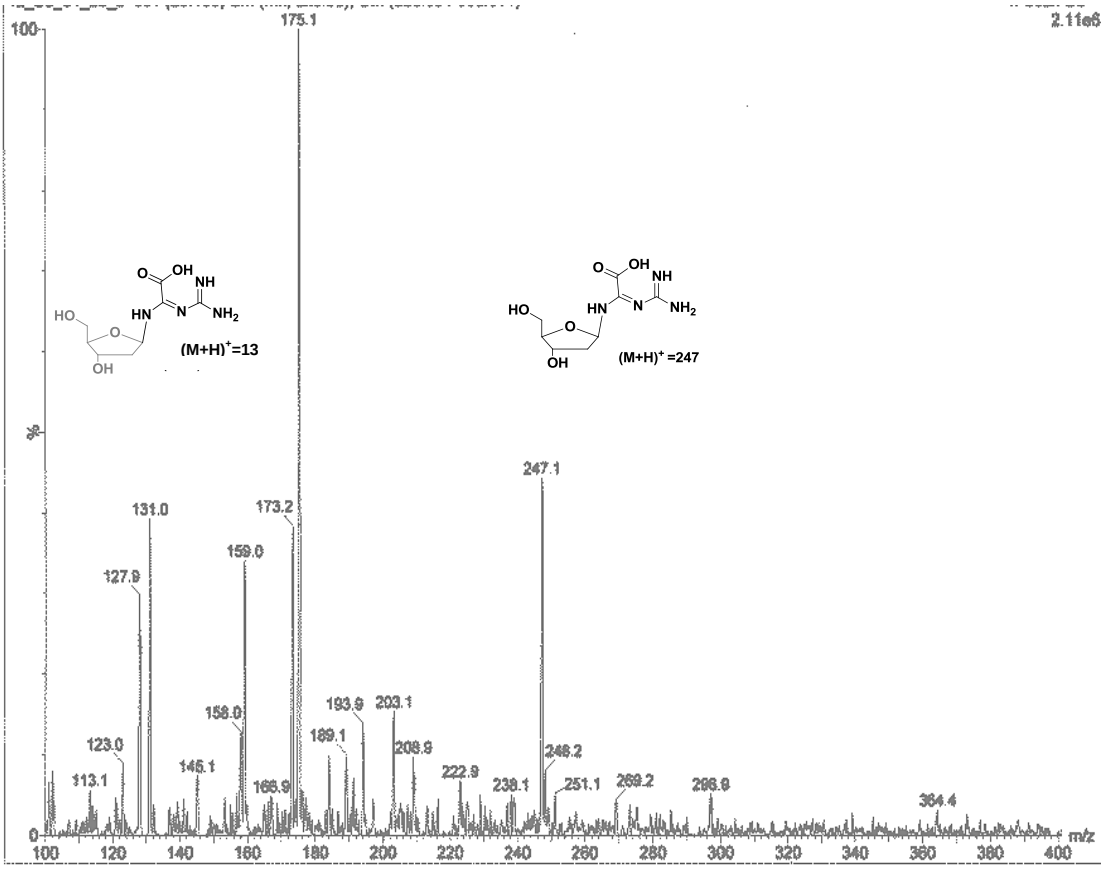


UPLC-ESI$^+$-MS for dZ nucleoside. The calculated mass $(M+H)^+$ = 247.2 and the calculated mass of the Z free base $(M+H)^+$ = 131.1.

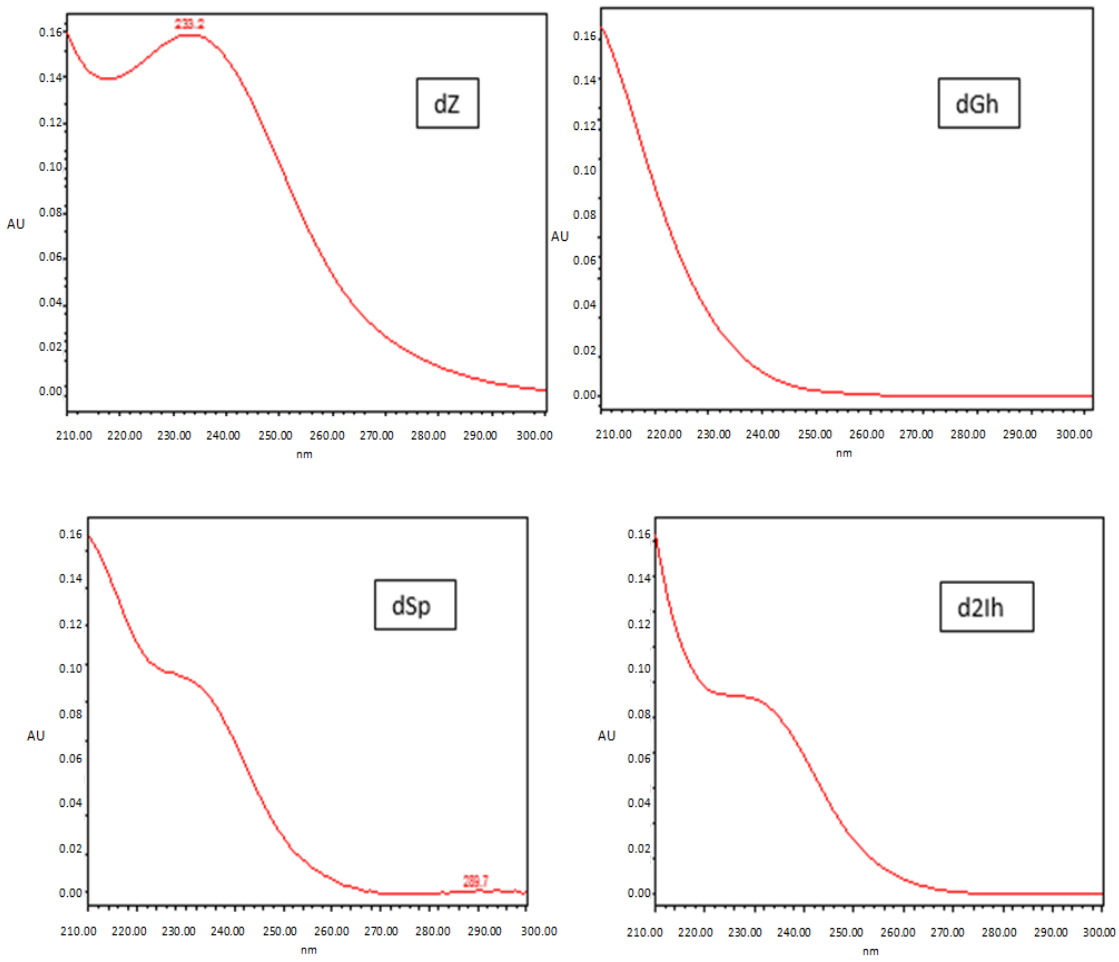


UV-vis spectra for dZ, dGh, dSp, and d2Ih.

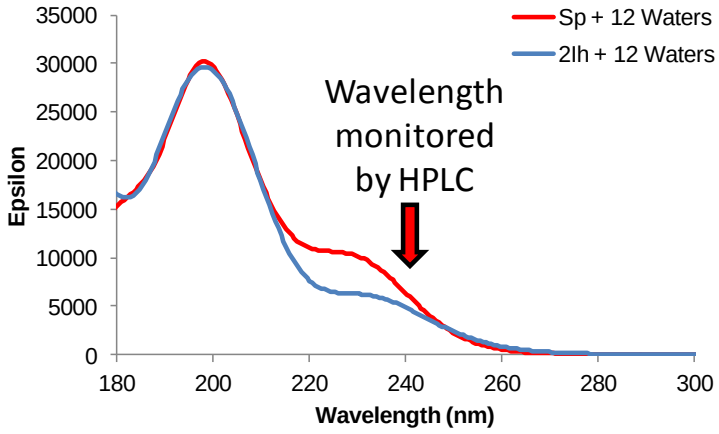


Comparison of dSp and d2Ih UV-vis spectra computed by TDDFT. The TDDFT simulations of the UV-vis spectra for Sp and 2Ih free bases were obtained using the M06-2X functional with the 6-311++G(2d,2p) basis set with implicit definition of water and 12 explict waters adding during the simulation. The Sp spectrum was red-shifted by 17 nm and the 2Ih spectrum was blue-shifted by 10 nm to line them up with the experimental spectra. Comparison of the these spectra support Sp having a larger extinction coefficent than 2Ih by ~30%. These results suggest that the quantities of 2Ih reported in the text are underestimates, and the correct values are significantly greater.

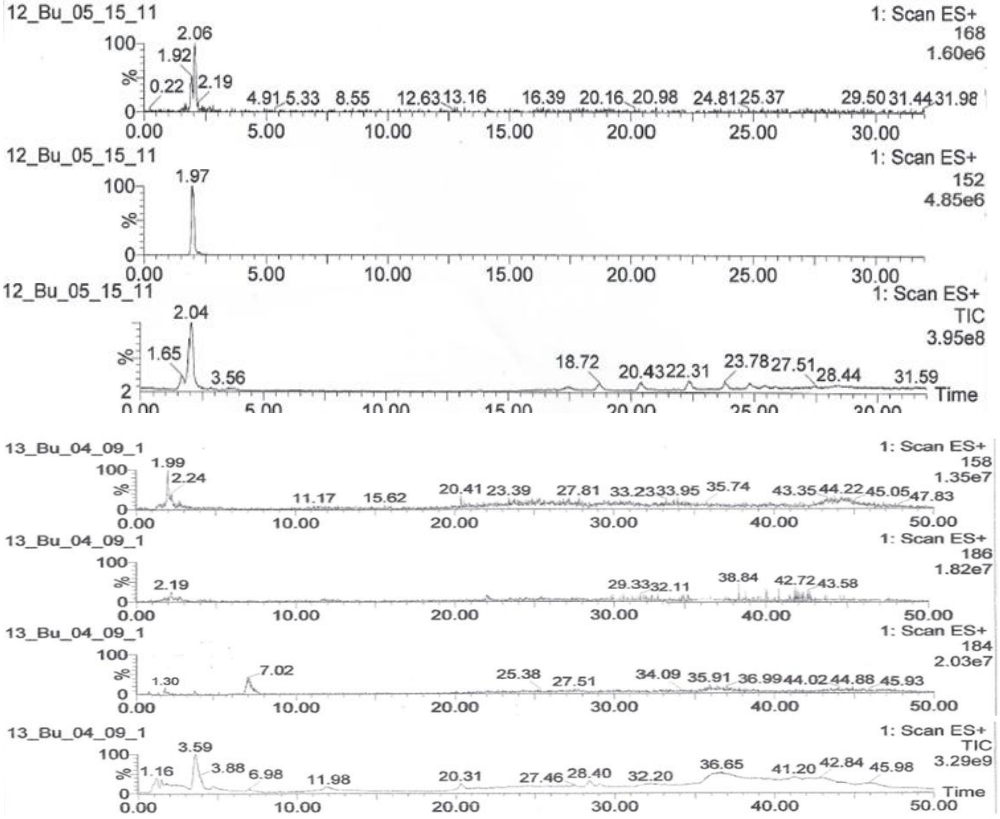


UPLC-ESI$^{+}$-MS dG products resulting from oxidation of ODNs and λ-DNA Free base guanine oxidation products: A: OG; B: Gua; C: Gh; D: 2Ih; E: Sp.

Detecting Fapy-dG under anaerobic condition.

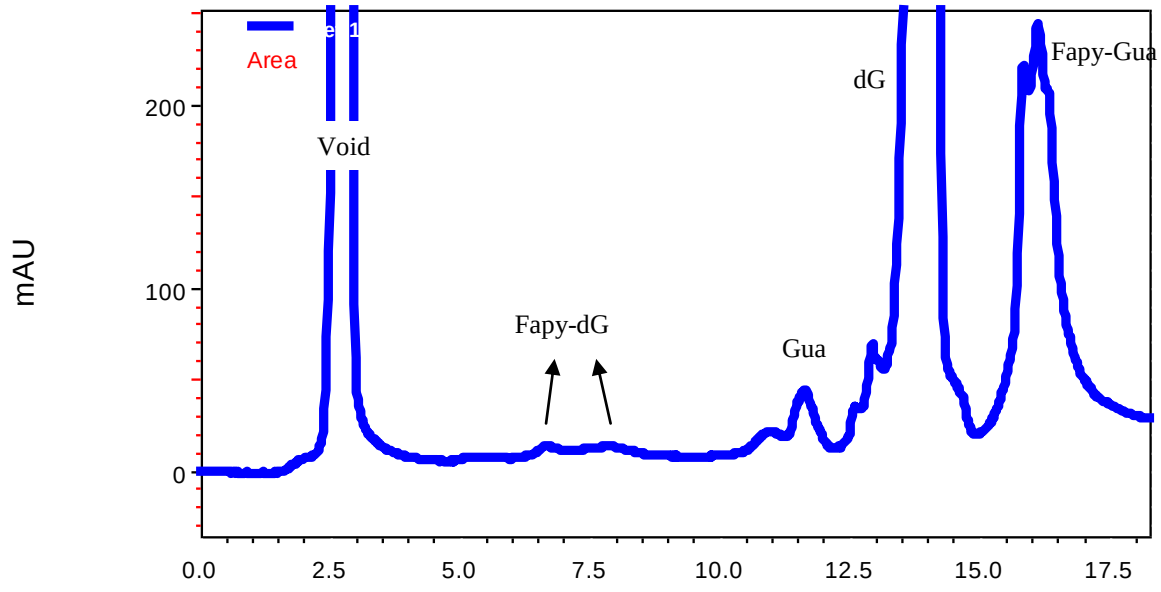


The RP-HPLC chromatogram for dG oxidation after argon purging for > 30 min. The HPLC mobile phase was water and acetonitrile.

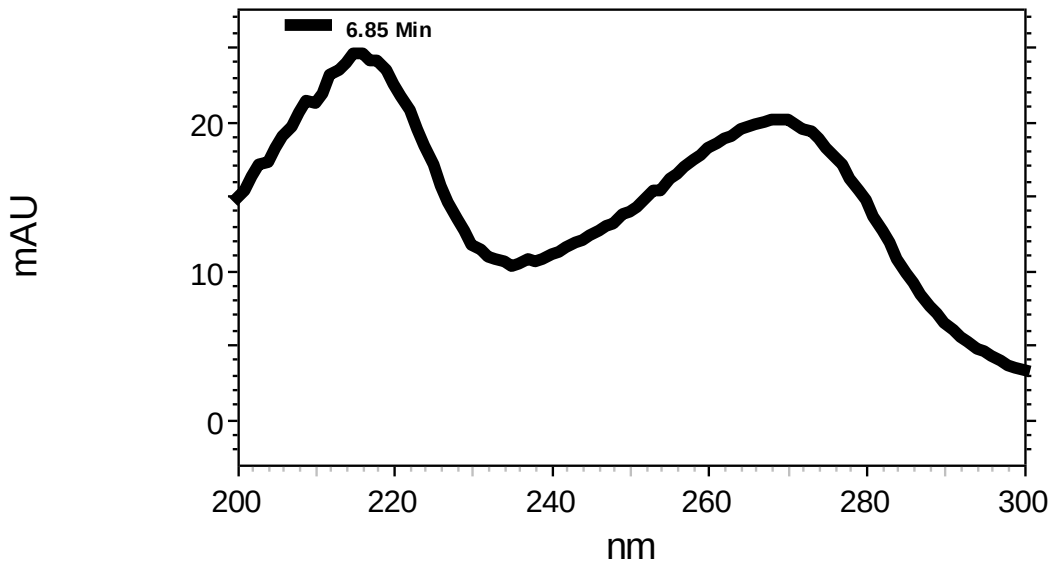


UV-absorbance of Fapy-Gua

# APPENDIX B

# MASS SPECTROMETRY AND GEL ELECTROPHORESIS FOR 2Ih-CONTAINING ODN

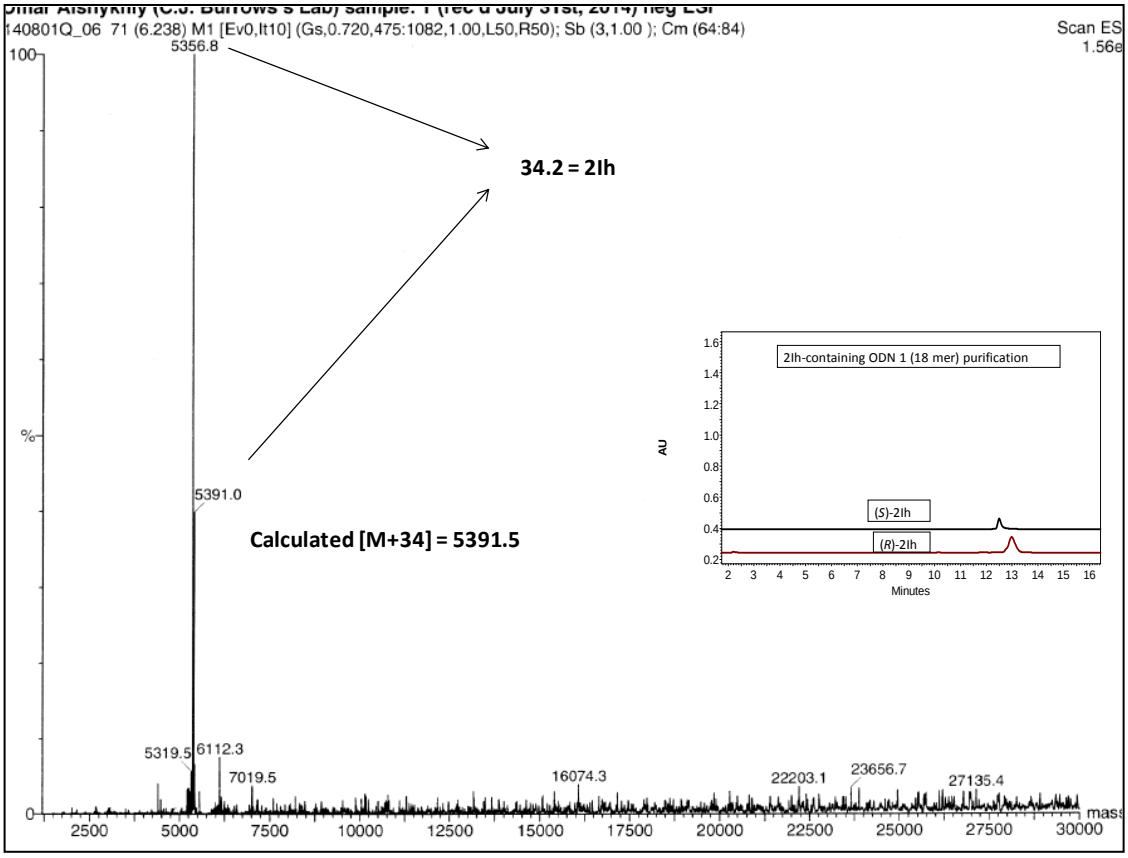


ESI-MS of an *S*-2Ih-containing ODN 1 (18 mer), calcd 5391.5, found 5391.0. The starting material G-containing ODN1, calcd. 5357.5, found 5356.8.

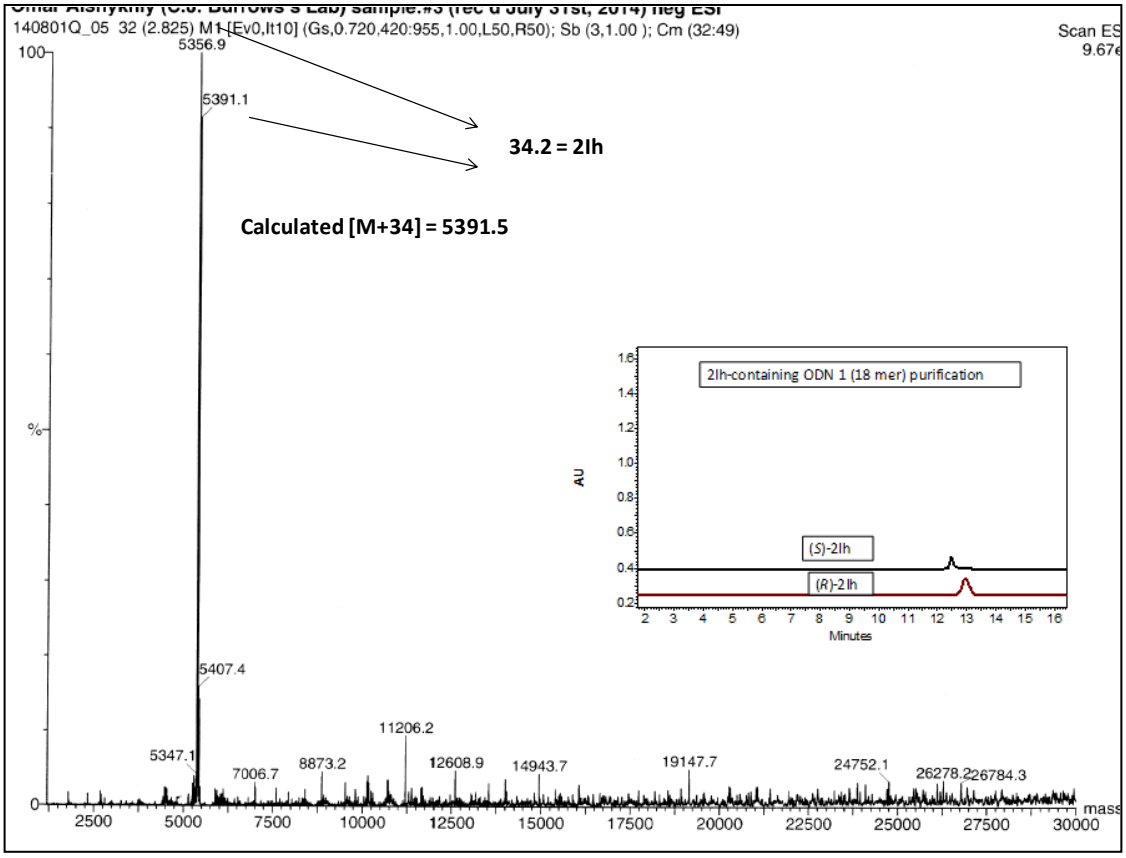


ESI-MS of an *R*-2Ih-containing ODN 1 (18 mer), calcd 5391.5, found 5391.1. The starting material G-containing ODN1, calcd. 5357.5, found 5356.9.

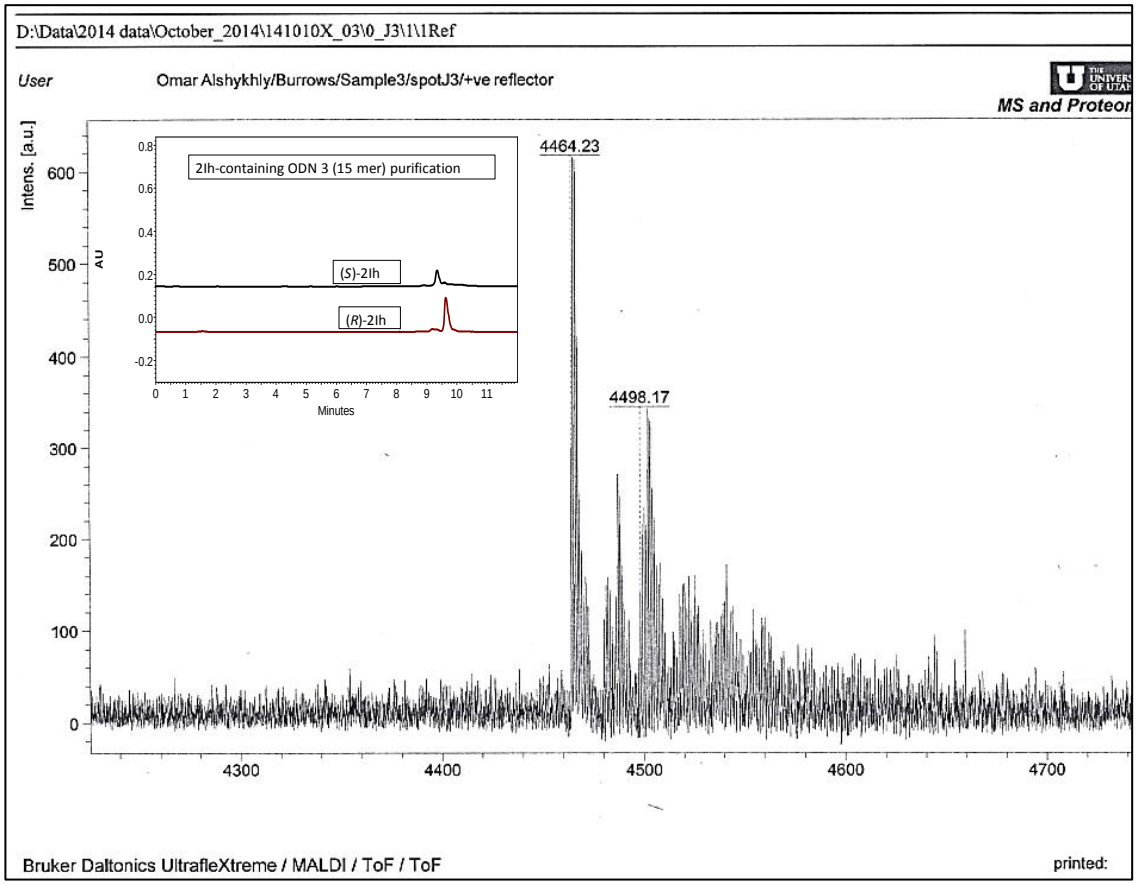


MALDI-MS of a mixture of two diastereomers of 2Ih-containing ODN 3 (15 mer), calcd 4497.80, found 4498.17. The starting material G-containing ODN1, calcd. 4463.80, found 4464.23.

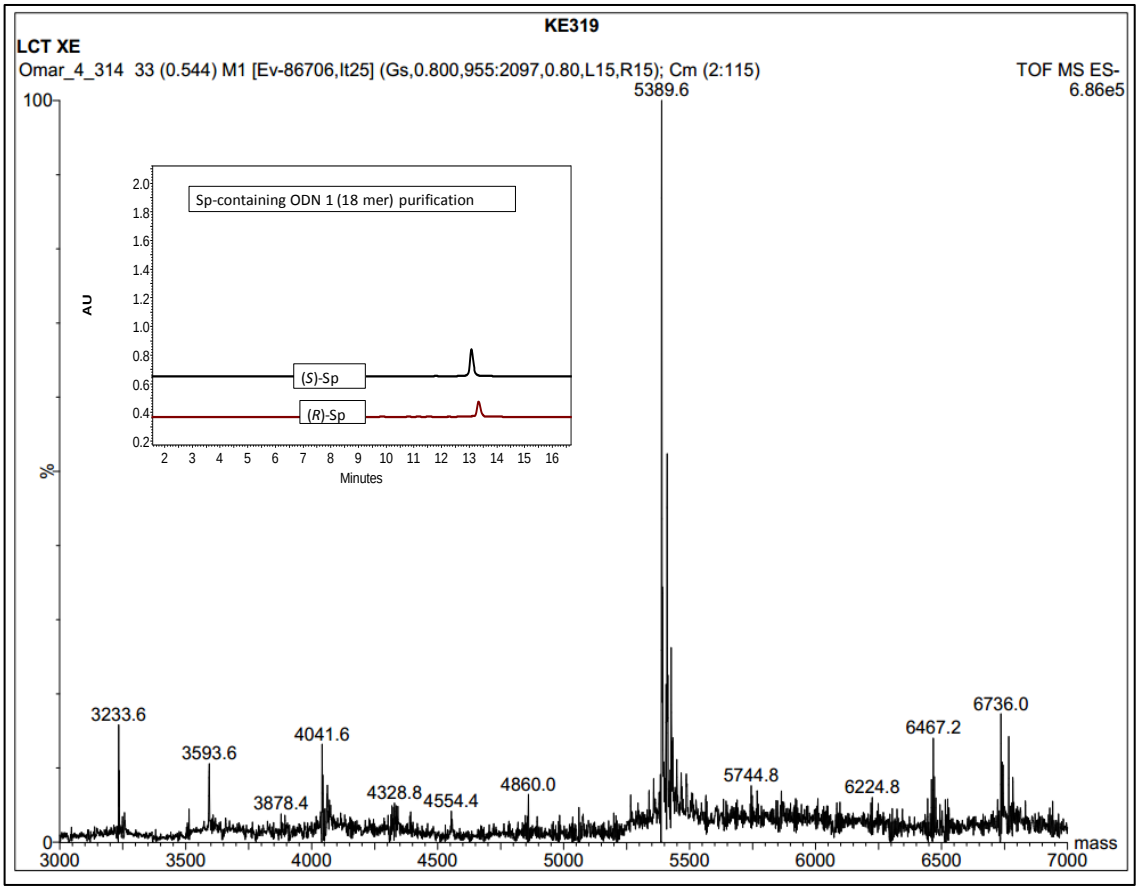


ESI-MS of a mixture of two diastereomers of Sp-containing ODN 1 (18 mer), calcd 5389.5, found 5389.6.

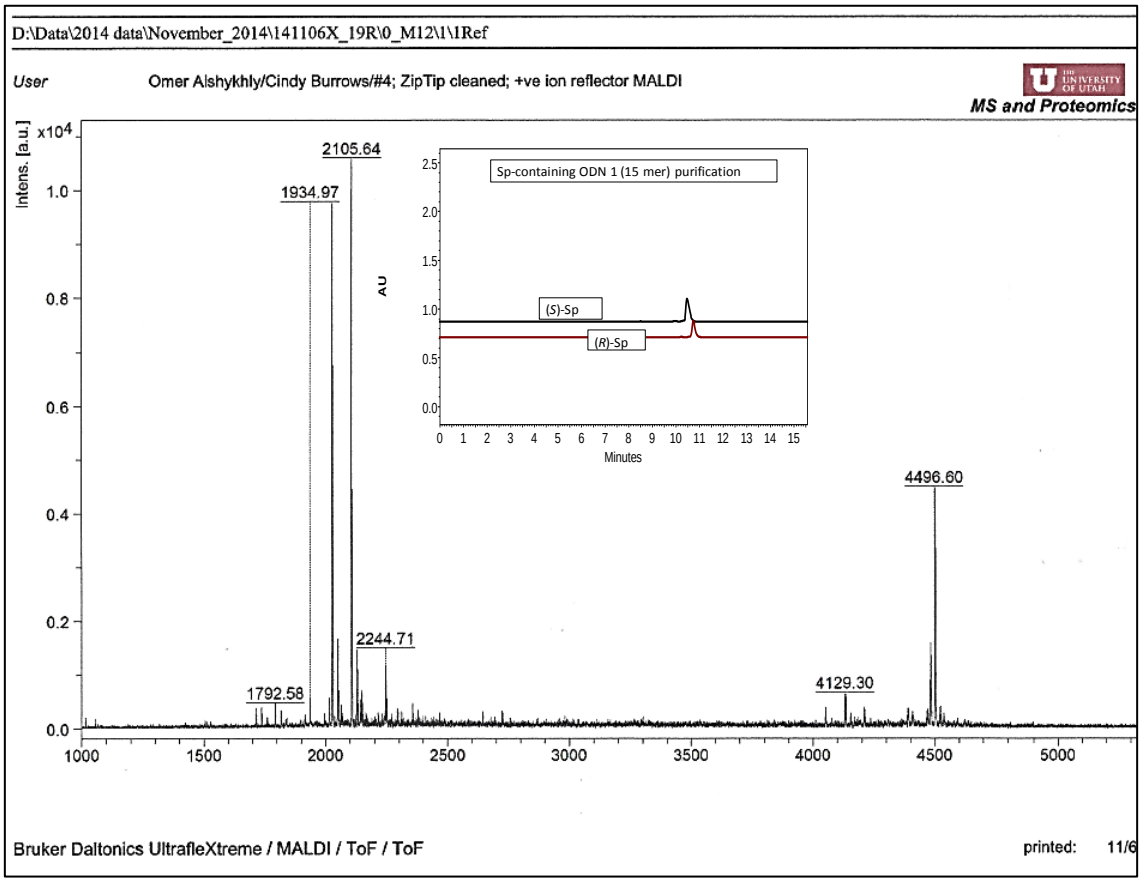


MALDI-MS of a mixture of two diastereomers of Sp-containing ODN 3 (15 mer), calcd 4495.8, found 4496.6.

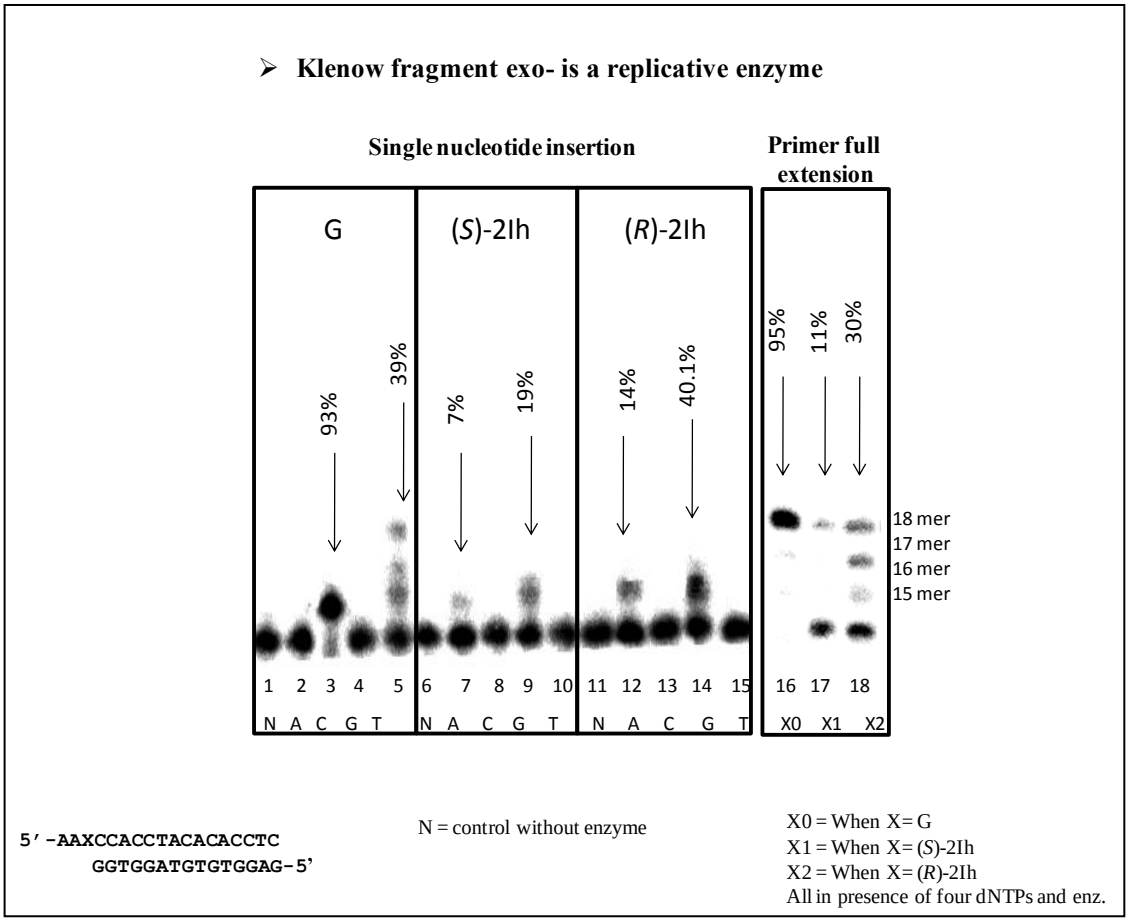


Gel electrophoretic study of Kf exo⁻ with 2Ih-containing ODN, single nucleotide and the four nucleotides insertion.

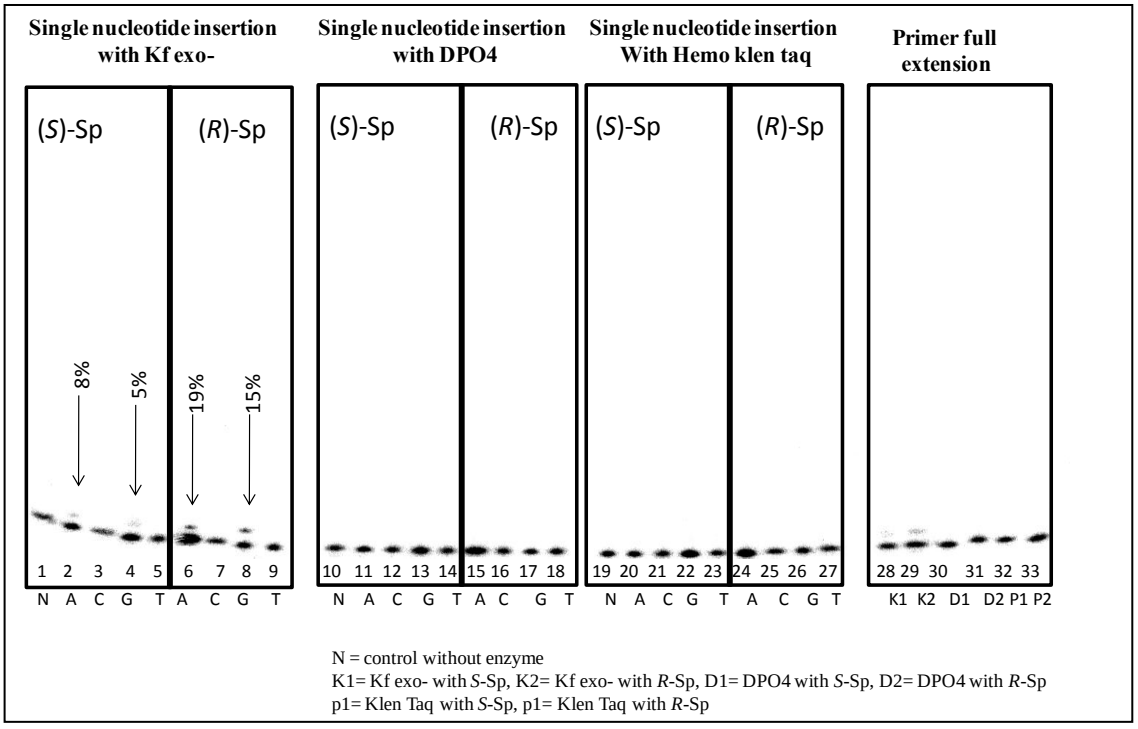


Gel electrophoretic study of Kf exo⁻, DPO4, and Hemo KlenTaq with Sp-containing ODN, single nucleotide and the four nucleotides insertion.

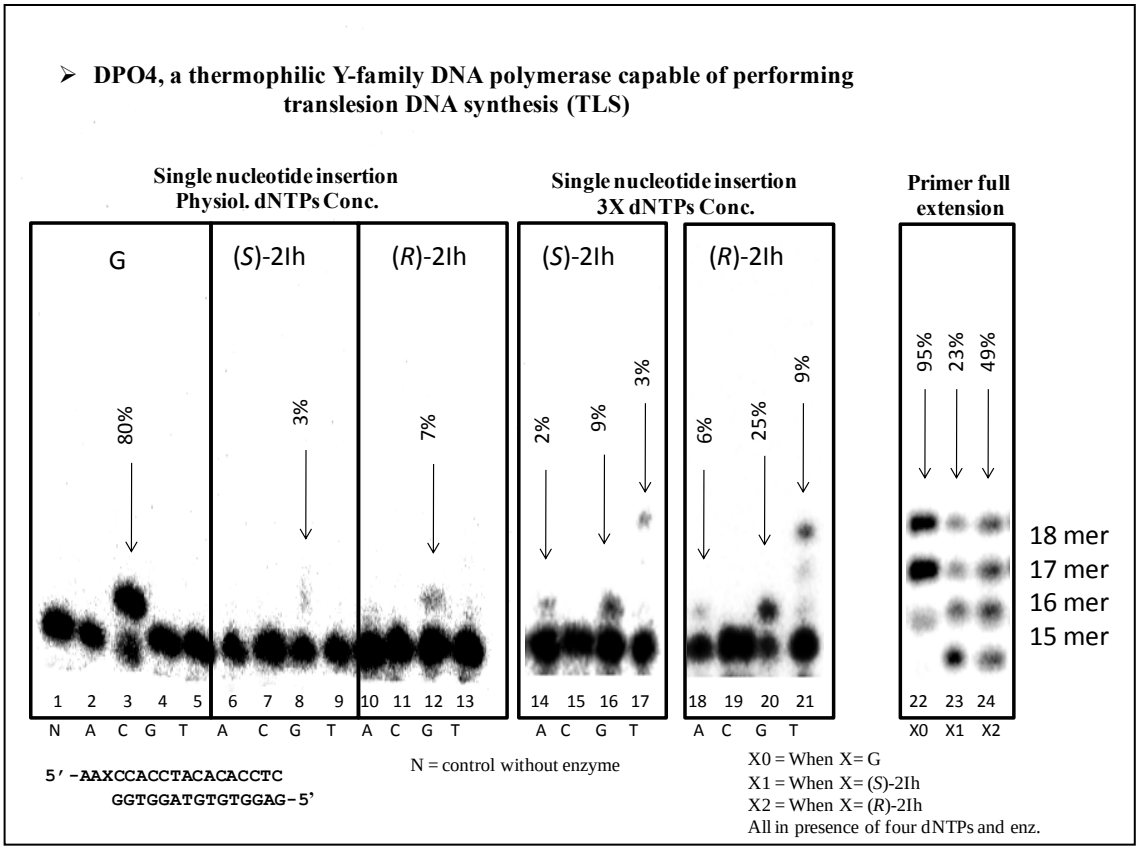


Gel electrophoretic study of DPO4 with 2Ih-containing ODN, single nucleotide and the four nucleotides insertion.

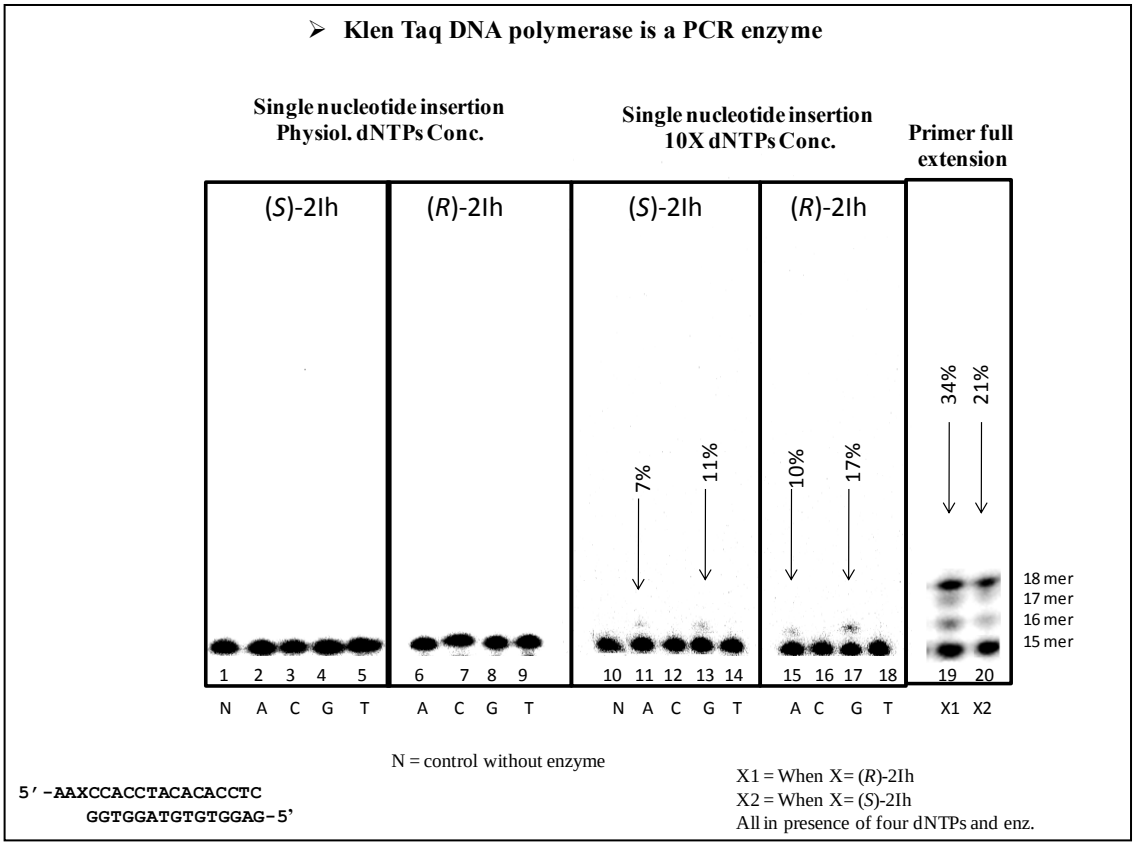


Gel electrophoretic study of Hemo Klen Taq with 2Ih-containing ODN, single nucleotide and the four nucleotides insertion.

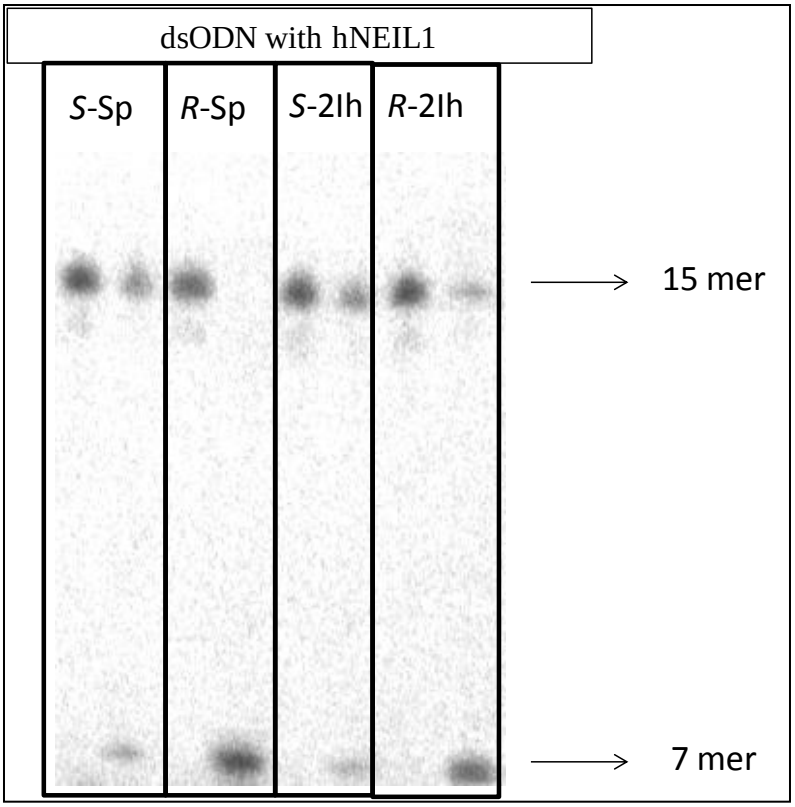


Gel electrophoretic study of NEIL1 activity toward 2Ih- and Sp-containing dsODN.

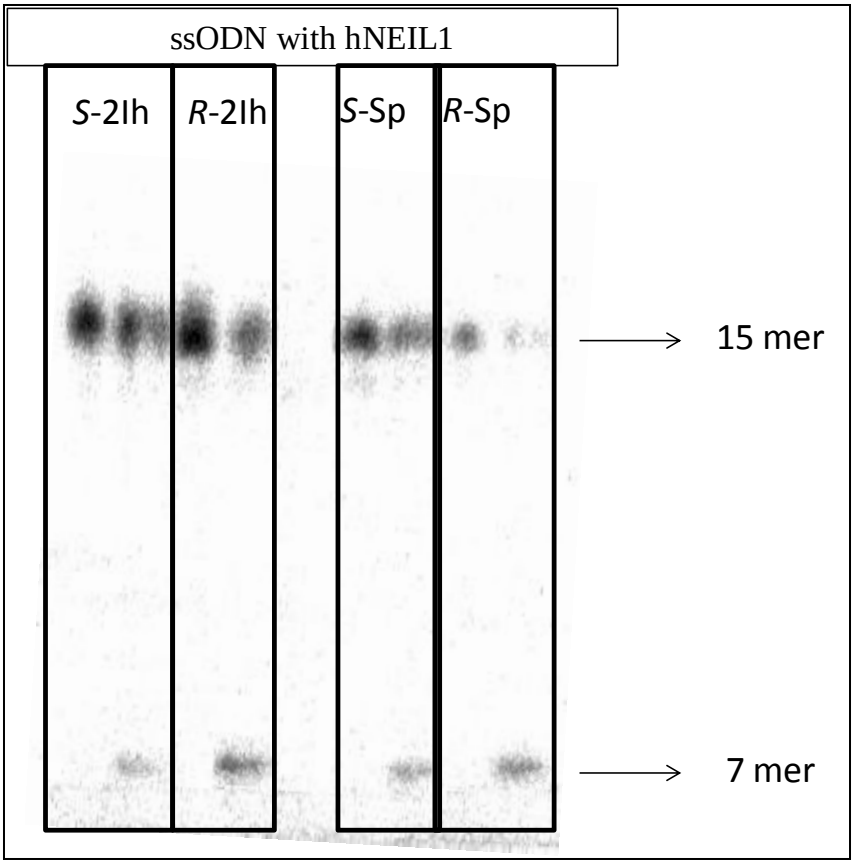


Gel electrophoretic study of NEIL1 activity toward 2Ih- and Sp-containing ssODN.

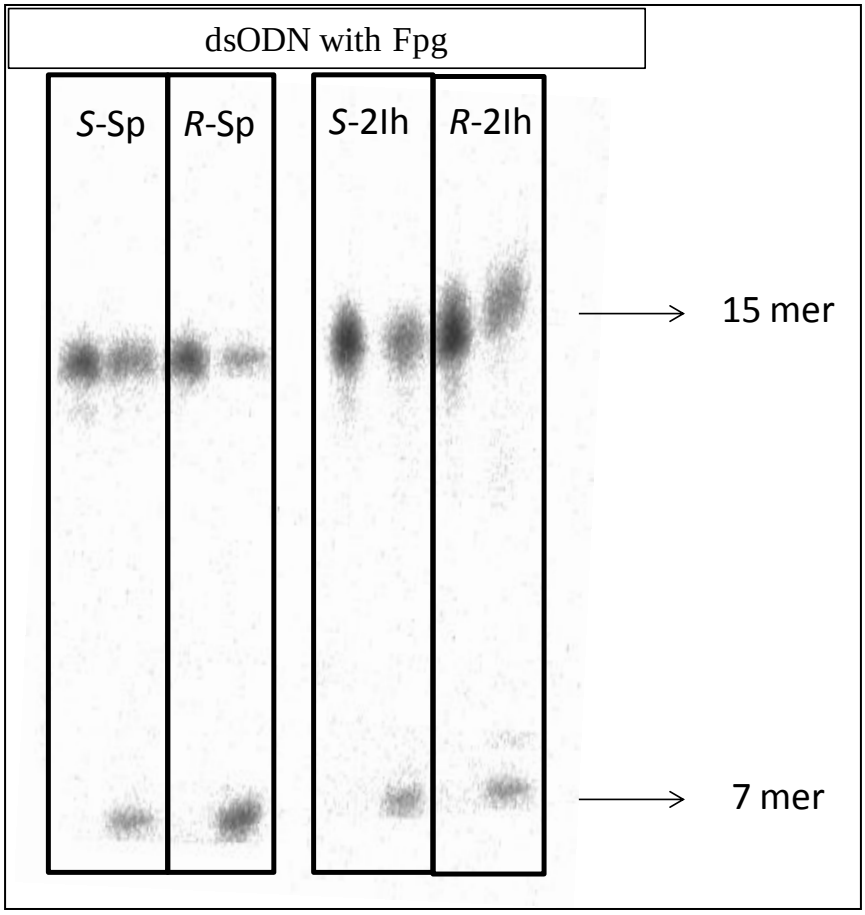


Gel electrophoretic study of Fpg activity toward 2Ih- and Sp-containing dsODN.

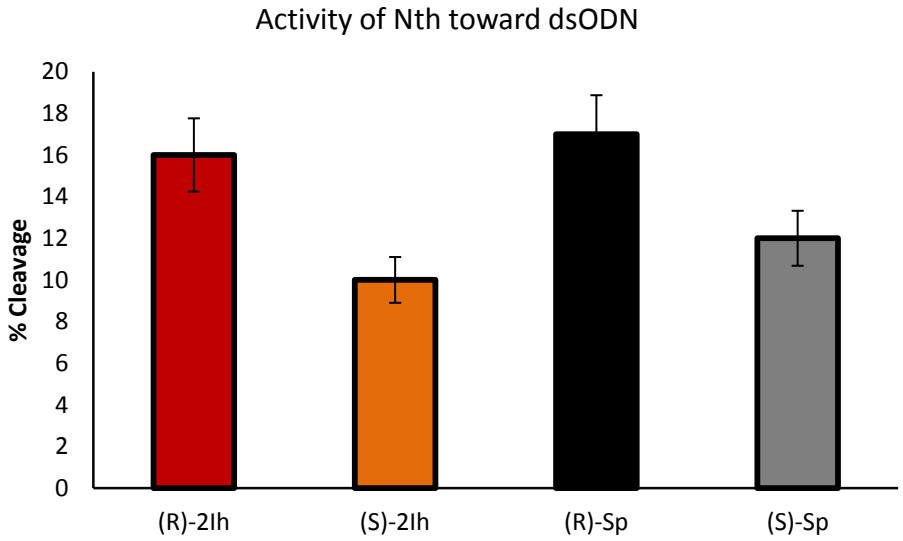


Nth activity toward 2Ih- and Sp-containing dsODN.

Coordinates and energies for the 2Ih diastereomer conformations with the lowest energies.

(*R*)-2Ih conformation 1

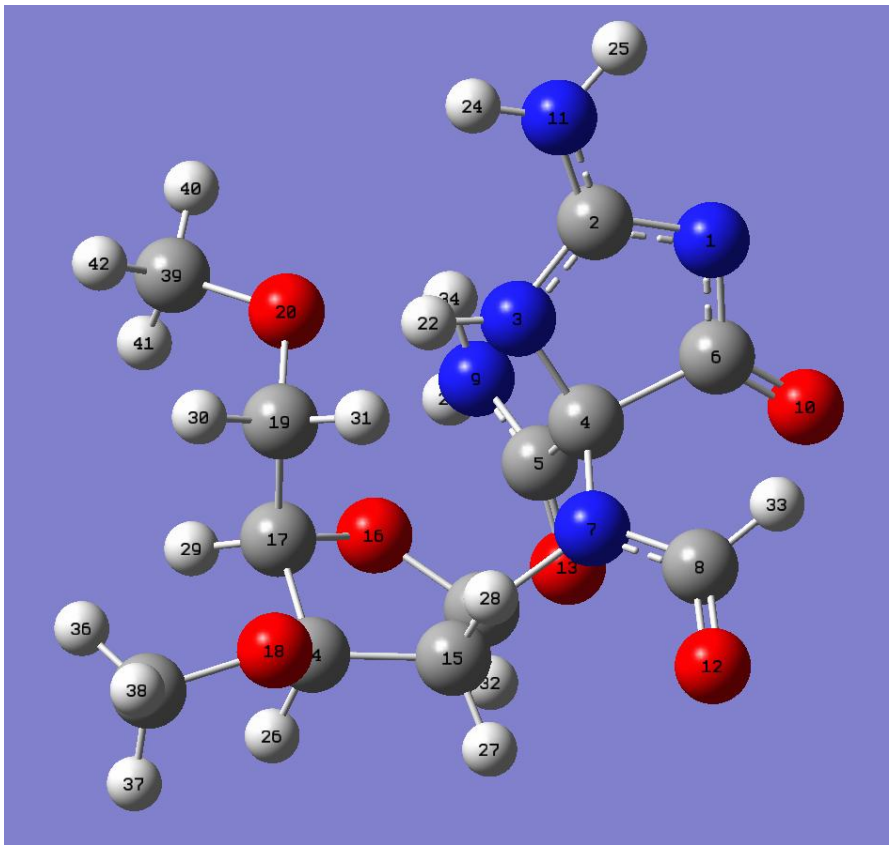


Energy = -1187.293005

| Symbol | X | Y | Z |
|---|---|---|---|
| N | 3.3155800 | 0.6584960 | 1.2870020 |
| C | 2.2314530 | 1.4806590 | 1.1998490 |
| N | 1.2777620 | 1.0612310 | 0.3297430 |
| C | 1.6293910 | -0.2493690 | -0.1981120 |
| C | 1.8241340 | -0.2664500 | -1.7348080 |
| C | 3.0834430 | -0.4068180 | 0.4667580 |
| N | 0.6907520 | -1.3151180 | 0.2055240 |

| | | | |
|---|---|---|---|
| C | 1.0625100 | -2.3325050 | 1.0374950 |
| N | 2.1006850 | 0.9170750 | -2.3125020 |
| O | 3.8545930 | -1.3549640 | 0.2140810 |
| N | 2.1280740 | 2.6112940 | 1.8979140 |
| O | 0.3638800 | -3.3521410 | 1.2531380 |
| O | 1.7984510 | -1.3570650 | -2.3536930 |
| C | -2.9626360 | -0.9187380 | -0.2175060 |
| C | -1.8245720 | -1.7721150 | 0.3615510 |
| O | -0.9098630 | -0.0794380 | -1.0602190 |
| C | -2.2523220 | 0.3896930 | -0.6372870 |
| O | -3.9875020 | -0.7446580 | 0.7939340 |
| C | -2.1377060 | 1.3991720 | 0.5054460 |
| O | -1.1239550 | 2.4194880 | 0.2379540 |
| C | -0.6175760 | -1.4116350 | -0.5112720 |
| H | 0.3736690 | 1.5289400 | 0.1814330 |
| H | 2.3014140 | 0.9531320 | -3.2993270 |
| H | 1.3161470 | 3.2031410 | 1.8328850 |
| H | 2.8752930 | 2.8858310 | 2.5130790 |
| H | -3.4009780 | -1.3956900 | -1.0981880 |
| H | -2.0505020 | -2.8318920 | 0.3287430 |
| H | -1.6605940 | -1.4898190 | 1.4008730 |
| H | -2.6893350 | 0.8418530 | -1.5239190 |
| H | -3.1014570 | 1.8782980 | 0.6867900 |
| H | -1.8115410 | 0.9187830 | 1.4241250 |
| H | -0.4931310 | -2.0875560 | -1.3541870 |
| H | 2.0276960 | -2.2063250 | 1.5197130 |

| | | | |
|---|---|---|---|
| H | 2.0483760 | 1.7826280 | -1.8017270 |
| C | -5.3092900 | -0.3845960 | 0.2755430 |
| H | -5.2992760 | 0.6043530 | -0.1875080 |
| H | -5.6488150 | -1.1273620 | -0.4494780 |
| H | -5.9731290 | -0.3777910 | 1.1347460 |
| C | -1.4997360 | 3.4646920 | -0.7172360 |
| H | -0.6802060 | 4.1768730 | -0.7189600 |
| H | -1.6338150 | 3.0554250 | -1.7192130 |
| H | -2.4171830 | 3.9546250 | -0.3877290 |

(*R*)-2Ih conformation 2

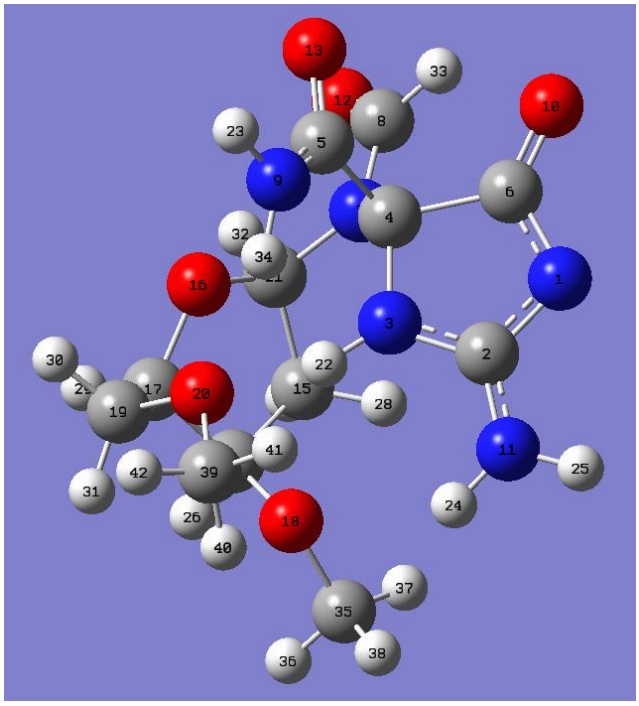


E = -1187.289309

| Symbol | X | Y | Z |
|---|---|---|---|

| | | | |
|---|---|---|---|
| N | -1.4948250 | 2.2981170 | -1.4380500 |
| C | -0.2117990 | 1.9980280 | -1.1247160 |
| N | -0.0769730 | 0.9605090 | -0.2558910 |
| C | -1.3667360 | 0.4093230 | 0.0806120 |
| C | -1.7166690 | 0.4707600 | 1.5935780 |
| C | -2.2963210 | 1.4222800 | -0.7515170 |
| N | -1.5060720 | -0.9901240 | -0.4331930 |
| C | -2.7665600 | -1.5617100 | -0.5187740 |
| N | -0.8681870 | 1.1283940 | 2.4114600 |
| O | -3.5411420 | 1.3846230 | -0.7752010 |
| N | 0.8389900 | 2.6616370 | -1.6157520 |
| O | -2.9608250 | -2.7900520 | -0.6769790 |
| O | -2.7956320 | -0.0392450 | 1.9801570 |
| C | 2.0757480 | -1.5524820 | -0.7216410 |
| C | 0.7202520 | -1.8455700 | -1.4126020 |
| O | 0.3364730 | -1.5758550 | 0.9544230 |
| C | 1.7932310 | -1.7106520 | 0.7913970 |
| O | 2.5948830 | -0.2176860 | -1.0268040 |
| C | 2.4647180 | -0.7679160 | 1.7818460 |
| O | 1.9451520 | 0.6032110 | 1.6785510 |
| C | -0.3509470 | -1.9087260 | -0.2964180 |
| H | 0.7916940 | 0.7225540 | 0.2240720 |
| H | -1.1100630 | 1.1855750 | 3.3888100 |
| H | 1.7784280 | 2.3463350 | -1.4485690 |
| H | 0.6952640 | 3.4370650 | -2.2377070 |
| H | 2.8399530 | -2.2701290 | -1.0233590 |

| | | | |
|---|---|---|---|
| H | 0.7569300 | -2.7973860 | -1.9377880 |
| H | 0.4774630 | -1.0676660 | -2.1305520 |
| H | 2.0718540 | -2.7293600 | 1.0746950 |
| H | 2.2590720 | -1.1124540 | 2.7949300 |
| H | 3.5417500 | -0.7667320 | 1.6177730 |
| H | -0.7792500 | -2.9026490 | -0.2173360 |
| H | -3.5817790 | -0.8481200 | -0.4930780 |
| H | 0.1097410 | 1.2482120 | 2.1757750 |
| C | 3.2524730 | -0.1380730 | -2.3336230 |
| H | 4.0508340 | -0.8800710 | -2.3993250 |
| H | 2.5374970 | -0.2944560 | -3.1430550 |
| H | 3.6745410 | 0.8599250 | -2.4044040 |
| C | 2.9698380 | 1.6523610 | 1.7577700 |
| H | 3.6929910 | 1.5175820 | 0.9559550 |
| H | 2.4485120 | 2.5983870 | 1.6439540 |
| H | 3.4594080 | 1.6179440 | 2.7305380 |

(S)-2Ih conformation 1

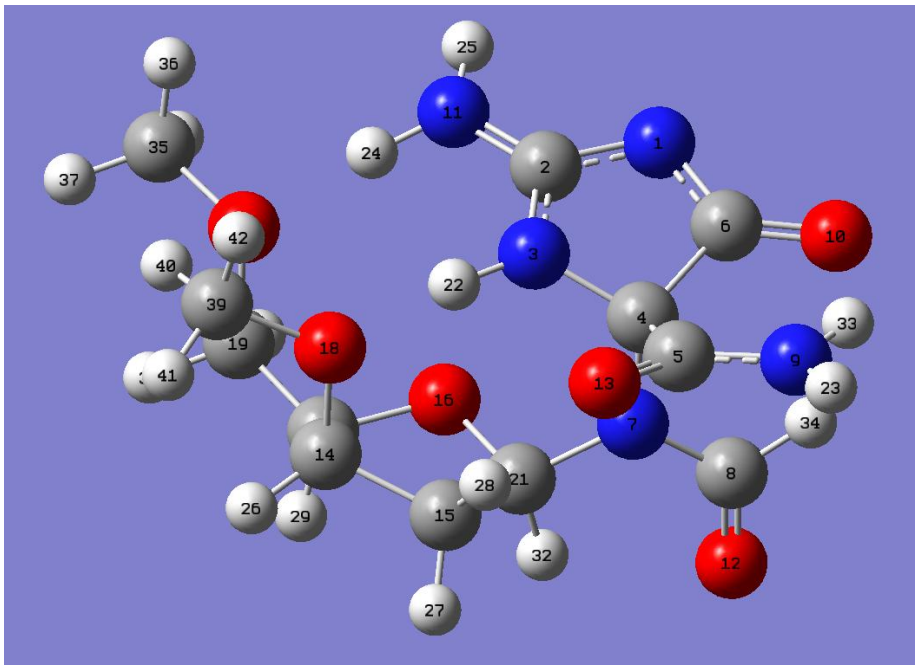


E = -1187.293005

| Symbol | X | Y | Z |
|---|---|---|---|
| N | 3.5633750 | -0.0152870 | 0.4914700 |
| C | 2.7612160 | -0.9423820 | 1.0469850 |
| N | 1.4616820 | -0.9548280 | 0.5800090 |
| C | 1.2691170 | 0.1909130 | -0.2860010 |
| C | 0.8409750 | -0.1901180 | -1.7258230 |
| C | 2.7800440 | 0.7286730 | -0.3682620 |
| N | 0.3618250 | 1.2176710 | 0.2847060 |
| C | 0.3292270 | 2.4198310 | -0.3950110 |
| N | 1.3756100 | -1.3670510 | -2.1280980 |
| O | 3.1295120 | 1.6627270 | -1.1000190 |
| N | 3.1800940 | -1.8143330 | 1.9587840 |
| O | -0.3333850 | 3.4343410 | -0.1015220 |
| O | 0.1787800 | 0.5719470 | -2.4459640 |
| C | -2.6765730 | 0.7227650 | 0.9311380 |

| | | | |
|---|---|---|---|
| C | -1.7253760 | 1.6995200 | 1.6505610 |
| O | -0.7218620 | -0.4390500 | 1.7538880 |
| C | -2.1736910 | -0.6384300 | 1.4763840 |
| O | -2.5098720 | 0.9777640 | -0.4819050 |
| C | -2.3122190 | -1.9166450 | 0.6643470 |
| O | -1.4554550 | -1.8386130 | -0.5140830 |
| C | -0.3643980 | 0.9781510 | 1.5739790 |
| H | 0.6206170 | -1.2662840 | 1.0920310 |
| H | 1.2482330 | -1.6771000 | -3.0853960 |
| H | 2.5686520 | -2.5192990 | 2.3555590 |
| H | 4.1485820 | -1.7864220 | 2.2581060 |
| H | -3.7227520 | 0.8680610 | 1.2353930 |
| H | -2.0077270 | 1.7855770 | 2.7035590 |
| H | -1.6820090 | 2.6655440 | 1.1586980 |
| H | -2.6728870 | -0.7968830 | 2.4392150 |
| H | -1.9930970 | -2.7597090 | 1.2939070 |
| H | -3.3657980 | -2.0735220 | 0.3972630 |
| H | 0.2982070 | 1.2323620 | 2.4037750 |
| H | 1.7899180 | -1.9974250 | -1.4510450 |
| H | 1.0270660 | 2.4126580 | -1.2313290 |
| C | -1.3957720 | -3.1342900 | -1.1995230 |
| H | -0.6641600 | -3.0091720 | -1.9967150 |
| H | -2.3693540 | -3.4137600 | -1.6223490 |
| H | -1.0653330 | -3.9301520 | -0.5178650 |
| C | -3.4833220 | 0.3095460 | -1.3483110 |
| H | -3.1923030 | -0.7275230 | -1.5183650 |

| | | | |
|---|---|---|---|
| H | -4.4999500 | 0.3578440 | -0.9324820 |
| H | -3.4611140 | 0.8538630 | -2.2959970 |